Identification of KLF13 Interacting Partners in the Heart

A Thesis Submitted to the
Faculty of Graduate and Postdoctoral Studies
University of Ottawa
In Partial Fulfillment of the Requirements for the Degree of Master of Science
Department of Biochemistry, Microbiology and Immunology
Faculty of Medicine
By
Rami Darwich

Abstract.

Identifying the molecular and genetic pathways important for heart development and deciphering the causes of CHD are still a challenging puzzle. A newly identified piece of this puzzle is KLF13, a member of the Krüppel-like family of zinc-finger proteins, was found to be important for atrial septation and ventricular trabeculation of Xenopus embryos. The protein is expressed predominantly in the heart, binds evolutionarily-conserved regulatory elements on cardiac promoters, and activates cardiac transcription.

In this study we examined KLF13 mechanism of action by investigating its transcriptional activity on the ANF promoter using a deletion/mutagenesis approach. We reported the identification of a new synergistic partnership between KLF13 and the individual cardiac transcription factors TBX5, NKX2.5, PEX1, and CATF1. Also, we localized KLF13's transcriptional activation domain, the nuclear localization region/zinc-fingers, and the DNA binding zinc-fingers. This study will provide insight into the contribution of KLF13 to the development of CHDs.

Acknowledgment:

Another two years have passed and I have gained a wealth of knowledge about cardiac development that has paradoxically emphasized that I know nothing. I am forcefully adopting the engineering motto "Question everything. Learn something. Answer nothing." However, I am certain that one day I will be reading the above lines with a smirk on my face, scrutinizing my foolishness.

I would like to express my most sincere gratitude to my supervisor Dr. Mona Nemer for mentoring me and providing a creative and open environment to work in. Her vast knowledge of cardiovascular research, positivity, innovative attitude towards scientific work, and guidance and encouragement throughout this project was of great importance. Thank you for paving my first stretch of road towards being an independent researcher. I would also like to express my appreciation to Dr. Alexandre Blais and Dr. Alexandre Stewart for their constructive criticism and insights during the course of this thesis.

I owe my gratitude to all present and former members of the "Nemer Lab": Hiba Komati and Brigitte Laforest for your thesis corrections and helpful discussions concerning my work; Abir Yamak and Wael Maharsy for friendship, cooperation and protocol guidance during the last couple of years; and Janie Beauregard for expert technical assistance, comic relief, and insight into life (without you I would have been studying chaos theory).

My deepest thanks go to my mother, family, and my better half Jessica, whose endless love, understanding, and confidence in me have been essential for the completion of this thesis.

Ottawa, April 2011

Rami Darwich

Table of Contents

List of Figures

List of Tables

List of Abbreviations

AD 293 cells	Human embryonic kidney cells
AHF	Anterior/secondary heart fields
ANF	Atrial natriuretic factor
ASD	Atrial Septal Defect
At	Atria
ATP	Adenosine triphosphate
BSA	Bovine serum albumin
BMB	Bone Morphogenetic proteins
BNP	Brain natriuretic peptide
CARE	Cardiac response element
CATF1	Cardiac response element transcription factor 1
CBP	CREB-binding protein: CREB = cAMP responsive element-binding protein
cDNA	complimentary deoxyribonucleic acid
CHD	Congenital heart diseases
CMV	Cytomegalovirus
DBD	DNA binding domain
DCM	Dilated cardiomyopathy
DMEM	Dulbecco.s Modified Eagles Medium
DMSO	dimethyl sulfoxide
dNTP	deoxynucleotide triphosphate
DNA	Deoxyribonucleic acid
DSMA1	Distal spinal muscular atrophy type 1
DTT	dithiothreitol
ED	Embryonic day
EDTA	Ethylene diamine tetraacetic acid
EMSA	Electromobility Gel Shift Assay
FCS	Fetal calf serum
FGF	Basic fibroblast growth factors
FHF	First Heart Field
FITC	Fluorescein isothiocynate
FOG	Friend of GATA
GATA	GATA binding protein
h	Hour
HA-tag	Haemagglutinin tag
HAT	Histone acetyltransferase
HDAC	Histone deacetylase
IGHMBP2	Immunoglobulin mu binding protein 2
LV	Left ventricle
kb	Kilobase
kDa	Kilodaltons
KO	Knockout
MEF2C	Myocyte Enhancer Factor 2
MHC	Myosin heavy chain
min	Minute
ml	Millilitre
µl	Microlitre

MLC	Myosin light chain
mM	Millimolar
mRNA	Messenger ribonucleic acid
NES	Nuclear export signal
NIH 3T3	Mouse embryonic fibroblast cell line
NKX	Nirenberg and Kim X=Mammalian class
NLS	Nuclear localisation signal
NMD	Neuromuscular degeneration
OFT	Outflow tract
p300	a 300kDa histone acetyltransferase
PBS	phosphate buffered saline
PCAF	p300/CBP associated factor
PCR	polymerase chain reaction
PERE	Phenylephrine response element
PEX1	Phenylephrine-induced Complex-1
PFO	Patent foramen oval
RANTES	Regulated upon Activation, Normal T-cell Expressed, and Secreted
RV	Right ventricle
Sin3	Swi-independent-3
SMARD1	Spinal muscular atrophy with respiratory distress type 1
SMC	Smooth muscle cells
TAD	transactivation domain
TAE	Tris-acetate-EDTA
TAZ	Transcriptional co-activator with PDZ-binding motive
TBS	Tris-buffered saline
TBST	Tris-buffered saline with Tween-20
TBX	T-box transcription factor
SDS	sodium dodecylsulphate
ToF	Tetralogy of Fallot
VSD	Ventricular Septal Defect
ZF	Zinc finger
ZFP	Zinc finger protein

1. Introduction

1.1 Morphology of heart development.

The heart is the first functional organ to develop during vertebrate embryogenesis, arising through a flawless spatiotemporal orchestration of cell fate specification, migration, differentiation, proliferation, and morphogenesis. The masterpiece of the orchestra is a four-chambered heart composed of diverse cell types including cardiomyocytes, conduction system, smooth muscle and endothelial [1]. The process starts during gastrulation as inductive signals from the underlying endoderm initiate the commitment of mesodermal cardiac progenitor cells into two distinct cardiac progenitor cell fields. These two cardiac fields are known as the first and the anterior/secondary heart fields (FHFs and AHFs). As development progresses, those progenitor cells undergo expansion, migration, and organization to form the cardiac crescent (**figure 1.1**). The cells of the FHF, located in the anterior lateral plate mesoderm on each side of the primitive streak, will migrate and fuse along the ventral midline to craft the beating linear heart tube. At this stage, the tubular heart consists of: 1) an interior layer of endocardial cells which will form the inner lining of the heart; 2) an exterior muscle-forming layer of myocardial cells; and 3) an extracellular matrix, the cardiac jelly, separating the two last layers, which eventually plays a central role in the septation of the heart and the formation of the atrioventricular canals [1-8]. In addition to the FHF, the anterior heart field (AHF), a Wnt-signalling-delayed line of progenitor cells located dorsomedially to the FHF, also contributes to the heart tube at the venous and arterial poles of the tube [1-7]. Ultimately, the FHF will form the left ventricle of the four-chambered heart, whereas the SHF will give rise to the outflow tract, right ventricle, and most of the atria [1-5]. Recently, multipotent epicardial progenitor cells were discovered to be contributors to the atrial and ventricular myocardium, coronary smooth

muscle, and cardiac fibroblasts [5].

As development continues, the heart tube loops to the right. This looping breaks the symmetry of the early embryo and initiates the correct alignment of the atrial and ventricular chambers along with the aorta and the pulmonary artery [9]. The looping step is followed by the ballooning of the archetypal vertebrate four-chambered structure, in which the chambers will form along the outer curvature of the balloons, and the inner curvature will form the septa and valves. At later stages, the ballooned structure is refined further by septation, trabeculation, and maturation to form the definitive four-chambered heart [10, 11].

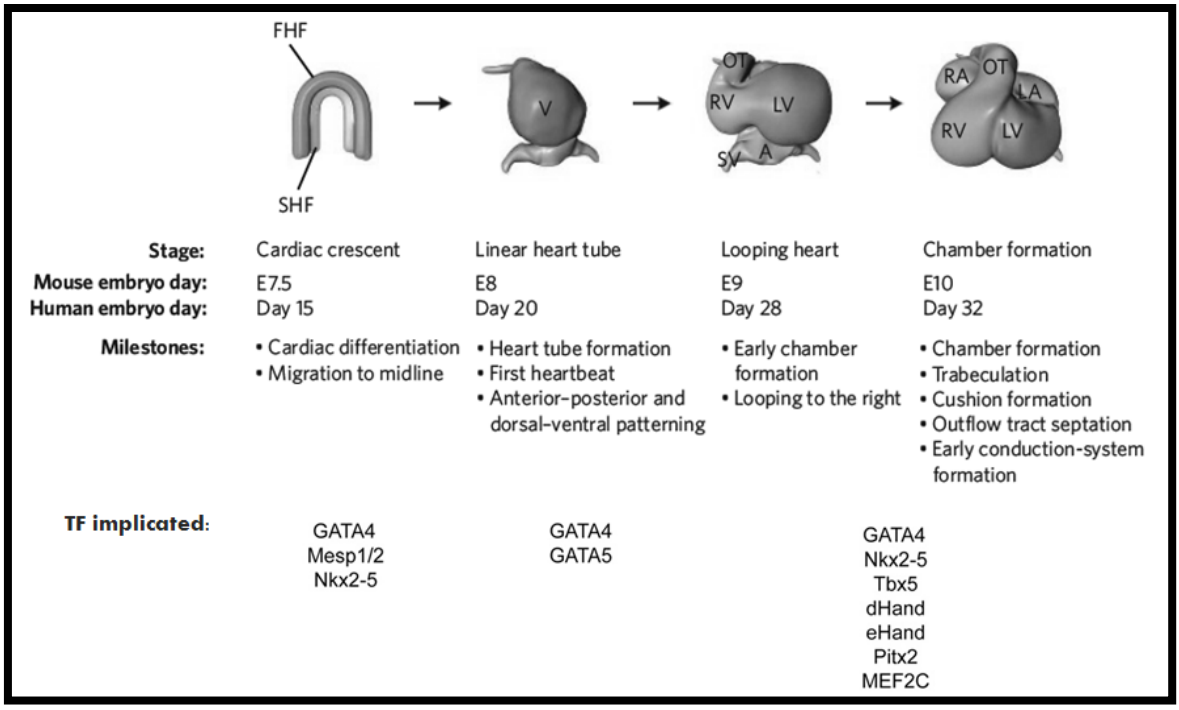

Figure 1.1: Overview of mammalian heart development. At the earliest stages of heart formation (cardiac crescent), two pools of cardiac precursors exist. The first heart field (FHF) contributes to the left ventricle (LV), and the second heart field (SHF) contributes to the right ventricle (RV) and later to the outflow tract (OT), sinus venosus (SV), and left and right atria (LA and RA, respectively). Outflow tract septation separates the common outflow tract (OT) into the aorta (AO, connected to the left ventricle) and the pulmonary artery (PA, connected to the right ventricle). Modified figure from [5, 11]

1.2. Cardiac transcription: Different levels of control

The control of lineage commitment and expansion of the cardiac progenitor populations is coordinated via positive and negative inductive signals [from the adjacent endothelial, endocardial, and other mesodermal derived cells] along with a cascade of interacting transcription factors. These inductive signals include, among others, bone morphogenetic proteins (BMPs), basic fibroblast growth factors (FGF), and Wnt proteins. Exemplifying the importance of these inductive signals for cardiac differentiation, FGF8 deficient embryos were shown to have multiple cardiovascular lethal malformations affecting primarily SHF derivatives, including the outflow tract (OFT) [12, 13].

Following the inductive signals, a handful of cardiac-specific evolutionarily-conserved transcription factors including GATA [11], NKX2 [14], TBX [15], MEF2 [16], SRF [17] and HAND [18] proteins (to be discussed in later sections), were found to be activated within the cardiac progenitor cells of the FHF and AHF. The earliest of these is the zinc finger containing TF, GATA-4, which is essential for cellular response to cardio-inductive factors; and its combined action with the homeodomain TF, NKX2.5, mediates BMP signalling [11]. Cooperatively and through direct interactions, these cardiac regulators activate the expression of genes that control cardiac cell fates and morphogenesis of cardiac structures, as well as genes encoding muscle specific proteins such as α-myosin heavy chain (α-MHC), cardiac α-actin, atrial natriuretic factor (ANF) and brain natriuretic peptide (BNP) [19]. Adding to the complexity of cardiac gene expression, these transcription factors also participate in transcriptional feedback loops that induce one another's expression, resulting in the stabilization and maintenance of the cardiac gene program [20]. For example, GATA4 and TBX20 cooperatively activate both the NKX2.5 and MEF2C enhancers [21].

Chromatin remodelling and histone modification add another level of transcriptional complexity in which the transcriptional activity of TFs is highly dependent on chromatin structure and accessibility to binding sites. Examples are the Swi/Snf-like Brg1/Brm-associated (BAF) chromatin remodelling complexes which are polymorphic assemblies of numerous components that modify the structure of the DNA–nucleosome complex. Mice embryos deficient in Baf60 subunit isoform c, a BAF complex subunit enriched in precardiac mesoderm, demonstrated cardiac lethality at embryonic day (ED) 10.0–11.0. Additionally, *in vitro* studies have indicated that the primary function of Baf60c is to create an interaction between DNA-binding transcription factors, such as GATA-4, NKX2.5, and TBX5, and the BAF complexes, presumably to augment their transcriptional activities [22].

On the histone modification front, acetylation of lysine residues is an active process controlled by the actions of two large families of enzymes, the histone acetyltransferases (HATs) and the histone deacetylases (HDACs). Several histone modifying enzymes are known to interact with various cardiac transcription factors [23, 24]. For example, the histone acetyltransferase (HAT) protein p300 acetylates lysine residues on H3 as well as on GATA4, thereby enhancing DNA-binding and transcriptional activity [25]. The importance of p300 is demonstrated by the lethal cardiac malformations exhibited at ED 9 -11.5 [26]. On the other hand, inhibiting histone deacetylation in embryonic stem cells via histone deacetylases (HDACs) inhibitors was shown to increase the levels of acetylated GATA4 and the cells differentiated into cardiomyocytes [27]. Therefore, the regulation of distinct gene programmes depends on multiple levels of transcriptional control dictated by transcriptional regulators that bind specific DNA sequences, guiding the modification of chromatin structure, which in turn directs the accessibility of DNA to regulatory factors [23, 28].

1.3. Natriuretic peptides: A tool to decipher cardiac transcription.

De Bold's and Sudoh's milestone discoveries of atrial natriuretic peptide/factor (ANF/ANP) and brain natriuretic peptide (BNP), respectively, have triggered the spark of understanding cardiac development and homeostasis [29, 30]. The highly homologous cardiac natriuretic polypeptides are also being used in clinical practices as quantitative biomarkers of heart failure. The two polypeptide hormones are synthesized as precursor forms that are activated by proteolytic cleavage giving rise to biologically active forms of ANF and BNP peptides that can be stored in atrial-specific granules [31]. Although the two hormones are continuously released from the heart, various mechanical and neuroendocrine stimuli modulate their rate of synthesis or/and release. The hormones regulate wide cellular spectra that converge to execute related tasks that are predominantly mediated through increases of cGMP in target cells. In these cells, the secondary messenger cGMP targets include cGMP-dependent protein kinases, cGMP-gated ion channels, and cGMP-regulated cyclic nucleotide phosphodiesterases. Thus, ANF and BNP regulate their effects by modulating their cellular targets in various manners at the integrative level [32, 33].

The imperative nature of natriuretic hormones in all facets of cardiac function is indicated by the fact that ANF is expressed even in pre-cardiac cells prior to primitive heart formation [34]. During early stages of embryogenesis, the ANF gene is expressed both in the atrial and ventricular, but not in the skeletal, muscle cells. In the later stage of fetal development, ANF expression is dramatically reduced in the ventricular cells whereas its expression remains high in the atria [33, 35]. However, ventricular ANF gene expression is reactivated in response to hemodynamic overload [33, 36].

ANF and BNP are secreted from the cardiac atria and ventricles, respectively. Interestingly, while disruption of the murine ANF gene, Nppa, resulted in marked hypertension [37], disruption of the murine BNP gene, Nppb, showed no signs of systemic hypertension or ventricular hypertrophy. However, Nppb-/- mice had ventricular fibrotic lesions that were exacerbated in response to pressure overload. Thus, it was suggested that while ANF is a regulator of blood pressure, BNP is a paracrine regulator of cardiac remodeling [38]. Moreover, neural and endocrine factors are directly involved in stimulating ANF secretion and examples include α-adrenergic agonists, β-adrenergic agonists, ET-1, glucocorticoids, prostaglandins, thyroid hormone, NO inhibition and Ang II [33, 39, 40].

At the genetic level, analyses of the ANF and BNP promoters and patterns of expression have led to the characterization of key cardiac regulators and pathways that converge onto these sensitive markers of cardiac stress. Among these cardiac transcription factors are GATA4, TBX5, and NKX2.5, which are fundamental to cardiac development and their mutations were found to be linked to wide array of cardiac defects [31].

1.4. Congenital Heart Diseases:

Congenital heart diseases (CHD) refer to the prenatal abnormalities affecting heart structure or function. These defects represent the most common developmental abnormalities, with an approximate incidence of nearly 1% of all live births, and are estimated as a major cause for prenatal birth losses [5, 41]. Of the CHDs, septal and valvular defects are the most frequent. The defects range in severity from relatively minor, which can later lead to cardiovascular complications like patent foramen oval (PFO), to complex malformations that can be fatal and require corrective surgery to restore heart

function like Tetralogy of Fallot (ToF). However, even the minor, subclinical, or undiagnosed inborn defects can often lead to progressive phenotypes. For example, defects in valve differentiation may progress to valve deterioration requiring valve replacement in young adults; therefore, early interventions are crucial for the avoidance of future CHD complications such as valve replacement, stroke, or heart failure [11]. In addition, congenital heart diseases are frequently accompanied with secondary neurological disorders. Thus it is essential to analyze the intricacies and understand the effects of congenital heart diseases on prenatal and postnatal physiology [5].

Understanding the genotype-phenotype relationship, deciphering the molecular basis of CHD variability, and identifying the contributing genes are key paradigms for understanding the pathophysiology of CHDs [11]. Although sporadic random isolated cases of CHDs are common patients often have a familial history. The identification of several genomic loci linked to CHDs revealed two important patterns: first, a given structural defect is often linked to more than one locus; second, the mutation-linked phenotypes often display variable penetrance and expressivity, pointing to the influence of modifier genes, genetic polymorphisms, and environmental influences on cardiac phenotypes [11, 42]. The penetrance variability is even observed on the level of autosomal dominant diseases such as Holt-Oram Syndrome (HOS), which is caused by mutations in TBX5, where the associated cardiac manifestation among affected family members can vary from asymptomatic conduction system defects to severe structural anomalies [11] .

The combinatorial interaction of transcription factors can explain the linkages of the same malformation to more than one gene, as seen with the case of ASD or VSD and the transcription factors NKX2.5, GATA-4 and TBX5 **(table 1.1)** [11]. Since heart

development is an interplay of different genetic pathways, disturbances in each or all unit(s) of a particular circuit (eg. ligand, receptor, transcription factor, or extracellular matrix proteins) can result in correlated phenotypes. Take the example of the BMP signalling pathway during atrioventricular valve formation, where the conditional deletion of BMP (ligand), ALK2, 3 or 6 (receptors), or SMAD transcriptional factors were shown to result in similar cardiac defects [43].

On the other hand, a buffering model might explain the penetrance variability of CHD [44, 45]. This buffering might be contributed to a functioning second allele, a duplicated gene, a pathway that maintains residual function, and/or from epigenetic and environmental mechanisms. Therefore, if the buffering properties of a network are lost by increased mutation loading on different components, the tolerant window of gene-loss anomaly becomes narrower [46]. Take, for example, GATA4+/- and GATA6+/- double heterozygous mice. Although mice that are heterozygous for either GATA-4 or GATA-6 are viable, the compound heterozygosity of GATA-4 and GATA-6 results in embryonic lethality by ED13.5 due to a spectrum of cardiovascular defects that includes thin-walled myocardia, ventricular and aortopulmonary septal defects, and abnormal smooth muscle development [47]. Therefore, a specific environmental background is required for heterozygous mutation carriers to develop cardiac defects [11].

Thus, the elucidation of the genetic architecture of CHD and the underlying function of key cardiac regulators such as GATA-4, NKX2.5, and TBX5 (Section 1.4), their interacting partners, downstream target genes, upstream signalling pathways, and the characterization of their functions are all essential for the identification of additional regulators and effectors that are potential disease-causing genes. An understanding of gene–

gene as well as gene–environment interactions is indispensible in improving patient care and may help to prevent secondary health risk factors in postnatal and adult life.

With the previous points in mind, our lab has uncovered a novel role for KLF13, a member of the Kruppel-like family of zinc-finger proteins, in the transcriptional network during cardiac development. KLF13- the focus of this study- is conserved across species and *Xenopus* embryos deficient in KLF13 were associated with atrial septal defects and hypotrabeculation similar to those observed in humans or mice hypomorphic to GATA-4 alleles [48]. Analysis of the contribution of KLF13 on the genetic architecture of CHD and its underlying transcriptional networks, including the interplay between transcription factors and epigenetic mechanisms, will definitely provide new insights for the discovery of novel molecular targets for diagnostics and therapeutics.

1.5. Essential cardiac regulators

The production of animal models in which specific genes were inactivated has not only allowed the identification of proteins involved in cardiac development and their associated congenital defects (CHD), but also those involved in postnatal cardiac development and homeostasis (summarized in **table 1.1**). Importantly, the knowledge gained from developmental biology studies can be used more broadly for cardioprotection of the postnatal heart. This section will provide an overview of some of the literature pertaining to the major genes that have been shown to be important prenatal and postnatal cardiac regulators.

Table 1.1: Transcription factors associated with cardiac development.

Transcription Factor	Cardiac Expression	Role	Human Cardiac Phenotype	Ref.
NKX2.5	pan-cardiac	Cardiac specification and patterning, conduction system development	ASD, VSD, conduction	[49-54]
GATA-4	pan-cardiac	Cardiac differentiation, ventral morphogenesis	ASD, VSD	[55]
GATA-5	pan-cardiac	Cardiac differentiation, ventral morphogenesis	ASD, VSD	[56]
FOG2	pan-cardiac	GATA-4 cofactor, modulator	ASD, TOF	[57]
MEF2C	pan-cardiac	Specifies cardiomyocytes	N/A	[58]
FGF10	AHF	Ventricular patterning	N/A	[59]
Isl-1	AHF	AHF development	N/A	[60]
Hand1	LV, AVC, OFT	Cardiac patterning, proliferation	N/A	[61]
Hand2	RV, Endocardium	Cardiac proliferation, RVt identity	N/A	[3, 62]
TBX1	PA	AHF proliferation, OFT development	Conotruncal abnormalities	[63]
TBX2	Primitive myocardium	Inhibits chamber differentiation	N/A	[64]
TBX3	Primitive myocardium, CCS	Inhibits chamber differentiation; Sinoatrial node patterning	N/A	[65]
TBX5	LV, At	Atrial and left ventricle identity	ASD, VSD, conduction defect	[66]
TBX20	pan-cardiac	Repress TBX2, endocardial cushion development	N/A	[21]

Legend: ASD: Atrial Septal Defect; VSD: Ventricular Septal Defect; ToF: Tetralogy of Fallot; N/A: Not Associated with Phenotype; AHF: Anterior/SecondaryHeart Field; N/R: Not Reported; LV: Left Ventricle; AVC: Atrioventricular Canal; OFT: Outflow Tract; RV: Right Ventricle; PA: Pharyngeal Arches; CCS: Central Conduction System; At: Atria.

1.5.1 GATA4

GATA-binding proteins are a subfamily of zinc finger transcription factors with six mammalian members (GATA1-to-6) that interact with the DNA consensus sequence A/G GATA A/T. GATA members are lineage-restricted and are known to be pivotal during cellular growth and development [67]. The cardiac expression pattern of GATA-3, -4 and -6 is differentially regulated throughout development. While GATA-4 is predominantly expressed in all cardiac progenitors and cardiomyocytes at all stages, GATA-5 transcripts are largely restricted to endocardial cells. On the other hand, GATA-6 is mainly found in myocardial as well as vascular smooth muscle cells [11].

By far, GATA-4 is the most comprehensively analyzed member of the family, first identified as a direct regulator of NPPB, the gene encoding BNP [68]. Several characters support GATA-4's candidacy for the position of "master" regulator during earliest stages of cardiogenesis [11]: Firstly, GATA-4 is one of the earliest cardiac developmental markers, detected in the murine precardiac splanchnic mesoderm as early as ED 7.0 [11, 69]. Its transcript is abundantly detected as early as ED 8.0 in both the endocardium and myocardium of the folding heart tube and in cardiomyocytes throughout prenatal and postnatal life [70]; secondly, GATA-4 is a central intricacy of the self-reinforcing feedback loop during cardiogenesis as well as being pivotal to the onset of cardiogenic competency and the expression of several cardiac TFs that control diverse genetic programs imperative for heart progenitor formation. For example, the combined action of GATA-4 with the SMAD proteins, the signalling intermediates of the TGF/BMP signalling pathway, activates the expression of the early cardiac TF, NKX2.5 [71]; thirdly, there are more than 30 cardiac promoters and enhancers that are regulated directly by GATA-4 [11]; and finally, the essentiality of GATA-4 to cardiogenesis is clearly evident by the cardiac defects of GATA-4 null mice and the manifested congenital heart diseases (CHD) in mice and human with GATA-4 haploinsufficiency [11, 72, 73]. The null mice embryos exhibited severe cardiac abnormalities at ED 7.0 and ED 9.5 that were characterized by the absence of a primitive heart tube due to the failure of the FHF to migrate and fuse along the ventral midline [72].

Structurally (**figure 1.2.A**), GATA4 contains two zinc-fingers located at the N- and C-terminals of the C2C2-type that are formed by four cysteine residues [73, 74]. While the C-terminal zinc finger is necessary and sufficient for DNA binding, the N-terminal zinc finger does not independently bind DNA and instead is required for the stabilization and

specification of DNA binding [74, 75]. In addition, GATA-4 contains a nuclear localization sequence (NLS) located within the basic domain flanking the C-terminal zinc finger. In addition, two separate transcriptional activation domains (TAD1 and TAD2) were identified within the N terminal of the protein. The partial conservation of these activation domains between GATA-5 and -6 may partially explain some functional redundancy and the similarities with GATA-4 in transcriptional activation mechanisms [75, 76]. In vitro analysis of GATA4 elucidated interactions with a number of cardiac cofactors including NKX2.5 [77] , TBX5 [15], and the multi zinc-finger protein friend of GATA (FOG2) [78]. Most of these protein-protein interactions are mediated via the C-terminal zinc finger of GATA-4, except for FOG2 and KLF13, which are directed via the N-terminal zinc finger of GATA-4.

1.5.2 NKX2.5

NKX2.5 (Nirenberg and Kim X=Mammalian class 2.5) is a member of the NK2 class of homeodomain transcription factors that are conserved in evolution and bind to the DNA consensus sequence T(C/T) AAGTG [71, 73]. Just like the GATA members, members of NK2 are lineage-restricted and are known to play a vital role during cellular growth and development. Of the NK-2 genes expressed in vertebrates NKX2.3, NKX2.5, NKX2.6, NKX2.7, NKX2.8, and NKX2.10 are referred to as the cardiac group due to their high cardiac expressivity [71].

NKX2.5 is the most extensively studied member of the NK-2 genes; it was isolated in a screen for mammalian homologues of tinman, a homeobox gene, which is required for the development of the dorsal vessel which is the insect equivalent of the vertebrate heart [11, 71]. Nkx2.5 is expressed quite early during development, at ED 7.5 in mice, and it continues to be expressed at a high level in the heart throughout adulthood [52].

While mutation of the *drosophila's* tinman showed a complete absence of dorsal vessel formation [11, 71], a targeted disruption of the murine homolog resulted in embryonic lethality at ED 9–10. Although the NKX2.5 null mice maintained the ability to form a heart tube, the tube failed to progress to the looping stage [52]. The discrepancy in the phenotype severity in mice may reflect a buffering effect from other NK factors that remain to be identified [11]. Humans carrying mutations in the NKX2.5 homolog (**Figure 1.2.B**), most of which occur within the homeodomain, suffer septal defects, conduction abnormalities, and thinning of the ventricular myocardium and hypotrabeculation [11, 71]. Despite the homogeneous expression of NKX2.5 throughout the heart, mutant analyses propose the requirement of Nkx2.5 for the initiation of ventricular/septal gene expression programs that are key for proper chamber specification [11]. The discrepancy between NKX2.5's homogenous expression in the heart versus its role in heart regionalization is likely to be a function of the combinatorial interaction with other cardiac regulators, such as GATA-4 and TBX5 [11, 77, 79]. Species conservation of NKX2.5 suggests a conserved regulatory mechanism during cardiogenesis [80]. At the molecular level, the expression of a number of cardiac-specific genes are down-regulated in NKX2.5 mutant mice, including the atrial neutratic protein (ANF) and the basic helix-loop-helix TF (eHand).

Structurally (**Figure 1.2.B**) similar to the other members of the NK2 family, NKX2.5 is comprised of four conserved motifs. The motifs, starting from the amino terminus of the protein, are the TN domain, the homeodomain, the NK-2 domain, and the sequence GIRAW. The homeodomain is the DNA-binding domain of the protein and it holds three helices (I/II/III); of the three helices, helix III is responsible for DNA binding specificity. The three helices form a hydrophobic core with a tyrosine (Y) at position 54 that is characteristic of the NKX2 family members [71]. The homeodomain was also shown

to mediate the protein-protein interaction with the cardiac transcription factors GATA-4, TBX5 and SRF [77, 81, 82]. The functions of the TN-Domain and NK-2 domain remain a work in progress. The TN domain, also found in some basic helix-loop-helix (bHLH) factors such as Olig2, is a decapeptide domain that was shown to mediate the interaction of NKX2.5 with the Groucho family of co-repressors. Groucho family are implicated in the formation of a repressed chromatin state in several genetic loci in order to control major developmental decisions ranging from dorsal–ventral patterning to eye development [83, 84]. Interestingly, point mutations of the TN domain were shown to modify the interaction of NKX2.5 and p300 [85]. The NK-2 domain, on the other hand, is unique to the NK-2 class and lies just beyond the C-terminus of the homeodomain [71]. The NK-2 domain is thought to mediate interactions with other proteins and contains a proline-rich region, a hydrophobic core, and a group of flanking basic amino acids [71, 80]. Lastly, the function of the amino acid sequence "GIRAW" is still to be determined [71]. Interestingly, it appears that the c-terminal of NKX2.5, holding the NK2 domain and the GIRAW sequence, contains an autorepression domain since its deletion leads to super-activation of the ANF promoter.

Mechanistically, at least part of the regulatory mechanism assumed by the NK-2 proteins is due to the choice of the heterodimer binding partner. For example, ANF transcription is stimulated by the NKX2.5-GATA4 dimer and inhibited by the NKX2.5-TBX2 dimer [71].

1.5.3 TBX5

TBX5 is a member of the phylogenetically conserved Brachyury (T) gene family that shares a highly conserved 180-amino acid DNA-binding domain termed the T-box [86]. The family plays diverse roles in metazoan embryogenesis and germ cell differentiation [87]. Seven members of the TBX family (TBX1-5, TBX18 and TBX20) are expressed in

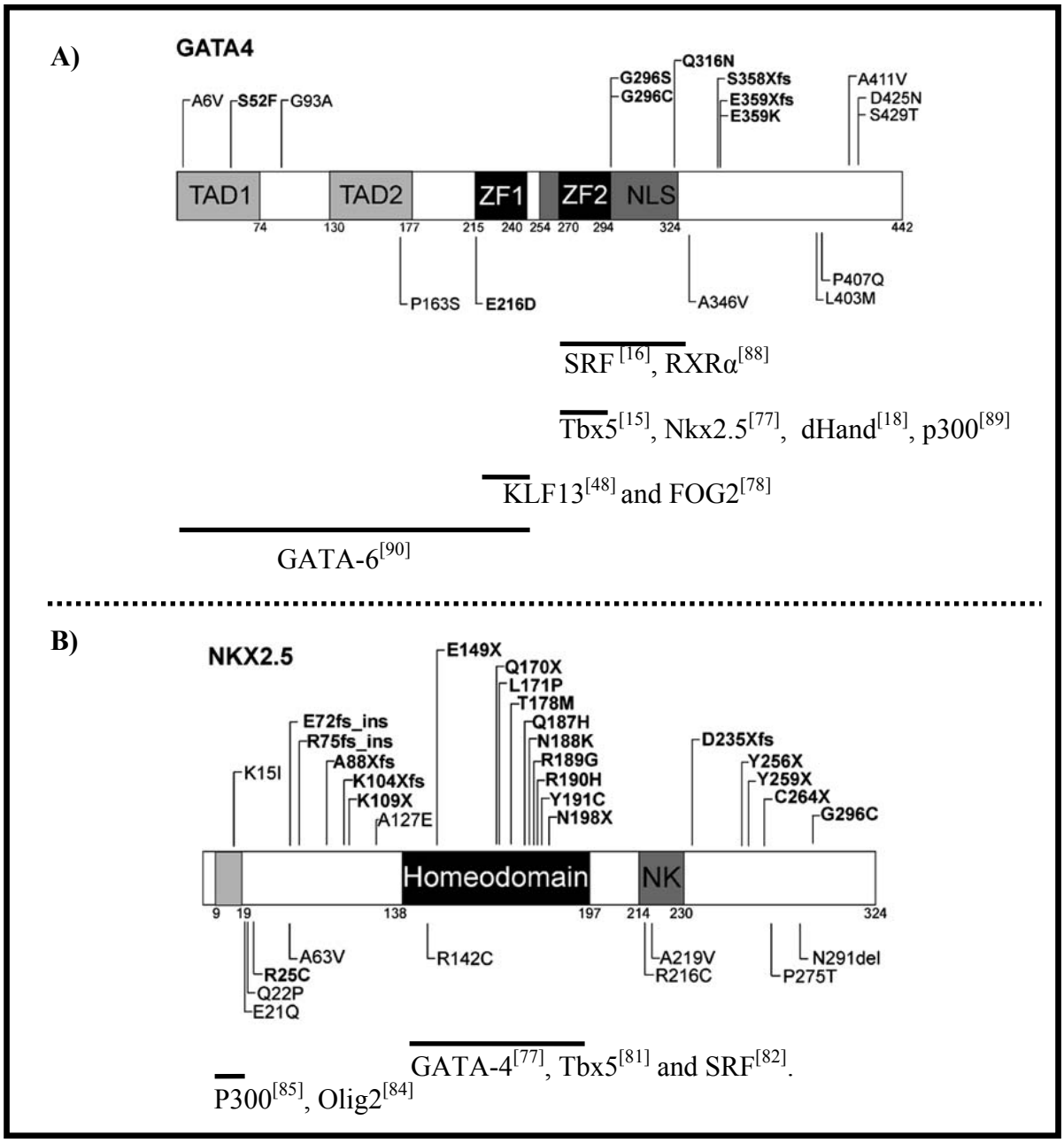

Figure 1.2: Schematic representation of A) GATA4 and B) NKX2.5 protein structure.
The exonic germline mutations related to nonsyndromic CHD are also indicated. All mutations related to ASDII are represented on the top. Mutations found in patients with CHD other than ASDII are shown below the structural domains. All mutations which were evaluated by family and/or functional studies are represented in bold letters. Mutations which were found in patients with dilated cardiomyopathy are marked with an asterisk. Somatic and intronic mutations are not included. The lines represent the regions required for the interaction with the protein identified under the line. The figure is modified from [41].

the embryonic heart in vertebrate models in overlapping expression patterns [86]. Knock-out of any of these seven genes is embryonically/prenatally lethal due to the wide range of cardiac defects. Yet, it is only TBX5 heterozygosity that is associated with embryonic lethality [86].

TBX5 is the most extensively studied member of the T-box genes. The importance of Tbx5 is due in part to the fact that it is the gene mutated in human Holt-Oram Syndrome (HOS), a dominant disorder characterised primarily by upper fore-limb defects and heart abnormalities [91]. The latter abnormalities include atrial and ventricular septal defects, Tetralogy of Fallot, hypoplastic left heart, and conduction anomalies [86]. Tbx5 is expressed at the earliest stages of cardiogenesis, throughout the heart primordia, and is co-localized with other cardiac transcription factors such as NKX2.5 and GATA-4 [92]. As the heart differentiates, TBX5 expression is graded along the heart tube as a result of the retinoic acid signalling gradient, with a peak in the posterior sinuatrial segments of the heart.

Mechanistically, TBX5 associates directly, and synergistically, with other conserved cardiac transcription factors, including NKX2.5 and GATA-4 to activate the expression of chamber-specific genes such as ANF and Gja5 (which encodes connexin 40) in vitro [74]. Therefore, it appears that TBX5 plays an instructive role in lineage specification and morphogenesis of future chambers [74, 77].

Structurally (**figure 1.3**), the coding region of TBX5 contains eight exons that give rise to a protein with a short N-terminus of approximately 56 amino acids, followed by a 180-amino acid DNA binding domain, and a 282-amino acid C-terminal half [81]. Structure-function analysis of TBX5 is still a work in progress. Most works were conducted on the T-box domain which mediates DNA-binding, to consensus sequence (A/G)GGTGT

(C/G/T)(A/G), and protein-protein interactions [82]. To date, over 37 mutations in the TBX5 gene have been associated with Holt-Oram syndrome; the majority introduce a premature stop codon within the T-box domain. Hence, these mutations reduce its DNA-binding to target genes, leading to decreased transcriptional activation by TBX5 and a reduction in the synergistic transcriptional activation with NKX2.5, GATA-4, and the MAD box cardiac transcription factor MEF2C [83-85]. The N-terminal domain of TBX5 is also shown to be necessary for the interaction with MEF2C and NKX2.5 [86, 87]. Thus, it is possible that in addition to the loss of DNA-binding, premature truncation of TBX5 in the N-terminus may lead to HOS through the loss of TBX5 interaction with GATA4, NKX2.5 and Myocyte Enhancer Factor 2 (MEF2C) [81]. On the other hand, the C-terminus of TBX5 possess a transactivating domain (TAD), amino acids 339–379; however the mechanism underlying the transactivation by the C-terminus of TBX5 is largely unknown [81, 88]. Another structural features of TBX5 are two functional NLS motifs , one in the DNA-binding domain and the other in the C-terminus of the protein, and one NES motif in the DNA-binding domain[86]. Nuclear import and export sequences are also important regulators of the subcellular localization of proteins. It is interesting to note that even increased TBX5 dosage, chromosome 12q2 duplications, has been reported to cause HOS[90]. Interestingly, the protein LMP4, a member of the PDZ-LIM protein, has been identified to interact with the C-terminal transactivation domains of both TBX5 and TBX4 to induce their re-localization from the nucleus to the cytoplasm. As LMP4 negatively regulates the nuclear availability of TBX5, it works as a controller of the transcriptional activity of the TBX5 protein [86]. Recent work, has revealed that the family of LMP4, PDZ-LIM protein family, is crucial for the assembly of protein complexes with the cytoskeleton and can act as signal modulators regulating cell lineage specification and organ

development [89]. These observations suggest that hitting a balanced level of TBX5 protein in the cell, nucleus in particular, is critical for its function [86].

Mechanistically, the deleterious effect of TBX5 mutations on the interaction with GATA4 and NKX2.5 support the existence of a tri-complex composed of the three TFs to regulate the expression of a subset of genes required for cardiac septal formation. Analysis of TBX5 point mutations is considered as the "Rosetta stone" in deciphering how disruption of the combinatorial interactions of transcription factors can lead to specific birth defects [15]. In addition, the novel transcriptional co-activator TAZ (transcriptional co-activator with PDZ-binding motive), was recognized as a key TBX5 co-activator. The co-activational properties of TAZ were found to be mediated via interactions with histone acetyltransferases p300 and PCAF. Interestingly, truncated HOS mutants of TBX5 were unable to associate with and be stimulated by TAZ [91].

1.5.4 PEX1

Recently we reported the isolation and the identification of a novel cardiac transcription factor that we named PEX1 (Phenylephrine-induced Complex-1) which is implicated in α1-adrenergic (phenylephrine and endothelin-1) signalling in the heart. PEX1, a 13-zinc-finger-containing protein, is grouped with the Krüppel family of zinc-fingers that binds to an evolutionarily-conserved phenylephrine response element (PERE) on the proximal ANF promoter. The protein is expressed in a tissue-restricted manner in the heart, skeletal muscle, and adrenal gland. In the heart the protein is developmentally regulated, resembling the expression profile of ANF, with a robust expression in the embryonic heart and is usually down-regulated postnatally.

The protein was initially isolated in a screen for regulatory proteins binding to an evolutionarily-conserved phenylephrine response element, termed PERE. PERE is essential for the α1- adrenergic receptor agonist's (phenylephrine) stimulation of the ANF promoter [93, 94]. It is well established that α1-adrenergic receptors mediate several biological effects of catecholamines including the regulation of myocyte growth and contractility and the transcriptional regulation of several cardiac genes including ANF. Not only was it found that PEX1 transcripts are induced by the α1-adrenergic agonist phenylephrine [94], but also its transcriptional activity is potentiated in a PKC-dependant manner, by endothelin-1 (ET-1), another α1-adrenergic receptors agonist [95]. Physiologically, PEX1 transcripts were shown to be elevated in genetic models of hypertension and cardiac hypertrophy; this finding was further confirmed when conditional upregulation of PEX1 expression was sufficient to induce the morphologic and genetic changes characteristic of cardiac hypertrophy [94, 95]. On the other hand, knocking down PEX1 using an antisense strategy in cardiomyocytes eliminated the endogenous ANF gene response to α1-AR stimulation [94]. Thus, understanding the PEX1 mechanism of action as a transcriptional regulator and as a nuclear effector of α1-Adrenergic receptor activation is critical in deciphering the poorly understood signalling cascade linking the α1-adrenergic receptor activation to its accompanied genetic changes.

Structurally (**figure 1.4**), the 407-amino-acid translated PEX1 protein is characterized by the presence of thirteen zinc fingers of the C2H2 type with H/C links which groups the protein under the Kruppel family of ZF proteins. There are no published reports of a structure-function analysis of PEX1. *In silico* sequence analysis gave no hits on any conventional transactivation domain in the coding region [94], yet the protein contains several putative phosphorylation sites for PKC, PKA, and casein kinase II [94].

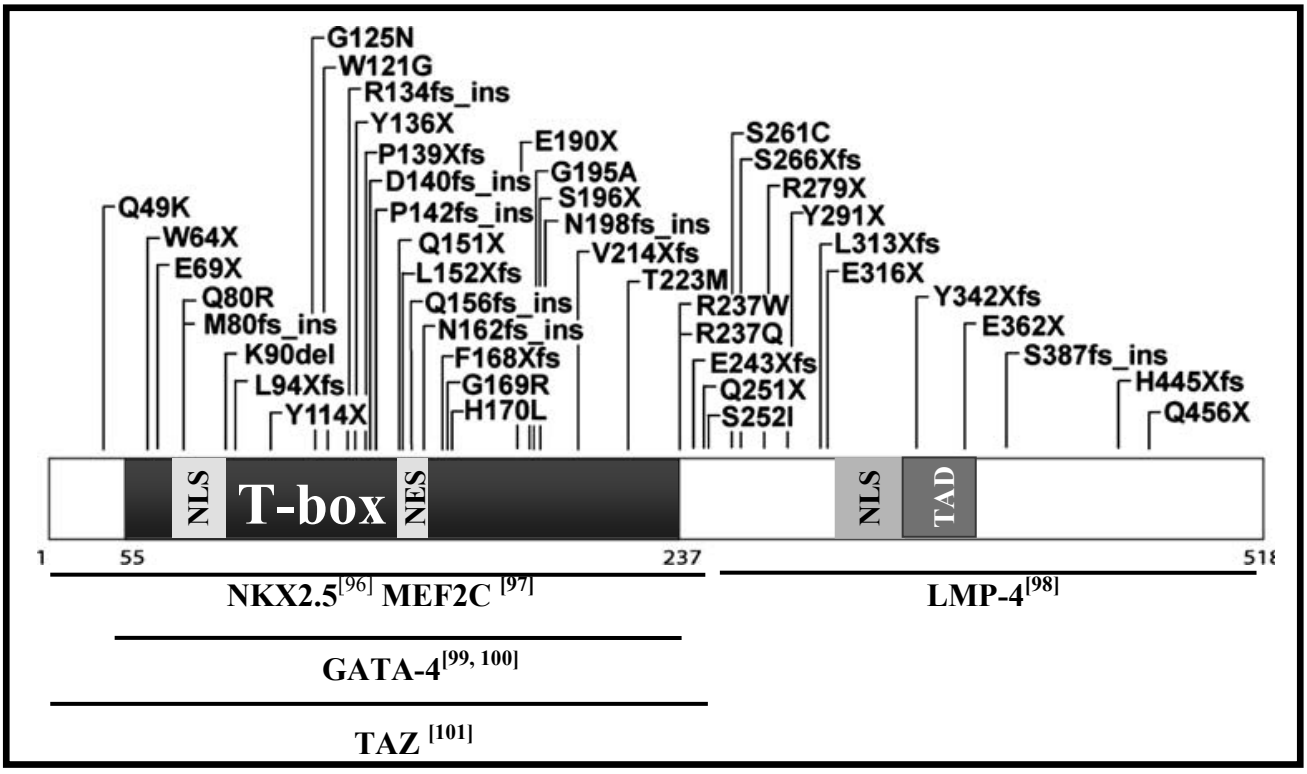

Figure 1.3: Schematic representation of Tbx5 protein structure. The exonic germline mutations related to HOS are also indicated. The majority of mutations are located in the DNA-binding T-box domain of TBX5. Intronic and somatic mutations are not included. The lines represent the regions required for the interaction with the protein identified under the line. NLS: Nuclear localization signal, NES: Nuclear export signal, TAD: Transactivation domain. The mutations are located according to reference [41].

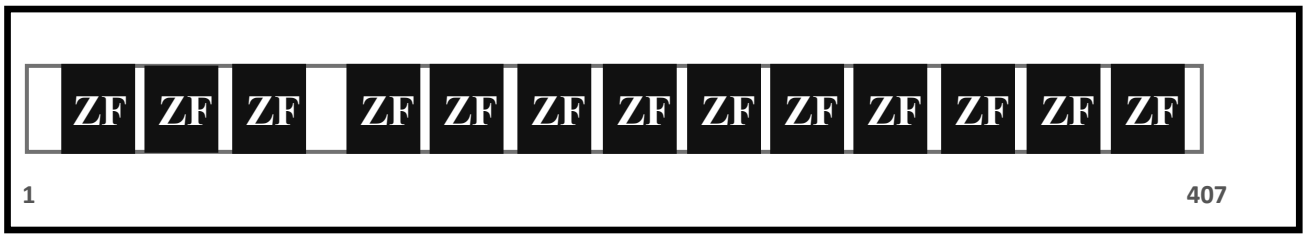

Figure 1.4: Schematic representation of PEX1 protein structure.

Mechanistically, PEX1 is one of a handful of transcription factors, including GATA4, which appear to be required for nuclear signalling of α1-adrenergic receptors. Not only does PEX1 physically and functionally interact with GATA4 to cooperatively activate the transcription of ANF and other hypertrophy induced genes, but ET-1 enhances PEX1 transcriptional activity via a PKC dependent pathway which phosphorylates the protein and further potentiates its synergy with GATA4. Thus, it appears that the PEX1/GATA-4 interaction is critical for transducing the nuclear and cytoskeletal effects of α1-adrenergic agonists [94, 95].

1.5.5 CATF1

The cardiac response element transcription factor 1(CATF1) is a member of the DEXDc DEAD-like superfamily of DNA/RNA helicases. CATF1 has been implicated in broad cellular processes including DNA replication, pre-mRNA splicing, and transcription [102, 103]. In E15 mice, CATF1 is broadly expressed with the highest levels in brain, spinal cord, and muscle, and its lowest levels are in the lung, heart and liver [104]. In postnatal and adult rats, CATF1 is highly expressed in a tissue-specific fashion, the highest being in the heart [105].

CATF1 was first isolated in mice by virtue of its binding to a GGGG stretch sequence motif of the immunoglobulin Sμ region and thus it is also known as immunoglobulin mu binding protein 2 (IGHMBP2) [106]. Simultaneously, in our lab the protein was isolated in a rat cardiomyocyte cDNA library searching for the protein(s) interacting with the hypersensitive cis-acting myocyte-specific cardiac response element (CARE), located in the proximal region of the ANF promoter, and thus named CATF1 [105, 107].

Later, several mutations in CATF1 were linked to distal spinal muscular atrophy type 1 (DSMA1), formerly known as spinal muscular atrophy with respiratory distress type 1 (SMARD1) [108]. This autosomal recessive disorder manifests in early childhood as a severe degeneration of spinal cord α-motorneurons and axonal loss leading to muscular atrophy. One of the earliest and most severe clinical symptoms is respiratory distress due to diaphragmatic paralysis and muscle weakness that is more prominent in the distal limbs and typically leads to early infant death [108, 109]. Moreover, neuromuscular degeneration (NMD) in mice and distal spinal muscular atrophy type 1 (DSMA1) in humans were also accompanied by dilated cardiomyopathy (DCM) [108]. DCM is a disease of the myocardium defined by ventricular chamber enlargement and systolic dysfunction that ultimately manifests itself in progressive heart failure, arrhythmias, thromboembolism, and premature death [110]. Interestingly, NMD mice with conditional rescuing of CATF1 in cardiac muscle had a normal cardiac phenotype and an extended lifespan in comparison to their NMD counterparts [108].

The 15 exons of the CATF1 gene encode a 989-amino acid protein containing a putative DNA helicase region, nucleic acids binding R3H motifs, as well as a zinc-finger AN1-like domain. Encompassed by the putative DNA helicase region are DEAD/DEAH box helicases and AAA ATPase domains. *In vitro* analysis found that CATF1 directionally (5' --> 3') unwinds RNA and DNA double helices [109]. Interestingly most of the mutations associated with the DSMA1 disease were located in the DNA helicase domain of the gene, impairing the ATPase and helicase activity and suggesting a particular role for this domain in the disease-causing mechanism (**figure 1.5**). CATF1 is preferentially localized in the cytoplasm of neuronal and non-neuronal cells and is physically associated with ribosomes, tRNAs, and in particular with tRNATyr. Moreover, the transcription factor IIIC-

220 kDa (TFIIIC220), an essential factor required for tRNA transcription, and the helicases Reptin and Pontin, which function in transcription and in ribosome biogenesis, were also found to be part of cytoplasmic CATF1-containing complexes [109]. It is speculated that the phenotypes associated with DSMA1 patients are due to the requirement of CATF1 by particular neuron to efficiently translates certain mRNAs (e.g. RNAs with excessive secondary and/or tertiary structures). Therefore, dilated cardiomyopathy (DCM) in DSMA1 might be due to less efficient translation of myocyte-specific mRNAs. Thus, discovery of tissue specific mRNAs whose expression depends on CATF1 may give further insight into the cell-type specific features of the disease [102]. Thus, further detailed functional and structural analysis of this protein is required to address this issue [102].

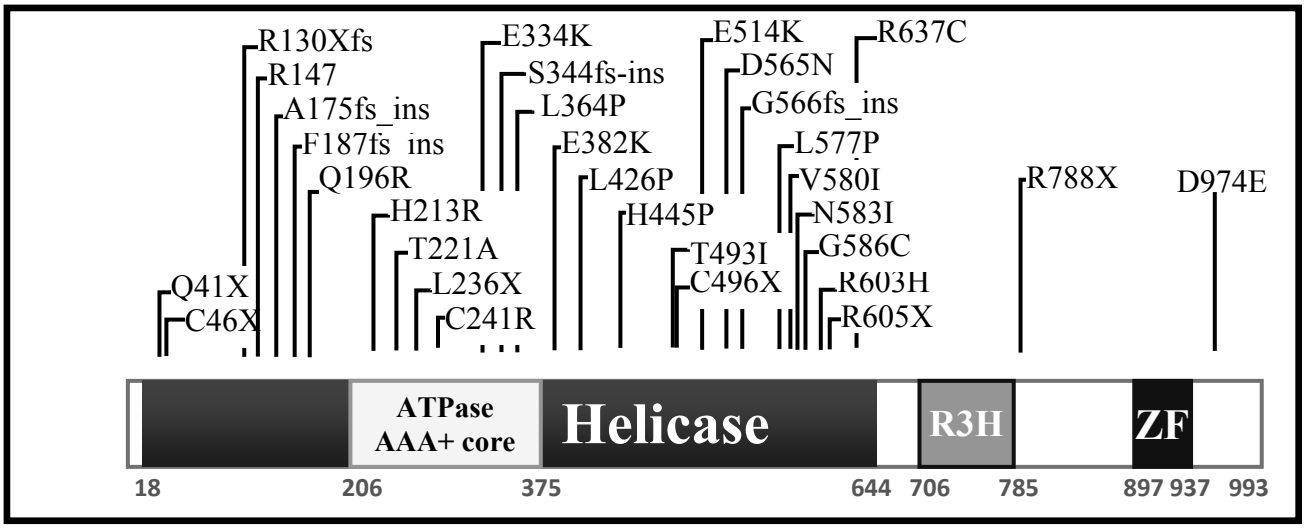

Figure 1.5: Schematic representation of CATF1 protein structure. The protein contains the helicase superfamily 1 domain, a nucleic acid binding domain of the R3H type, as well as an AN1-type zinc finger motif. The positions of each IGHMBP2 domain are numbered according to Interpro database (http://www.ebi.ac.uk/interpro). The exonic germline mutations related to DSMA1 are also indicated. The mutations are identified and localized from data in [102] and [111]. The majority of mutations are located in the ATPase and helicase domains and they were shown to severely impair the activity of the two domains.

1.6 The Kruppel-like transcription factor KLF13

1.6.1 Introducing the family

Transcription factors are categorized based upon their DNA binding structural domains including the helix-loop-helix, homeodomain, leucine zipper, and zinc finger protein (ZFP) families [112]. The Kruppel-like transcription factor KLF13 is a member of the ZFPs kruppel-like factors (KLFs), so named for their homology to the *Drosophila* segmentation gene product Kruppel [113]. KLFs are categorized along with the specificity protein (Sp) family of transcription factors under the Sp/KLF family of which there are currently 26 members. There are 17 distinct members of the KLF family, a few of which (e.g. KLF6, KLF10, and KLF8) exhibit splice variants [112, 114]. According to the rules of the new nomenclature, these proteins are numbered as KLFX factors, where X corresponds to the approximate order in which the genes were described (KLF1-KLF16). The family is found to be conserved across species with variability in numbers probably due to multiple gene-duplication events throughout evolution (**figure 1.6** depicts a phylogentic tree for the Sp/KLF family**)** [115].

These proteins are characterized by C-termini Cys2/His2 zinc-finger motifs that confer preferential binding to GC/GT rich sequences in gene promoters and enhancer regions in order to mediate activation and/or repression of transcription [112, 114]. Although initially regarded to simply function as silencers of Sp1 transactivity, the KLF family are now implicated in a broad range of cellular processes including proliferation, apoptosis, differentiation, and development [113, 114]. Most of the Sp/KLF members display a dispersed expression pattern, but some show a tissue restricted expression (**table 1.2** highlights their expression pattern and cellular function). Despite the volumes of studies

describing the role of KLFs in human health and disease over the past decade, their role in the heart is just beginning to be elucidated. Currently, there are only five published reports describing the function of KLFs in the heart—KLF13 (embryonic) in cardiomyocytes [48], KLF5 in cardiac fibroblasts [116], KLF15 (postnatal) [117], KLF4 (postnatal) [118] and a brief report describing a cardiac phenotype in systemic KLF10-null mice [119]. **Table 1.3** highlights some of these published findings pertaining to KLFs in the heart and the two other muscle types. Among the five reports, only KLF13 was implicated with embryonic cardiac malformations upon disruption, thus making it a candidate for the regulation of cardiac development.

The existence of multiple KLF proteins with preferential binding to similar GC/GT rich sequences grants the nucleus numerous modes to precisely manipulate gene expression under various physiological conditions by utilizing the diverse biochemical mechanisms attributed to these proteins. It is the N-terminus region that bestows the functional identity to each member of this family. The heterogeneity of the N-terminal domain may explain in part the diverse biochemical mechanisms by which KLFs regulate transcription, and as a consequence, explain their influence on cellular processes [112, 120]. It is not radical to assume that these proteins have structurally evolved in a way that provides a strategic opportunity for interaction with distinct cofactors. Thus, the differential interactions with a distinct repertoire of cofactors not only allow the distinct Sp/KLF members to regulate a distinct subset of genes, but also to participate in the divergent regulation of the same gene [120]. For example, it was recently reported that while Sp1 can activate the ANF promoter in cardiomyocytes, Sp3 has opposing negative effects on ANF expression [101]. In addition, while KLF15 can inhibit GATA4 DNA-binding and

transcriptional activity, KLF13 was shown to transactivate multiple cardiac promoters synergistically with GATA4 [52, 97]. On the physiological front, **table 1.2** and **table 1.3** show how multiple KLFs can be involved in the regulation of the same cellular processes and that different KLFs may exert opposing effects. For example, while KLF5 overexpression promotes smooth muscles cell (SMC) proliferation, KLF15 overexpression prevents SMC proliferation. Furthermore, while KLF5 (-/+) mice have reduced neointimal growth and perivascular fibrosis in response to vascular injury, KLF15 (-/-) mice exhibit an exaggerated neointimal response to vascular injury [121]. Recent reports have also pointed to KLFs' regulatory effect on the expression of other family members. For example, expression of KLF3 is regulated by KLF1 in erythroid cells [113].

Unlike other gene clusters' encoded developmental regulators (e.g Hox transcription factors) the loci of Sp/KLF proteins are arbitrarily scattered throughout the genome and are thought to function independently except for the locus containing KLF2 and KLF3 genes. The genes structure of Sp/KLF family is to be determined [115].

An unexplored additional layer of functional regulation of the Sp/KLF family members in both health and disease is the existence of alternative splicing isoforms [93, 95]. For example, while the wild-type KLF6 acts as a classic tumor suppressor, the splice isoform KLF6 SV1, which lacks a nuclear localization signal, displays a markedly opposite effect on cell proliferation, colony formation, and invasion [122].

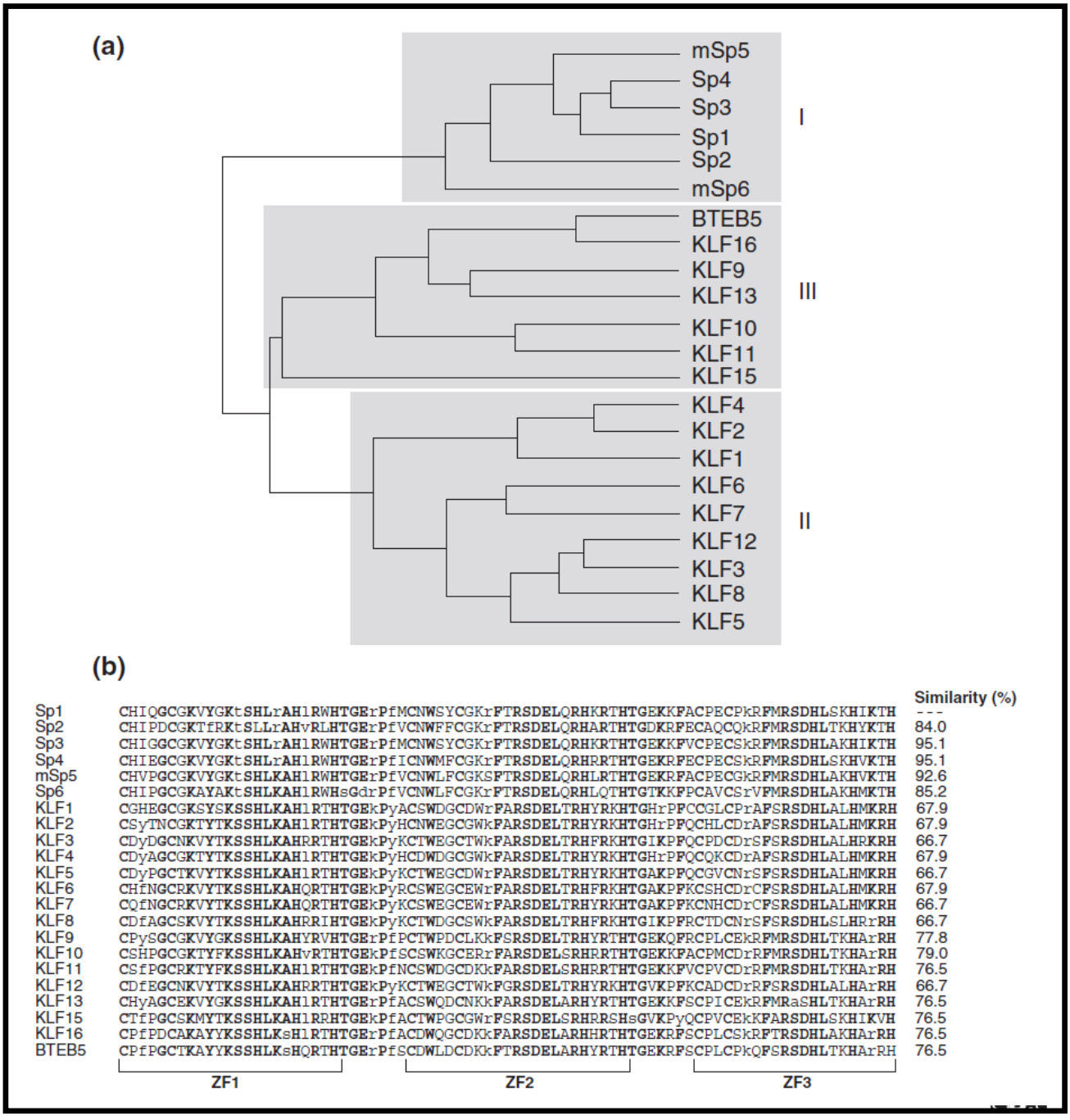

Figure 1.6: Mammalian members of the Sp1-like/KLF family. (a) A phylogenetic tree of human Sp1-like/KLF proteins and mouse Sp5 and Sp6 (mSp5 and mSp6) identified three general subgroups. The tree was generated using Genetic Computer Group (GCG) sequence analysis software. (b) Sequence alignment of the zinc-finger domains of Sp/KLF protein family members in comparison to zinc-finger motifs of human Sp1. Identical residues are in black, similar residues in gray and different residues in lower case. The percentage similarity between the Sp1 and the other Sp1-like/KLF zinc-finger domains is indicated on the right. The figure is modified from **[115]**

Table 1.2: The functional features of Sp1-like/KLF family.

Protein*	KLF #	Expression pattern	Interacting co-activator / co-repressor	Cellular function
Sp1	-	Ubiquitous	CRSP, p300/CBP, TAFII130	Embryogenesis
Sp2	-		Unknown	Unknown
Sp3	-	Ubiquitous	Unknown	Unknown
Sp4	-	Brain-enriched	Unknown	Post-natal survival and male fertility
mSp5	-	Ubiquitous	Unknown	Unknown
Sp6	**KLF14**	Ubiquitous	Unknown	Unknown
EKLF	**KLF1**	Erythroid and mast cells	p300/CBP, PCAF, SWI/SNF and mSin3A	Erythropoiesis
LKLF	**KLF2**	Lung, blood vessels, lymphocytes	Unknown	Blood vessel, lungdevelopment, T-cell survival
BKLF	**KLF3**	Erythroid tissue-and brain-enriched	CtBP2	Unknown
GKLF	**KLF4**	Gut-enriched	p300/CBP	Anti-proliferation, survival
IKLF	**KLF5**	Gut and epithelial tissues	Unknown	Cell growth
CPBP	**KLF6**	Ubiquitous	Unknown	Putative tumor suppressor
UKLF	**KLF7**	Ubiquitous	Unknown	Cell-cycle arrest
BKLF3	**KLF8**	Ubiquitous	CtBP2	Unknown
BTEB1	**KLF9**	Ubiquitous	mSin3A	Neurite outgrowth and carcinogen metabolism
TIEG1	**KLF10**	Ubiquitous	mSin3A	Apoptosis, anti-proliferation
TIEG2/ FKLF	**KLF11**	Ubiquitous	mSin3A	Anti-proliferation
AP-2rep	**KLF12**	Brain, kidney, liver and lung	CtBP1	Unknown
BTEB3/ RFLAT-1 / FKLF-2	**KLF13**	Ubiquitous	mSin3A, p300/CBP and PCAF	Anti-proliferation and carcinogen metabolism
KKLF	**KLF15**	Unknown	Unknown	Unknown
BTEB4 / mDRRF	**KLF16**	Ubiquitous	mSin3A	Carcinogen metabolism

The table is modified from [115].

Table 3: The Kruppel-like Factors in muscle biology

	Function / observation	Ref.
	Heart	
KLF13	• Expressed in developing cardiomyocytes with substantial reduction postnatally • Can bind and activate the BNP promoter • Transactivates multiple cardiac promoters synergistically with GATA4 • Interacts with the N-terminal zinc finger domain of GATA4 • KLF13 knockdown in Xenopus embryos causes cardiac developmental defects (atrial septal defects and ventricular hypotrabeculation) that can be rescued by GATA4	[48]
KLF5	• Expressed in cardiac fibroblasts and induced by angiotensin II • Regulates expression of PDGF-A and TGF-β • KLF5(+/−) mice have reduced hypertrophic remodeling in response to angiotensin II infusion • Interacts with retinoic acid receptor alpha whose activation modulates KLF5 function	[116]
KLF15	• Expressed in cardiomyocytes and cardiac fibroblasts • Not expressed in heart developmentally, but upregulated postnatally • Downregulated with hypertrophic stimulation • Functions as a transcriptional inhibitor of hypertrophy • Can inhibit GATA4 and MEF2 DNA-binding and transcriptional activity • KLF15(−/−) mice develop severe eccentric hypertrophy and LV dysfunction with pressure overload	[117]
KLF10	• Cell-specific and temporal expression within the heart not reported • KLF10(−/−) mice (males only) develop spontaneous pathologic hypertrophy by 16 months age • Regulates expression of Pituitary Tumor Transforming Gene (Pttg1), although significance of this finding is not known	[119]
KLF4	• KLF4 was expressed in the heart from late embryonic development through adulthood. • KLF4 (−/−) mice were born at the expected Mendelian ratio but they gradually died after birth. Mice survived beyond postnatal day 28 exhibited marked growth retardation and significant decrease in cardiac output. • KLF4 (−/−) mice had a reduction in expression of multiple cardiac genes, including Gata4	[118]
	Smooth muscle	
KLF13	• Activates the minimal promoter for the SMC differentiation marker SM22α	[123]
KLF5	• Expressed in fetal SMC but downregulated postnatally • Robust re-induction with vascular injury or angiotensin II stimulation that may involve signaling through survivin and MAP-kinase pathways • KLF5 induces PDGF-A/B, PAI-1, iNOS, and VEGF-R and promotes SMC proliferation • KLF5(+/−) mice have reduced neointimal growth and perivascular fibrosis in response to vascular injury and angiotensin II infusion • KLF5 activity is regulated by RARα as well as by interactions with p300, HDAC1 and the SET oncoprotein	[124]
KLF15	• Robust expression in SMC at baseline with significant downregulation after vascular injury • KLF15 overexpression prevents SMC proliferation • KLF15(−/−) exhibit an exaggerated neointimal response to vascular injury	[125]
KLF4	• SMC expression is low under basal conditions but rapidly induced following vascular injury • PGDF-bb mediated repressive effects on SMC gene expression/differentiation are, in part, KLF4 dependent and may involve inhibition of myocardin • KLF4 can inhibit the TGFβ1-mediated induction of SMC differentiation markers α-SMC actin and SM22α	[126]
	Skeletal muscle	
KLf13	• Expressed in skeletal muscle but role not known	[127]
KLF15	• Regulates expression of glucose transporter GLUT4. • Interacts with MEF2A • Regulates fasting-induced transcriptional activation of mitochondrial acetyl-CoA sythetase-2	[128]
KLF6	• Expressed in skeletal muscle but role not known	[129]

The table is modified from[121].

1.6.2. KLF13 in embryogenesis: emphasis on cardiogenesis

KLF13 (also known as RFLAT1/FKLF-2/BTEB3) was first identified as the transcriptional regulator of the chemokine RANTES in T lymphocytes three to five days after T lymphocyte activation [130]. Later reports illustrated its role as a transcriptional regulator of the human γ globin promoter, other erythroid-specific genes, ANF, BNP, other cardiac genes, SV40, and SM22α promoters [48, 127, 131]. KLF13 expression was detected as early as ED 8.0 in mice with a succeeding robust expression in the heart, cephalic mesenchyme, thymus, dermis, skeletal muscles, and epithelial layers of the gut and urinary bladder [121, 132]. The earliest cardiac expression of KLF13 was at ED 9.5 with subsequent expressions in the developing atrial myocardium, ventricular trabeculae, AV cushions, and truncus arteriosus. Postnatally, KLF13 is substantially downregulated with expression predominantly restricted to the valves and the interventricular septum [121]. The first study regarding the role of KLF13 during embryogenesis was one describing a knockout mice phenotype and the protein's implication on controlling erythropoiesis. Although the Klf13−/− mice were viable, they exhibited a reduced Mendelian inheritance ratio (<25) and were characterized with reduced numbers of circulating erythrocytes and a larger spleen and thymus [133].

On the cardiac front, our lab had the initiative in describing the role of KLF13 in the embryonic myocardium by deciphering its contribution to BNP gene regulation and Xenopus cardiogenesis. Examination of the BNP promoter identified an evolutionarily-conserved KLF consensus CACCC box essential for promoter activity and flanked by nearby GATA sites. This sequence was found to have a greater transcriptional contribution in atria compared to ventricles. Using *in-silico* analysis complemented by *in-vitro* assays, we identified KLF13 as the most likely member of the KLF family regulating BNP promoter

activity via the identified CACCC box. Emphasizing its possible role as a cardiac gene regulator, KLF13 was capable of activating multiple cardiac promoters (BNP, ANF, β-MHC, α-cardiac actin) in a synergistic fashion with GATA4 through the N-terminal zinc finger domain of GATA-4 [48, 121, 134]. To determine the role of KLF13 in the early stages of cardiogenesis, a functional knockdown of the protein was created in Xenopus embryos using antisense morpholinos. The knockdown embryos exhibited a cardiac phenotype with ventricular hypotrabeculation, atrial septal defects, and delayed atrioventricular cushion formation and maturation of valves. The first evident sign of cardiac malformation occurred after heart tube formation, beating at a slower pace and showing signs of pericardial edema. These results suggested a critical role of KLF13 in cardiac cell fate specification and morphogenesis. No change in the expressions of NKX2.5 and GATA6, early cardiac markers, at the neurula stage 15 was detected in the knockdown mice revealing that KLF13 is not essential for initial specification of cardiac cell fates. However, at stage 20 both genes exhibited a decreased expression. At stage 30, prior to the formation of the cardiac tube, several cardiac specific transcription factors, including GATA-4, GATA‑5 and TBX5, were severely reduced in expression. At later developmental stages, other late cardiac differentiation markers such as ANF and αMLC, were shown to be delayed. Negative TUNEL assays for apoptotic nuclei eliminated the probability of an attribution of cardiomyocytes lost to these anomalies. This left us with the hypothesis that KLF13 might be involved in cardiac cell proliferation. On that note, we found that KLF13 is a potent transactivator of the cyclin D1 promoter, which not surprisingly contains several KLF binding sites.

In addition to the phenotypes exhibited in the aforementioned animal model, 18% of human patients with heterozygous microdeletions of the chromosomal band 15q13.3,

harbouring at least seven genes including KLF13, were associated with cardiac defects [135]. Thus, it is likely that KLF13 is an important intricacy in the mechanism patterning the embryonic heart.

1.6.2 KLF13: A portrait of the family's structural features

To understand the function ascribed to a transcription factor, a dissection of its basic structural features and properties should be pursued. A minimum of three domains are required to comprise a site-specific transcription factor: a DNA-binding domain, a nuclear localization signal (can be dispensable), and a transcriptional regulatory domain [120]. This section will describe the structure–function aspects of KLFs with a primary focus on KLF13 features (**figure 1.7 represents the structural features of KLF13**).

The distinguishing feature of the KLF family is the presence of a DNA-binding domain composed of three contiguous and highly conserved classical Cys2/His2 zinc-fingers at the carboxyl terminus. These zinc-fingers enable the KLF family to bind to related GC/GT rich sites on the major groove of DNA [112, 113]. The architecture and sequences of the three zinc-fingers are well conserved among the family members (**figure 1.6**). Each zinc-finger contains a beta-hairpin and an alpha-helix where a single zinc atom is co-ordinately chelated by two cysteine and two histidine residues in a tetrahedral array, producing a finger-like tertiary structure [136]. The zinc-fingers are separated by the highly conserved seven-amino acid spacer TGEKP(Y/F) X. The critical residues that directly interact with the DNA bases and determine sequence specificity are four highly conserved amino acids positioned at −1, 2, 3, and 6 from the N-terminal end of the α-helix in each ZF. Each zinc-finger recognizes a nucleotide triplet, and thus the three zinc-finger repeats of the KLFs recognize nine base pairs in total [136].

The DNA recognition modes of the ZF motifs were predicted from previous structural analysis of non-KLF C2H2 zinc-fingers [136, 137]. Despite these robust studies, complementary *in-vitro* studies illustrated that some members of the family prefer slightly different DNA sequences from those predicted from the amino acid sequence analysis. For example, while KLF13 is predicted to bind to GC rich sequences, DNA binding studies demonstrated that KLF13 binds to CTCCC boxes on the RANTES promoter and CACCC boxes of the γ-globin and BNP promoters [48, 127, 130]. Thus, it is important to complement the *in-silico* DNA binding studies with *in vitro* studies. Several explanations were laid for *in silico/vitro* DNA-binding discrepancy. These included a "co-operative binding" model of the zinc-fingers and a 'wobble" effect similar to that during peptide synthesis [120, 138]. In addition, the effect of post-translational modifications is another untouched mechanism. Since there are several thousands of GC/GT rich sites throughout the genome, deciphering the zinc-fingers' wobbling code for DNA-binding would be indispensible for studies that are focused on the mechanism of gene expression [120].

In contrast to the conserved zinc finger motifs, the location and structure of the NLSs are variable [120]. NLSs, usually rich in basic amino acids, are important for protein translocation across the nuclear membrane via nuclear transport proteins in an ATP-dependent fashion [112]. Although some members of the KLF family, including KLF1 and KLF13, possess a basic amino acid (Arg/Lys)-rich region (AA 147 – 168) just before the repeated zinc-fingers, but they proved non-functional for nuclear localization in some KLFs including KLF1 [115, 136]. Instead several basic residues within the zinc-fingers were found to be the critical determinants for nuclear localization. Furthermore, these basic regions may also be utilized for interactions with other nuclear proteins [136].

In addition, members of the KLFs have highly variable N-terminal regions. It is the N-terminal region that gives the functional identity to each member of this family. The heterogeneity of the N-terminal domain may explain in part the diverse biochemical mechanisms by which KLFs regulate transcription, their specific spatiotemporal expression and, as a consequence, explain their influence on cellular processes [112, 120]. Several activation and repression domains that interact with various co-activators and co-repressors, determined by the cellular environment, were localized within the amino-terminal region in several KLFs. Thus, the characterization of these motifs will help to elucidate the distinct function of each member [112, 120]. The amino-terminal region of KLF13 (AA 1–146) is rich in proline (24/146), serine (10/146), and alanine (30/146) residues [112]. The use of truncated KLF13 constructs, in GAL4 DBD fusion, co-transfected into NIH 3T3 cells with a reporter construct, has revealed that AA 1–35 contain a possible transactivational domain. Unlike other transactivational domains that are rich in hydrophilic acidic moieties (Asp and Glu) or glutamine residues, KLF13's is rich in hydrophobic amino acids (Ala, Pro and Val). Interestingly, this transactivational domain has a high homology to the transactivational domain of KLF9. In addition, similar co-transfectional studies demonstrated the presence of a unique repression domain rich in alanine (19%) and prolines (20%) located between AA 67–112 of the protein [112]. Although they are known to mediate protein-protein interactions, proline and alanine rich domains are also found in a few of the known repression domains. It is worth mentioning that while KLF13 acts as an activator for the RANTES gene, it also acts as a repressor when fused with GAL4 DBD. Other KLFs were also noted to work as activators and repressors depending on the targeting promoters, their interacting partners, and the cellular context [112, 120, 121].

KLF13 also contains a serine-rich carboxyl-terminal tail (AA 250–288), but the exact function of the Ser rich regions in the KLFs has not been elucidated [112].

1.6.3. KLF13: Mechanisms of regulation

Several members of the Sp1-like/KLF family were identified as having bifunctional activities by interacting with co-repressors or co-activators to regulate transcription. It is suggested that histone modification is the molecular switch for Sp1/KLF proteins to function as activators or repressors. Volumes of studies have implicated histone acetylation and deacetylation with repression and activation of transcription, respectively [115]. Our protein of interest, KLF13, was shown to activate several promoters including human γ globin promoter, ANF, BNP, SV40, and SM22α promoters [48, 115, 127, 131]. KLF13 was also shown to repress promoters such as the cytochrome P450 CYP1A1[115, 139]. These studies point to a promoter-dependent trans-regulatory activity of KLF13[115].

Song *et al, 2002* demonstrated that the coactivators p300/CREB-binding protein (CBP) and p300/CBP-associated factor (PCAF) act synergistically in stimulating KLF13 transcriptional activity indicating that both acetyltransferases are involved in KLF13 transcriptional activation [140]. The co-activational properties of CBP and PCAF were previously attributed to their intrinsic acetylase activities on histones and/or transcription factors. The modification of transcription factors by acetylation has been shown to regulate the activation function at multiple levels, including DNA binding, interaction with other proteins, and stability. A later report by the same group pointed to an antagonistic relationship between CBP and PCAF on the DNA binding properties of KLF13 that is dependent on the status of KLF13 acetylation [140]. PCAF was found to directly bind to and acetylate specific lysine residues at the first and third zinc-fingers of KLF13 enhancing

DNA-binding activity. Unexpectedly, they also provided the first example of CBP acetylation that is disruptive for DNA binding of a TF, KLF13. Based on these findings, they concluded stating "… transcription is a very dynamic process involving the assembly and disassembly of pre-initiation, initiation or elongation complexes. Therefore, in the context of the complex process of transcriptional regulation, CBP and PCAF may function at distinct steps of the transcription process to facilitate the assembly or disassembly of the complex through acetylation of target proteins in the complex. " [140].

With respect to histone deacetylation, KLF13, along with KLF9, KLF10, KLF11, and KLF16, were shown to repress transcription via a mechanism that includes a direct interaction with Sin3, a histone deacetylase co-repressor. KLF13's recruitment and direct interaction with Sin3 was mapped to the N terminus through three hydrophobic pockets within AA 1-114 named the SID, R2 and R3 domains [115, 120, 141]. Interestingly, the residues of the SID domain overlap with the previously described amino-terminal activation domain of KLF13 [115]. Swi-independent-3 (Sin3) is a master transcriptional scaffold and corepressor capable of transcriptional silencing via the associated histone deacetylases (HDACs). The core Sin3–HDAC complex interacts with a wide variety of repressors and corepressors, providing flexibility and expanded specificity in modulating chromatin structure and transcription [142]. Thus, it is necessary to decipher the mechanistic code, written by co-activators and co-repressors, that dictates KLF13's effects on a given gene [115].

In addition to acetylation, KLF13 is highly phosphorylated in activated T lymphocytes, suggesting that its activity is regulated by posttranslational modification. Huang et all, illustrated that PRP4, a MAPK family member, phosphorylates KLF13 and

plays an important role in the regulation of RANTES expression in human T lymphocytes. Although KLF13 phosphorylation by PRP4 resulted in a lower promoter binding, co-expression of PRP4 and KLF13 increases nuclear localization of KLF13 and RANTES transcription [143]. However, no structural information on KLF13 or other KLF members complexed with other transcription factors has been reported. To understand the molecular mechanisms of KLF activities in the processes of self-renewal, proliferation, differentiation, and development, structural analyses of the KLF complexes must be performed.

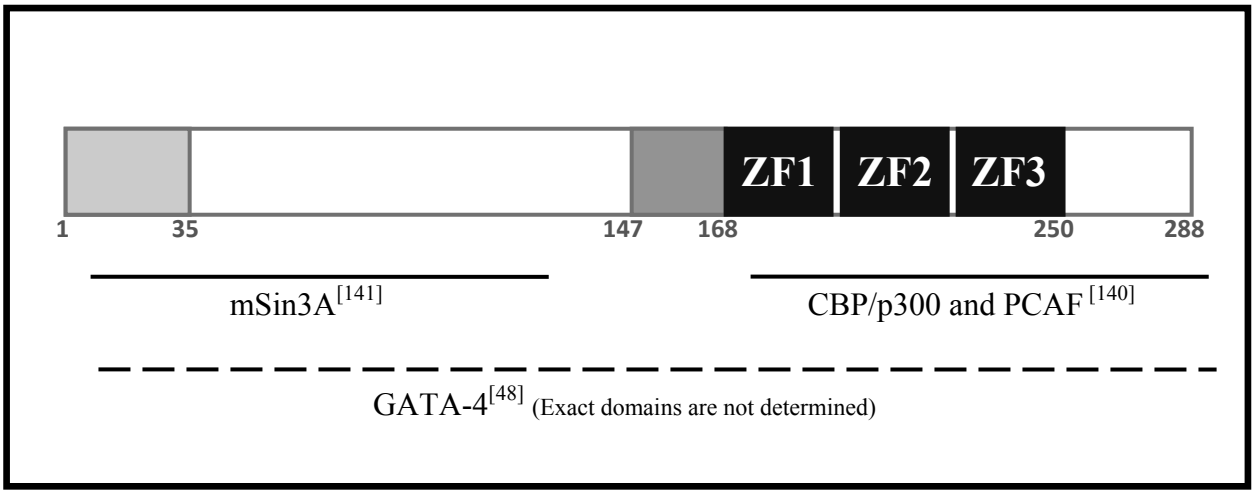

Figure 1.7: Schematic representation of KLF13 protein structure. The lines represent the regions required for the interaction with the protein identified under the line.

Hypothesis and Objectives:

Congenital heart defects (CHD) comprise the largest class of birth defects in humans and are a major cause of infant mortality and morbidity. However, identifying the molecular and genetic pathways important for heart development and deciphering the causes of CHD are still a challenging puzzle. A newly identified piece of this puzzle is KLF13, a member of the Krüppel-like family of zinc-finger proteins. The protein is expressed predominantly in the heart, binds evolutionarily-conserved regulatory elements on cardiac promoters, and activates cardiac transcription. Xenopus embryos that had KLF13 knocked down exhibited atrial septal defects and hypotrabeculation that recapitulated phenotypes observed in humans or mice with hypomorphic GATA-4 alleles.

Our hypothesis is that KLF13 is a critical component of the genetic network regulating heart development and its function is mediated via DNA-Protein and Protein-Protein interaction. Our research objective was to dissect the KLF13 mechanism of action by using the ANF promoter as a model. Our Specific aims were:

1. Mapping the KLF13 response element on the ANF promoter.
2. Identifying novel KLF13 transcriptional partners.
3. Pursuing structure-function analysis of KLF13.

Our analysis will provide insight into the contribution of KLF13 to the development of CHDs.

2. Material and Methods

2.1 Plasmid Constructions

ANF- and BNP-luciferase (BNP) constructs were obtained by subcloning the rat ANF and BNP promoters in the firefly luciferase-encoding pXP-2 vector [48]. Mutant ANF-luciferase and BNP-luciferase (BNP) constructs were generated using PCR-mediated mutagenesis utilizing the wild type ANF and BNP promoter constructs. The position of the mutations/deletions is indicated on the results section and the oligonucleotides used to produce the mutants are summarized in **Table 2.1**. All PCR-generated mutants were confirmed by sequencing.

KLF13, GATA-4, NKX2.5, TBX5, CATF1 and PEX1 expression vectors were obtained by subcloning the amplified reverse transcription (RT)-PCR cDNA constructs into the CMV-driven pCGN vector in phase with the hemagglutinin (HA) epitope. Internal, N- and C-terminal deletions of KLF13, TBX5 and NKX2.5 were generated in the same pCGN vector using PCR-mediated mutagenesis. Briefly, they were constructed via PCR amplification with appropriate primers, containing the appropriate restriction sites, corresponding to the deletion end points using the Phusion® High-Fidelity DNA polymerase (New England BioLabs). The produced PCR products were then digested using the appropriate restriction enzymes and then ligated to pCGN vector digested with the same restriction enzymes.

Similarly, the same KLF13 construct was also cloned into the mammalian expression vector pcDNA3, controlled by cytomegalovirus immediate-early promoter/enhancer, to produce in vitro-transcribed/translated protein. Also, NKX2.5, TBX5 and PEX1 constructs were also cloned in-frame either into pMALC or pGEX vectors to produce MBP and GST fusion proteins, respectively.

Table 2.1: List of the oligonucleotides used during the course of this study to produce the desired promoter and protein constructs.

Region	Oligonucleotides	Direction
Proximal Mutation of the distal CACCC element of the ANF promoter	AGGTCCACCCACGAGGCC	Sense
	GGCCTCGTGGGTGGACCT	Antisense
Proximal Mutation of the proximal CACCC element of the ANF promoter	AGGTCGACTCAGGAGGCC	Sense
	GGCCTCCTGAGTCGACCT	Antisense
Mouse KLF13ΔN (contains the C-ter=Exon2)	GCTCTAGAGAGAGGCCTTTCGCCTGC	Sense
	GGGGTACCTCAGGGTGAGCTGGCCGG	Antisense
Mouse KLF13ΔC (contains the N-ter=Exon1b)	GCTCTAGAGCAGCCGCCGCCTATGTG	Sense
	GGGGTACCCTAACCTGTGTGAGTTCTCAG	Antisense
Mouse KLF13 Δ 250-288aa	GCTCTAGAGCAGCCGCCGCCTATGTG	Sense
	GGGGTACCGTGGCGGCGTGCGTGCTT	Antisense
Mouse KLF13 Δ 221-288aa	GCTCTAGAGCAGCCGCCGCCTATGTG	Sense
	GGGGTACCTGTGCGTGCGATAGTGCC	Antisense
Mouse KLF13 Δ1-147	GCTCTAGACTCAGACAAAGGGGTCGGC	Sense
	GGGGTACCTCAGGGTGAGCTGGCCGG	Antisense
Mouse KLF13Δ 1-147/250-288aa (From KLF13 Δ 250-288aa)	GCTCTAGACTCAGACAAAGGGGTCGGC	Sense
	GGGGTACCGTGGCGGCGTGCGTGCTT	Antisense
Mouse KLF13Δ1-67aa	GCTCTAGAGCGGACCTCAACCAGCAG	Sense
	GGGGTACCTCAGGGTGAGCTGGCCGG	Antisense
Mouse KLF13Δ 67-147	GCTCTAGAGCAGCCGCCGCCTATGTG	Sense
	TAGGATCCGAGCCACCAC	Antisense
	CTCAGACAAAGGGGTCGG	Sense
	GGGGTACCTCAGGGTGAGCTGGCCGG	Antisense
	GTGGCTCGGATCCTACTCAGACAAAGGGGT	Sense
	ACCCCTTTGTCTGAGTAGGATCCGAGCCAC	Antisense
Mouse Second Isoform of KLF13 (Contains Exon 1a and Exon 2)	GCTCTAGAGCCTCCTGTTTTGCCAGG	Sense
	GGGGTACCTCAGGGTGAGCTGGCCGG	Antisense

Table 2.2: List of the oligonucleotides probes used for EMSA.

Region	Oligonucleotides	Direction
BNP Proximal CACCC Element	ATAACCCCACCCCTACTC	Sense
	GAGTAGGGGTGGGGTTAT	Antisense
BNP Proximal CACCC Element (Mutant)	ATAATCCTACTCCTACTC	Sense
	GAGTAGGAGTAGGATTAT	Antisense
ANF CARE Element	AGCTGGGTGTGGGCCAGC	Sense
	GCTGGCCCACACCCAGCT	Antisense
ANF CARE Element (Mutant)	AGCTGAGTCTGAGCCAGC	Sense
	GCTGGCTCAGACTCAGCT	Antisense
ANF Distal CACC Element	TAGGGTGGGGGTGGGCTG	Sense
	CAGCCCACCCCCACCCTA	Antisense
ANF Distal CACC Element (Mutant)	TAGGATGGAGGTAGGCTG	Sense
	CAGCCTACCTCCATCCTA	Antisense
ANF Proximal CACC Element	AGGTCCACCCACGAGGCC	Sense
	GGCCTCGTGGGTGGACCT	Antisense
ANF Proximal CACC Element (Mutant)	AGGTCGACTCAGGAGGCC	Sense
	GGCCTCCTGAGTCGACCT	Antisense

2.2 Cell cultures and transfections:

Human embryonic kidney cell line AD293 and Mouse embryonic fibroblast cell line NIH 3T3 were maintained in a controlled humidified environment of 5% (v/v) CO_2 at 37^{o}C. The cells were grown in 175cm^2 flasks in growth medium (Dulbecco's Modified Eagle Medium (DMEM) supplemented with 10% (v/v) fetal bovine serum (FBS) and 1% (v/v) penicillin/streptomycin (AD293 was supplemented with extra 1% (v/v) sodium pyruvate). Once reached confluencey the cells were washed briefly with PBS, incubated in trypsin for 5min to detach these cells from the flask, and then re-suspended in the appropriate growth media with a final dilution of 1/10.

Transient transfections were carried out on the cells by overnight calcium phosphate co-precipitation method on 10 cm dishes for AD293 and 12-well plates for NIH 3T3; seeded the previous day to give a maximum of 70% confluencey on the day of transfection. For the 10 cm dishes of AD293 the total amount of DNA was kept at 10ug per dish. For the 12-well plates of NIH 3T3 the amount of reporter was kept at 2.0 ug per well of 24 well plates and the total amount of DNA was kept constant (usually 2.5ug). After overnight incubation, the medium and precipitates were removed and replaced with the fresh medium. At 48 h post-transfection, cells were harvested, lysed, and luciferase activity was assayed with a GloMax®-96 Microplate Luminometer.

2.3 Preparation of nuclear extracts:

Nuclear extracts were prepared from at least 90% confluent AD293 cells transfected with the desired expression vectors. The cells were harvested 48 h post-transfection in ice-cold phosphate-buffered saline (PBS) containing 1 mM sodium orthovanadate. The cells were resuspended in hypotonic buffer (20 mM HEPES pH 7.9, 20 mM sodium fluoride, 1 mM sodium pyrophosphate, 1 mM sodium orthovanadate, 1 mM EDTA, 1 mM EGTA, 0.25

mM sodium molybdate, 10 μg/ml leupeptin, 10 μg/ml aprotinin, 10 μg/ml pepstatin, 2 mM DTT, 0.5 mM PMSF and 100 nM okadaic acid). After 10 min of swelling on ice 40 microliters of 10% NP-40, for membrane solublization, were added to the microtubes were then vortexed vigorously. The nuclei were then pelleted by centrifugation at 1500 rpm. at 4°C. The nuclei were extracted by resuspension a high salt buffer (hypotonic buffer containing 20% glycerol and 0.4% NaCl) and shaken vigorously at 4°C for 1 h. The nuclear extracts were cleared by centrifugation at 15 000 r.p.m. for 15 min at 4°C and the protein concentration was determined by the Bradford assay.

2.4 Western Blotting

Based on the molecular weight the protein of interest, 8~17.5% SDS-PAGE resolving gels, 1.0 and 1.5mm thick gels were casted with 10 wells. Following the quantification of all protein samples, the desired amount of protein (10 μg unless specified otherwise) was combined with 3X Laemmli Buffer (187.5mM Tris-HCl, 6% (w/v) SDS, 30% (v/v) glycerol, 15% (v/v) β-mercaptoethanol, 0.015% (w/v) bromophenol blue; pH 6.8) and heated at 95^{o}C for 5min before being loaded on to the gel. Protein molecular weight ladder (Bio-Rad), was also simultaneously run on each gel to assist in the estimation of protein molecular weight. Electrophoresis was typically carried out at 180V for 1.5 mm gels until the bromophenol blue dye front was at the bottom of the gel.

Following SDS-PAGE, the resolving gel was incubated in transfer buffer (48mM Tris, 39mM glycine, 1.2mM SDS, 20% (v/v) methanol; pH 8.0) for 10 min. Transfer of protein from the gel onto the nitrocellulose membrane was carried out using a Trans-Blot Semi-Dry electrophoretic transfer cell (Bio-Rad). Transfer was typically at 120 V for 60~90 min. Following transfer, the nitrocellulose membrane was blocked with a solution of 5% (w/v) non-milk powder in TBST (10mM Tris-HCl, 150mM NaCl, 0.1% (v/v) Tween 20; pH

7.5) for 60min at room temperature with gentle agitation. Then, the membranes were incubated with a primary rabbit polyclonal antibody against the HA probe overnight at 4^{o}C with gentle agitation (Y-11; Santa Cruz Biotechnology, dilution: 1 in 1000). Following the incubation with primary antibody, the membranes were washed 3 times with TBST with vigorous shaking and were then incubated in a solution of diluted secondary antibody peroxidase-conjugated goat anti-rabbit antibody (A 6154; Sigma, dilution 1:10 000) for 2h at room temperature with gentle agitation. Antibodies were diluted in 5% (w/v) milk/TBST for primary antibodies or 1% (w/v) milk/TBST for secondary antibodies. The membrane was then washed 3 times with TBST with vigorous shaking, excess TBST was removed and the membrane incubated in ECL Plus (Amersham Pharmacia Biotechnology). Western blots were then exposed to autoradiography film (Hyperfilm ECL, Amersham) for 1-5min depending on the strength of the signal.

Membranes were stripped by incubation for 20 minutes in a 60^{o}C incubator with strip solution (62.5mM Tris-HCl pH 6.8, 2% (w/v) SDS, 0.1% (v/v) β- mercaptoethanol), that had been pre-heated to 60^{o}C. The strip solution was then removed and the membranes were washed extensively in TBST. The membranes were then blocked in 5% (w/v) non-fat milk powder in TBST and then subjected again to the western blot protocol.

2.5 Electromobility Gel Shift Analysis

Double-stranded synthetic oligonucleotides containing wild-type or mutant CACCC elements of the rat ANF and BNP promoter were radioactively end-labeled using [γ-32P] ATP by T4-polynucleotide kinase (T4-PK, New England BioLabs). For the labelling reaction 5 pmol dsDNA was mixed with 4 μl [γ-32P] ATP (specific activity: 3000 Ci/mmole, 10 μCi/μl), water, 10X T4-PK reaction buffer (final concentration 1X), and T4-PK (5 units). The mixture was incubated at 37°C for 30 min. Samples were run on 15%

Polyacrylamide gel (40% acrylamide (Acrylamide:Bisacrylamide, 19:1) in 1X TBE at 100V for about 1 hour and stoopped when the blue color of the loading buffer is about 2/3 of the gel. One of the glass plates holding the gel was then detached, and the gel was wrapped tightly with saran-wrap and was then exposed to autoradiography film (Hyperfilm ECL, Amersham). After the DNA fragment of interest was located and extracted from the gel, the gel was excised, cut into smaller pieces and transferred to a 1.5 ml tube. The DNA probe was extracted by adding 300 µl elution buffer (1XTE + 250 mM NaCl) to the gel pieces. The extraction was performed by incubation at 37°C with agitation for overnight. DNA was then purified from the gel pieces using spin-X cloumn and radioactivity was measured using the scintillation counter.

For the binding reactions, 50,000 cpm of radioactive probe was incubated with 5 µg of crude nuclear extract contained in a binding buffer (1 µg of poly-(dI-dC)·(dI-dC) containing 10 mM HEPES pH 7.9, 1 mM MgCl2, 50 mM KCl, 1 mM DTT, 0.1 mM EDTA, 10 % glycerol, 0.025 % NP-40, 0.25 mM PMSF and 1 µM of each aprotinin, leupeptin and pepstatin, and when appropriate). Reactions were made at room temperature for 20 minutes and protein-DNA complexes were separated by electrophoresis on 5 % polyacrylamide gel in 0.5 × Tris-borate-EDTA buffer (TBE) at +4 ºC. Nonlabeled double-stranded oligonucleotides were also used as specific (wild type) and non-specific (mutant) competitor DNAs. For supershift experiments, 1 ul of polyclonal antibody against the HA probe were used (Y-11 sc-805, Santa Cruz). After the reactions were loaded on a gel and ran at 220 V at +4 °C, the gel was dried and exposed to either Phosphor Screens (Molecular Dynamics) and analyzed by Image Quant or exposed to autoradiography film (Hyperfilm ECL, Amersham).

2.6 Fluorescence microscopy.

AD 293 cells were grown directly on cover slips in a 12 wells plate and transfected as previously described (Section 2.2). After forty-eight hours, the cells were washed three times with PBS for 3 minutes each, fixed in 3% formaldehyde for 15 minutes, washed again three times with PBS, permeabilized with 0.1% Triton X-100 in PBS for 1 hour, and washed again for two times with PBS. The cover slips were then blocked with (3% BSA-PBS) pH 7.5 for 30 min to prevent unspecific binding of the antibodies. The cover slips were then incubated in primary antibody diluted in 1mL of TPBS-FBS (Y-11 sc-805, Santa Cruz) for 2h. Excess antibodies were then removed by washing the cover slips 3 times with TBS in 5min intervals. The cover slips were then probed with Goat anti-rabbit secondary antibody conjugated to Alexa 488 (A-11034, Molecular Probe). Excess antibodies were then removed by washing the cover slips 3 times with TBS in 5min intervals. To assess the nuclear localization of the desired proteins the nuclei were stained with Hoechst 33424. To remove any unbound secondary antibodies and prevent background fluorescence, the cover slips were again washed extensively with PBS. The coverslips were then mounted onto cover slides using ProLong Gold antifade reagent (P36930, Invitrogen) and observed by confocal laser scanning microscopy. Slides were stored for up to 3 months at -20°C.

2.7 Pull-down: a protein–protein binding assay:

For bacterial expression of the candidate transcription factors, NKX2.5 and TBX5 constructs were cloned in-frame into the pMALC vector to produce MBP fusion proteins. On the other hand, PEX1 was cloned in-frame into the pGEX vector to produce GST fusion proteins. These constructs were used to transform BL21 cells. The transformed cells were then grown in 200 ml of LB broth containing 100 μg/ml of ampicillin at 37°C to A = 0.8,

0.2 mM isopropyl-β-D-thiogalactopyranoside (IPTG) was added, and growth was continued for another 4 h at room temperature. The bacterial cells were then harvested using centrifugation and suspended in the appropriate GST/MBP binding buffer (MBP binding buffer: 20 mM Tris-HCl pH 7.5, 200 mM NaCl, 1 mM EDTA, 0.5 mM PMSF, 1 mM DTT) (GST binding buffer: 1XPBS, 100 mM Tris-HCl pH 7.5, 1 mM EDTA, 0.5 mM PMSF). The suspended cells were then sonicated and the cellular debris were then removed by centrifugation. The fusion proteins were then purified by binding to amylase/sepharose beads (New England Biolabs, Inc.). Estimating the concentration of the immobilized fusion protein was conducted using 10%SDS-PAGE stained with Coomassie blue and BSA as a standard (1-2-5-10-15ug).

For in vitro translated KLF13 we used TNT coupled in vitro transcription-translation system (Promega Corp., Madison, Wis.) with [^{35}S] methionine. In vitro binding studies were performed by incubating 10 µl of ^{35}S-labeled KLF13 with 500 ng of immobilized NKX2.5, TBX5 and PEX fusion proteins in 500 µl of binding buffer (150 mM NaCl, 50 mM Tris-Cl [pH 7.5], 10 mM ZnCl20.3% Nonidet P-40, 1 mM dithiothreitol [DTT], 0.5 mM PMSF, 0.25% bovine serum albumin [BSA]) overnight at 4°C with agitation and then centrifuged for 2 min at 15,000 rpm at room temperature. Beads were washed three times by vortexing in 500 µl of binding buffer at RT and three times by vortexing in 500 µl of binding buffer without BSA. The protein complexes were released after boiling in Laemmli buffer and resolved by sodium dodecyl sulfate-polyacrylamide gel electrophoresis. The gel was then dried and exposed to autoradiography film (Hyperfilm ECL, Amersham).

3. Results

3.1 Mapping of KLF13 response elements on the ANF promoter.

Recent studies from our lab have reported that KLF13 alone is capable of activating various cardiac specific promoters including -699 bp ANF and -114bp BNP in a dose dependent manner [48]. Interestingly, our promoter cotransfection assays into rat atrial and ventricular cardiomyocytes revealed that KLF13 activation may be context-dependent with efficient activation achieved in atrial but not in ventricular cardiomyocytes. This suggests a differential interaction of KLF13 with coactivators or corepressors in the different heart chambers.

Given the spatiotemporal expression of KLF13 and ANF in the atria, we chose to further our analysis of KLF13's role as a transcriptional activator of ANF by mapping KLF13 response elements on the promoter. *In silico* sequence analysis of the -699 bp ANF promoter indicated the presence of three evolutionarily-conserved putative KLF13 response elements (CACCC elements) centered around -535, -515 and -360bp **(figure 3.1.A)**.

To assess the contribution of these elements on ANF promoter activity we transfected NIH 3T3 cells with luciferase-reporter plasmids (pXP2) driven by different mutants of the ANF promoter. The mutant ANF promoters contained different 5'deletions (-699, -415, -331 and -137bp) that gradually truncated the putative CACCC elements. Consistent with our previous report [48], **figure 3.1.B** shows that KLF13 robustly and dose-dependently activated the -699 bp fragment of the ANF promoter. This activation was significantly and progressively reduced upon truncating the promoter to delete the putative KLF13 response elements. However, despite the absence of any identifiable CACCC elements, the -331bp and -137bp promoters were still responsive to KLF13 in a dose dependent manner, indicating a possible KLF13 response element located at that region.

To assess the contribution of the -360bp element, we conducted similar co-transfectional studies with an ANF construct containing a deletion of that specific element. Indeed, deleting the -360 bp response element significantly reduced, but did not abrogated, KLF13 dose dependent activation of the ANF promoter **(figure 3.2.A)**. These results implicate the two distal CACCC elements on the activation of ANF promoter by KLF13. Consistent with this, cotransfecting of KLF13 with ANF constructs containing an internal deletion along with different point mutations that disrupt the two distal -535 and -515 CACCC elements significantly decreased the activation of the ANF promoter (**figure 3.2.B**). Note that the internal deletion -137 to -492 was utilized to decrease the interference of other elements upon promoter activatation. Together, the data demonstrate the involvement of the three analyzed CACCC elements in the transcriptional activation of the -699 bp ANF promoter by KLF13.

To further substantiate that these elements are capable of recruiting KLF13, an EMSA experiment was performed using three sets of ^{32}P-labeled double stranded (ds) oligonucleotide probes, each covering one of the three putative KLF13 binding elements (the sequences are provided in **figure 3.3**). Each of these ^{32}P-labeled probes were then incubated with nuclear extracts of AD293 cells transfected with HA-taged KLF13 expression vectors. **Figure 3.3** shows that KLF13 was able to bind the -535, -515 and -360bp CACCC elements of the ANF promoter. Supershift experiments (Lanes #3 of **figure 3.3. A, B and C**) showed that the intensity of the protein-DNA complex was attenuated by the HA-antibody. To further establish that these elements are genuine KLF13 binding sites, competition EMSAs were performed using double stranded oligonucleotides that are either cold/non-radioactive probes (C.S) or cold/ non-radioactive mutant probes (CM). The specific DNA-KLF13 complexes were efficiently competed for by the cold self-probes, but

not by the cold mutant probe (Lane # 5 and 6 respectively of **figure 3.3.A, B and C**). Interestingly, our EMSA also shows that KLF13 might also participate in multimeric DNA-protein complexes. In **figure 3.3.C,** CARE elements showed the presence of heavy migrating complexes in the KLF13 transfected nuclear extracts. As the faster-migrating KLF13-DNA complex, but not the heavy multimeric complex, was abrogated by the addition of an HA-antibody, it appears that KLF13 was participating in a very strong multimeric protein complex. It also appears that other protein(s) in this complex are capable of binding to the CARE element as competition with cold mutants had significantly decreased the slower migrating complex. Further analysis to decipher the nature of such complexes is needed.

Overall, these experiments demonstrate that three evolutionarily conserved CACCC elements (centered around -535, -515 and -360bp) of the ANF promoter are high affinity KLF13 binding sites that mediate KLF13 dependent activation of the ANF promoter.

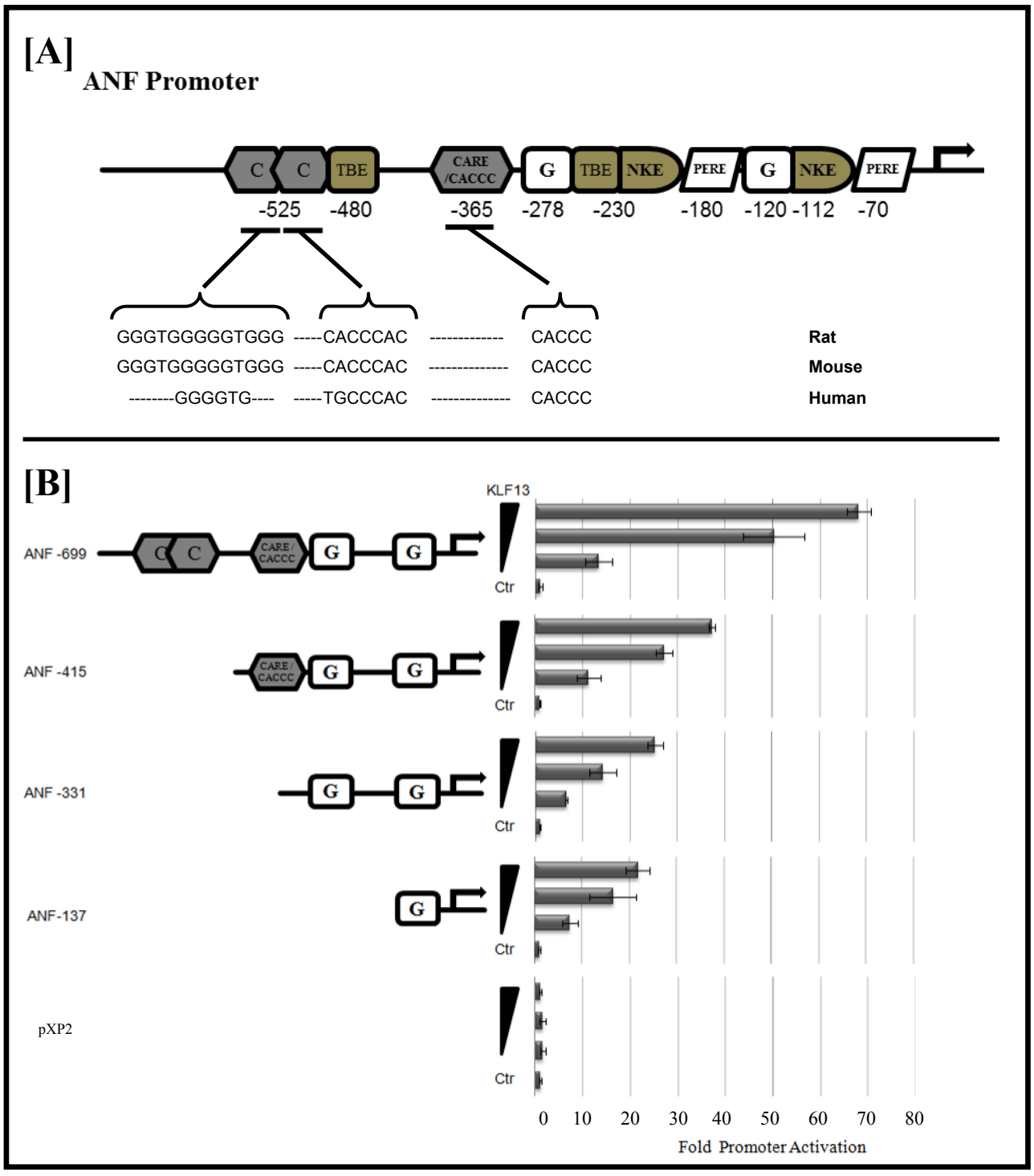
[A]
ANF Promoter
C
C
TBE
CARE /CACCC
G
TBE
NKE
PERE
G
NKE
PERE
-525
-480
-365
-278
-230
-180
-120
-112
-70
GGGTGGGGGTGGG -----CACCCAC ---------- CACCC Rat
GGGTGGGGGTGGG -----CACCCAC ---------- CACCC Mouse
--------GGGGTG---- -----TGCCCAC ---------- CACCC Human
[B]
KLF13
ANF -699
ANF -415
ANF -331
ANF-137
pXP2
Ctr
0
10
20
30
40
50
60
70
80
Fold Promoter Activation

Figure 3.1: Mapping of KLF13 response elements on the ANF promoter.

A) Representation of the -699bp ANF promoter with the location of the three putative KLF13 binding elements, centered at -365, -515 and -535bp. CARE is Cardiac Response element, TBE is T-Box element, NKE is the NKX element, G is GATA element, and PERE is Phenylephrine Response element. B) Transient co-transfectional assay of NIH 3T3 cells showing the mapping of KLF13 response elements on the ANF promoter. The mapping was investigated using 2ug of the luciferase reporters driven by a series of 5' deletions of the ANF promoters (-699, -415, -331 and -137bp) and different doses of KLF13 (25ng, 50ng and 100ng). Note that the total amount of DNA was kept constant using an empty pCGN vector. Fold promoter activity is expressed as the fold change relative to the control. The data shown is a representation of three different experiments, each carried out in triplicate.

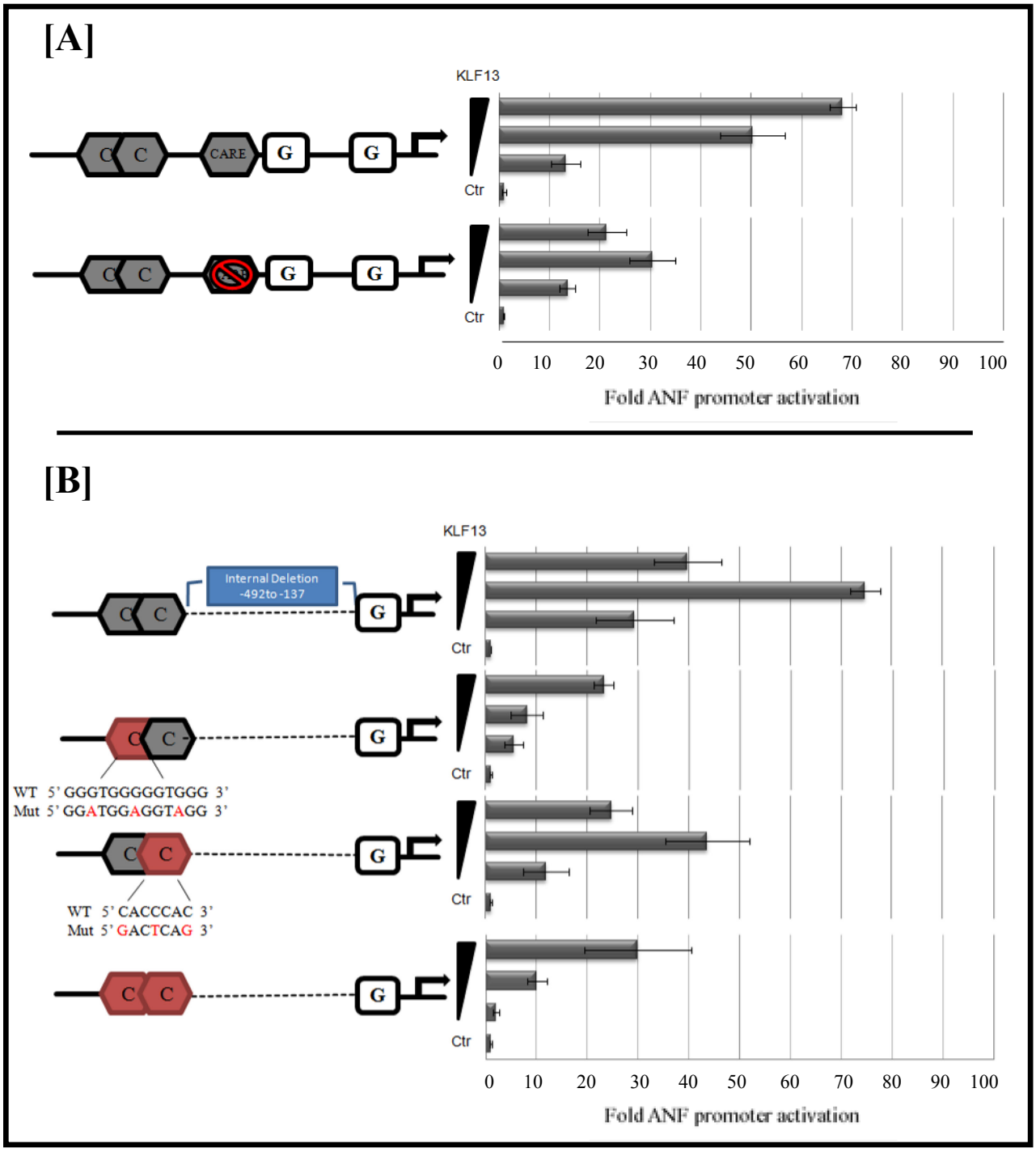
[A]
KLF13
C C
CARE
G
G
Ctr
C C
G
G
Ctr
0 10 20 30 40 50 60 70 80 90 100
Fold ANF promoter activation
[B]
KLF13
Internal Deletion
-492to -137
C C
G
Ctr
C C
G
Ctr
WT 5' GGGTGGGGGTGGG 3'
Mut 5' GGATGGAGGTAGG 3'
C C
G
Ctr
WT 5' CACCCAC 3'
Mut 5' GACTCAG 3'
C C
G
Ctr
0 10 20 30 40 50 60 70 80 90 100
Fold ANF promoter activation

Figure 3.2: Mutational studies on the putative KLF13 response elements on the ANF promoter.

A) Co-transfectional assays in NIH 3T3 cells showing the reduced KLF13-dependent activation of the ANF promoter upon the deletion of CARE element. B) A similar mutational study showing the reduced KLF13-dependent activation of the ANF promoter upon mutating the two distal CACCC elements centered around -535 and -515bp. The deletion/mutation studies were conducted by co-transfecting NIH 3T3 with 2ug of ANF promoter and different doses of KLF13 (25ng, 50ng and 100ng). Note that the total amount of DNA was kept constant using an empty pCGN vector. Fold promoter activity is expressed as the fold change relative to the control. The data shown is a representation of three different experiments, each carried out in triplicate.

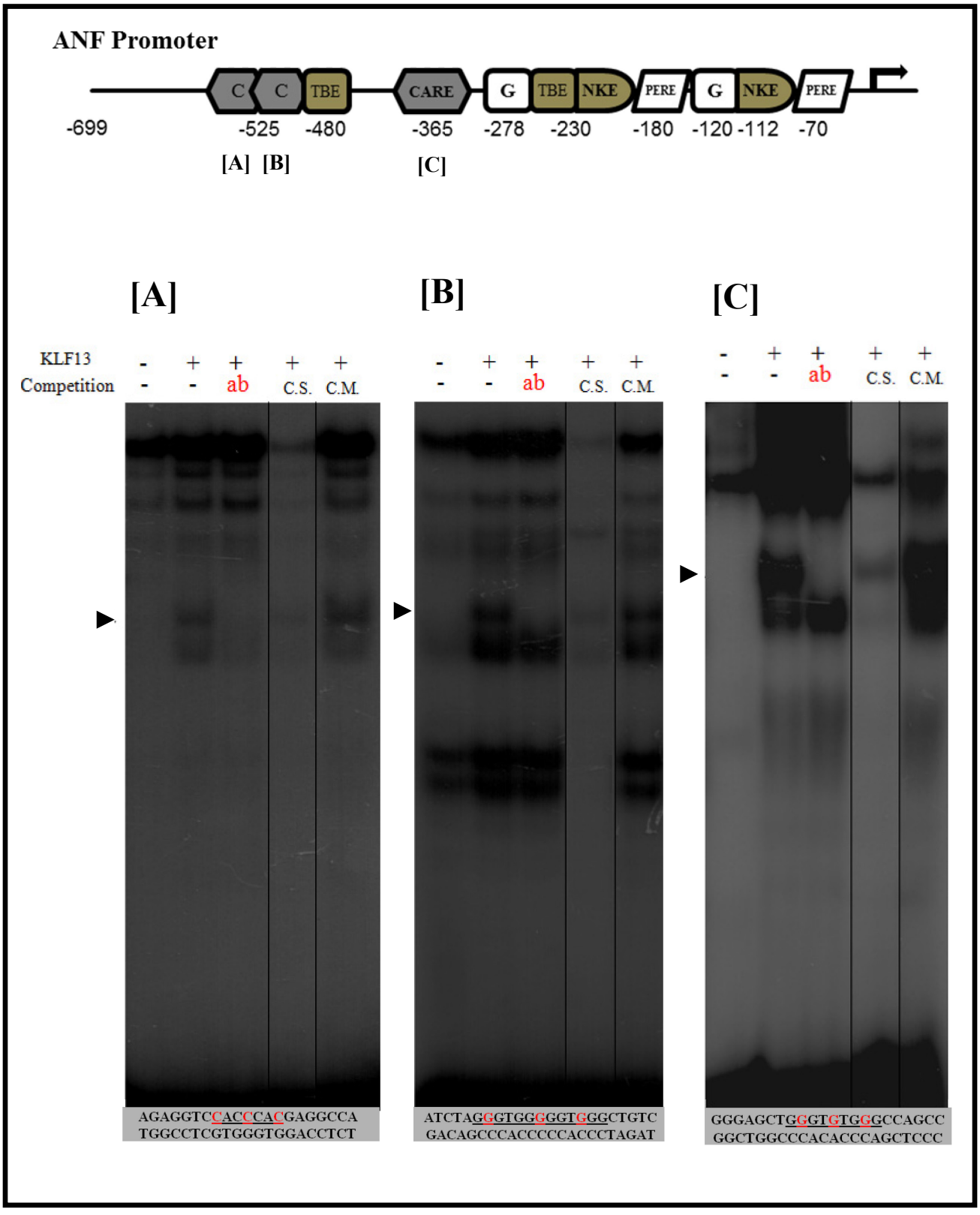
ANF Promoter
C
C
TBE
CARE
G
TBE
NKE
PERE
G
NKE
PERE
-699
-525
-480
-365
-278
-230
-180
-120
-112
-70
[A] [B]
[C]
[A]
[B]
[C]
KLF13
Competition
ab
C.S.
C.M.
AGAGGTCCACCCACGAGGCCA
TGGCCTCGTGGGTGGACCTCT
ATCTAGGGTGGGGGTGGGCTGTC
GACAGCCCACCCCCACCCTAGAT
GGGAGCTGGGTGTGGGCCAGCC
GGCTGGCCCACACCCAGCTCCC

Figure 3.3: Binding of KLF13 to CACCC elements of the ANF promoter.

The electrophoretic mobility shift assays (EMSA) show that KLF13 is able to bind to the three putative KLF13 response elements (A= -535, B= -515 and C= -365). The DNA probes utilized here are derived from the three putative elements; the probe sequences are provided under each EMSA and the red colored nucleotides are the nucleotides replaced in the mutant probes. The radioactive probes were incubated with either the nuclear extract of control or KLF13 transfected AD293 cells. The arrow heads show KLF13 binding. C.S: 100X cold self-competitor. C.M:100X cold mutant competitor. Ab: nuclear extract incubated with anti-HA antibody.

3.2 Combinatorial interactions of KLF13 on the ANF promoter.

In a recent study from our lab [48], the sequence and spatial conservation of the GATA and CACCC elements on the BNP promoter instigated our discovery of the functional and physical interaction between GATA-4 and KLF13. Here, localization of KLF13 response elements on the ANF promoter was used as a tool to examine the existence of other cardiac specific combinatorial interactions with other transcription factors. The partnering profile of KLF13 with other collaborators was conducted using a candidate approach that was guided by: i) the cardiac spatial co-localization of KLF13 and other cardiac transfection factors, ii) the conserved recurrence of KLF13 binding sites and other elements, and iii) known interactions between KLFs and other classes of TFs.

3.2.1 KLF13 and CATF1 synergistically activate the ANF promoter.

Previous studies have established the region located between -382 and -355bp of the ANF promoter as a hypersensitive DNA region/element; thus it was termed cardiac regulatory element (CARE) [107]. The CARE element was found to be necessary for the high cardiac-specific activity of the ANF element in embryonic cardiomyocytes and in postnatal atrial myocytes. Screening of cardiomyocyte cDNA library for cardiac protein(s) interacting with the CARE element has identified CATF1 as a CARE binding protein. As seen in **figure 3.4.A**, our identified KLF13 binding element positioned at -365 bp of the ANF is located within the CARE element. Thus, we investigated if KLF13 and CATF1 could functionally interact at the level of the ANF promoter. We tested this hypothesis by co-transfecting the -699 bp ANF promoter with KLF13, CATF1 or both factors in NIH 3T3 cells at limiting DNA concentrations in order to avoid squelching. For this study we used an increased concentration gradient of CATF1 with or without a constant concentration of KLF13. As shown in **figure 3.4.B**, CATF1 alone had little effect on ANF promoter activity

but, when co-expressed with KLF13, it potentiated by up to 4-fold the transcriptional activation by KLF13, resulting in a 17-fold induction of -699bp ANF promoter activity. The requirement of the CARE element for this synergy was determined utilizing 5' truncated ANF constructs that either contained or lacked a CARE element. As shown in **figure 3.4.B**, similar to the -699bp ANF promoter, the -415bp ANF promoter containing the CARE element was synergistically activated by the combination of KLF13 and CATF1 (Figure 3.4.B). However, CATF1 transcriptional and synergistic activity was lost upon deletion of the CARE element. Thus, the CATF1-KLF13 synergistic effect is dependent on the -365bp CARE element abrogated CATF1 transcriptional and synergistic effects.

3.2.2 KLF13 and PEX synergistically activate the ANF promoter.

As previously mentioned, despite the absence of any identifiable CACCC elements, the -137 fragment of the ANF promoter was responsive to KLF13 in a dose dependent manner indicating a possible KLF13 response element at that region. As the PERE element (GGGGAGGG) highly resembles the G-rich KLF13 response elements (CACCC or GTGGG elements), we speculated that the PERE element is a common binding element for KLF13 and PEX1. We expected that KLF13 and PEX1 would compete and antagonize in activating the ANF promoter. Intriguingly, co-transfectional studies of the two proteins showed that PEX1 is another synergistic collaborator of KLF13. As shown in **figure 3.5**, PEX1 alone had little effect on the -137bp ANF promoter's activities but, when co-expressed with KLF13, it potentiated by up to 3-fold KLF13's transcriptional activation, resulting in a 35-fold induction of -137bp ANF promoter activity. Furthermore, mutating the PERE element did not abrogate KLF13's activation of the -137bp ANF promoter, but rather totally abrogated the synergistic interaction of KLF13 with PEX1, and therefore indicating the essentiality of PEX1-DNA binding for the synergistic interaction with KLF1

3.2.3 KLF13 and NKX2.5 synergistically activate the ANF promoter.

Given the sequence and spatial conservation of the CACCC and NKE elements on the ANF promoter, we tested for functional cooperation between the KLF13 and NKX2.5. As shown in **figure 3.6**, NKX2.5 alone was capable of activating the -699bp ANF promoter and when co-expressed with KLF13 it potentiated by up to 3 to 4 -fold KLF13 transcriptional activation, resulting in approximately a 42-fold induction of the -699bp ANF promoter activity.

A structure-function study was conducted utilizing the NKX2.5 constructs Δ1-45aa, Δ 1-92aa, Δ203-318aa, and Δ246-318aa. These constructs were used to analyze the contribution of the TN domain, N-terminal domain, NK-2 domain, and the sequence GIRAW on the NKX2.5-KLF13 synergistic interaction, respectively. As expected, while deleting the transactivational domain of NKX2.5 (region 45-92aa) had abrogated promoter activation by NKX2.5 alone, deleting the C-terminal domain (Δ246-318aa and Δ203-318aa), which contains an inhibitory domain, showed a slight increase in promoter activity. Also, consistent with our previously published study [144], mutating tyrosine 54 located within the Homeodomain (HD), which impairs DNA binding, abrogated the transcriptional activity of the protein. On the synergistic front, although the Δ246-318aa construct still maintained the synergy with KLF13, the Δ203-318aa construct, having the NK domain deleted, had a significant reduction in synergy with KLF13. Most importantly, although KLF13 synergy was reduced with the Δ1-45aa NKX2.5 construct, the Δ1-92aa had a complete abrogation of synergy of NKX2.5 with KLF13. Thus, our data indicated that, in addition to intact DNA-binding activity of the homeodomain, synergy required an N-terminal region, 45-92aa, of NKX2.5. In addition, the NK domain located between 203 and 246aa seems to have an enhancing influence on NKX2.5-KLF13 synergy.

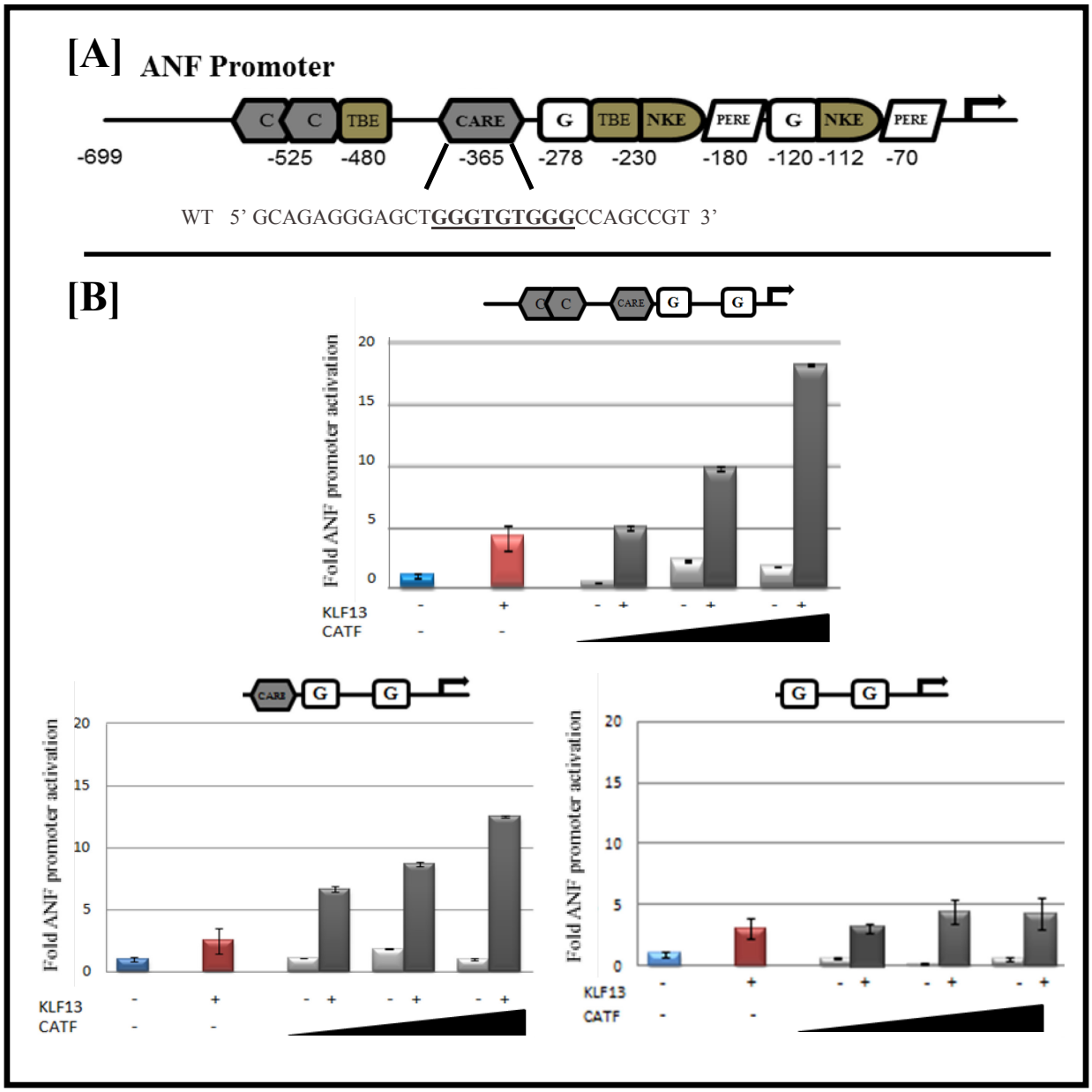
[A] ANF Promoter
C
C
TBE
CARE
G
TBE
NKE
PERE
G
NKE
PERE
-699
-525
-480
-365
-278
-230
-180
-120
-112
-70
WT 5' GCAGAGGGAGCTGGGTGTGGGCCAGCCGT 3'
[B]
Fold ANF promoter activation
KLF13
CATF
CARE
G
G

Figure 3.4: CARE element mediates the functional cooperation between KLF13 and CATF1.

A) Our identified KLF13 binding element centered at -365bp of the ANF promoter is located within the CARE element. The PERE corresponds to the phenylephrine response element, the NKE to the NK2 response element and the TBE to the T-Box element. (B) KLF13 and CATF1 synergistically activate the -699bp ANF promoter and this synergy is abrogated upon deletion of the CARE element. The study was conducted by co-transfecting NIH 3T3 with 2ug of ANF promoter, a constant dose of KLF13 (50ng) and different doses of CATF1 (25ng, 50ng and 100ng). Note that the total amount of DNA was kept constant using an empty pCGN vector. Fold promoter activity is expressed as the fold change relative to the control. The data shown is a representation of three different experiments each carried out in triplicate.

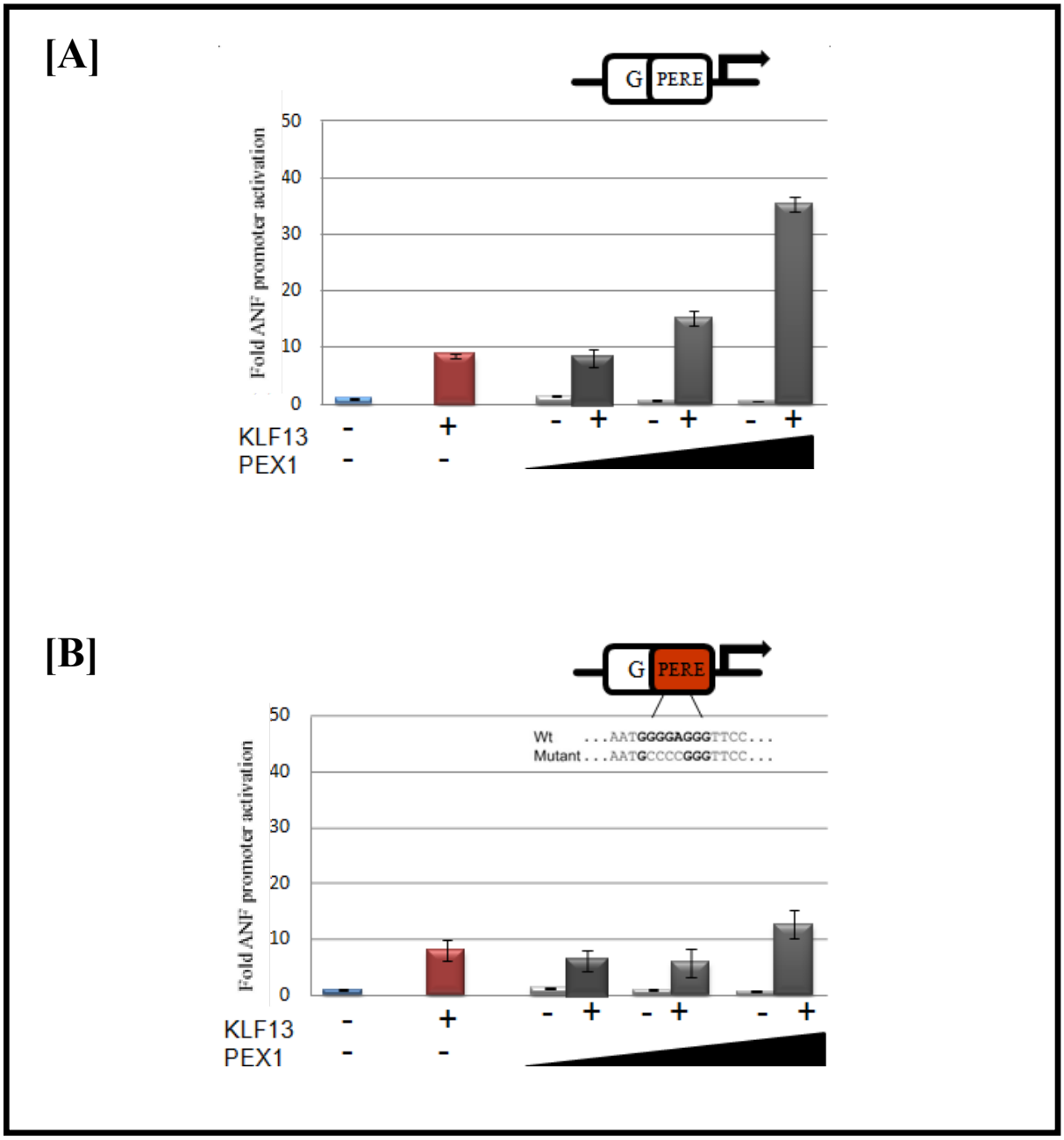
[A]
G PERE
Fold ANF promoter activation
50
40
30
20
10
0
KLF13 - + - + - + - +
PEX1 - -
[B]
G PERE
Wt ...AATGGGGAGGGTTCC...
Mutant ...AATGCCCCGGGTTCC...
Fold ANF promoter activation
50
40
30
20
10
0
KLF13 - + - + - +
PEX1 - -

Figure 3.5: PERE element mediates the functional cooperation between KLF13 and PEX1. KLF13 and PEX1 synergistically activate the -137bp ANF promoter (A) and this synergy was abrogated upon mutating the PERE element (B). The study was conducted by co-transfecting NIH 3T3 with 2ug of ANF promoter, a constant dose of KLF13 (50ng) and different doses of PEX1 (25ng, 50ng and 100ng). Note that the total amount of DNA was kept constant using an empty pCGN vector. Fold promoter activity is expressed as the fold change relative to the control. The data shown is a representation of two different experiments, each carried out in triplicate.

3.2.4 KLF13 and TBX5 synergistically activate the ANF promoter.

Similar to the KLF13 and NKX2.5 investigation, sequence and spatial conservation of the CACCC and TBE elements on the ANF promoter motivated us to test the possibility of functional cooperativeness between KLF13 and TBX5. As shown in **figure 3.7,** TBX5 alone was capable of activating the -699bp ANF promoter and when co-expressed with KLF13, it potentiated by at least 15-fold KLF13 transcriptional activation, resulting in at least a 50-fold induction of the -699bp ANF promoter activity.

To study the structure-function of TBX5-KLF13 synergy, we utilized TBX5 constructs that contained deletion - mutations (Δ1-52aa, Δ400-518aa and Δ251-518aa). Our previously published study [145] has indicated the presence of two transactivational domains within the C-terminal of TBX5 in the regions 400-518aa and 250-300aa. Consistently, deleting these two TADs and using Δ400-518aa and Δ251-518aa has led to a significant drop in promoter activation. Deletions of the N-terminal domain did not significantly decrease promoter activation but caused a right shift in the dose-response curve; our previous study indicated that this is likely reflective of a lower level of protein accumulation of the N-terminal deletion construct [145]. Synergistically, although deleting the two C-terminal TADs (Δ400-518aa and Δ251-518aa) or the N-terminal domain (Δ1-52aa) had a reduced synergistic interaction with KLF13, these deletions did not abrogate the strong synergistic interaction between KLF13 and TBX5. Thus, it appears that TBX5's T-box domain is required for functional interaction with KLF13. Thus, our data indicates for the possible implication of the DNA-binding T-box domain of Tbx5 in mediating the synergy with KLF13 on the ANF promoter .

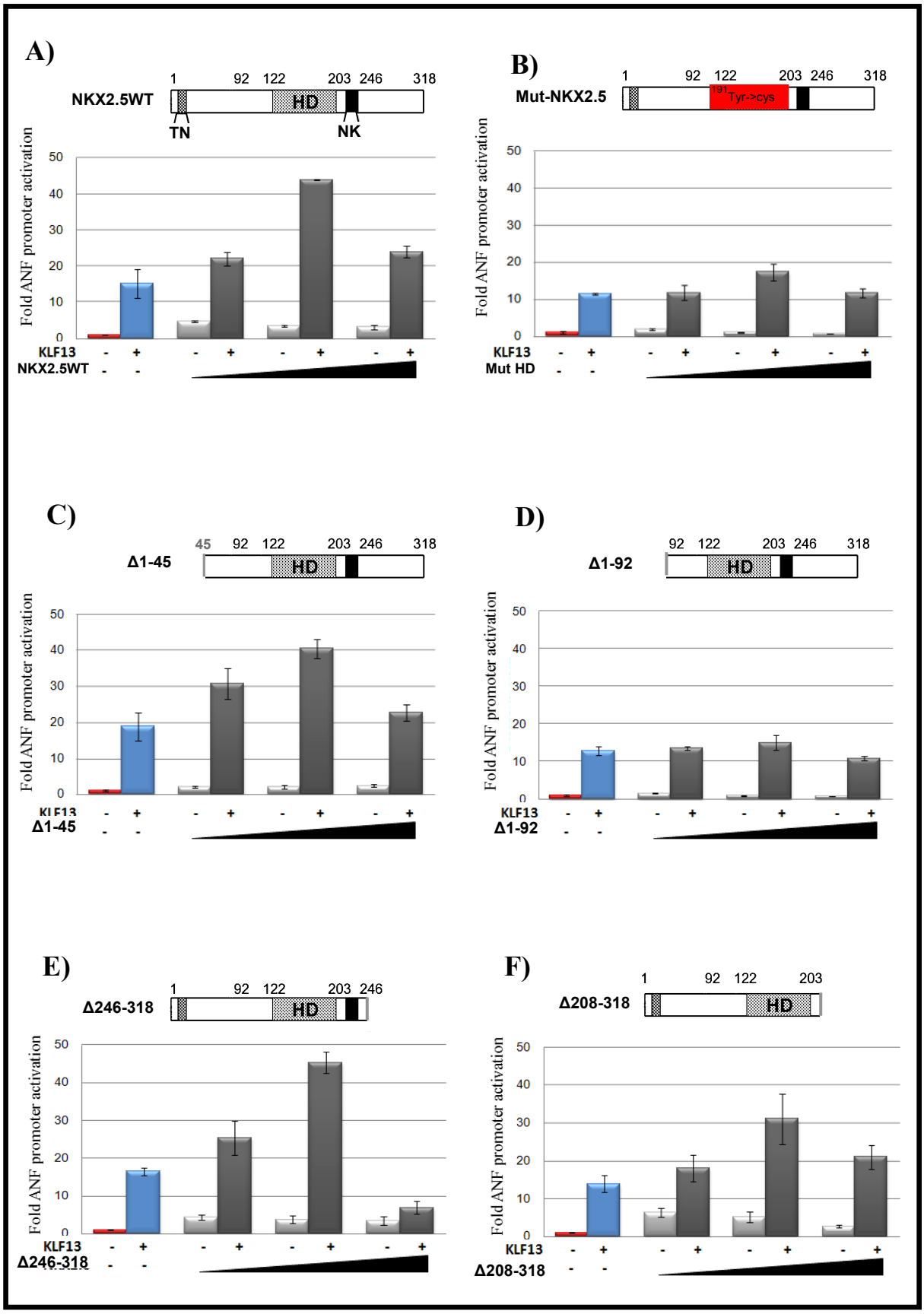
A)
NKX2.5WT
1 92 122 203 246 318
HD
TN
NK
Fold ANF promoter activation
KLF13
NKX2.5WT
B)
Mut-NKX2.5
191 Tyr->cys
Mut HD
C)
Δ1-45
45 92 122 203 246 318
Δ1-45
D)
Δ1-92
92 122 203 246 318
E)
Δ246-318
1 92 122 203 246
F)
Δ208-318
1 92 122 203

Figure 3.6: Domains of NKX2.5 important for KLF13 and NKX2.5 synergy.

KLF13 and NKX2.5 synergistically activate the expression of the -699 ANF promoter. Deletion/mutation analysis of the NKX2.5 protein (using the NKX2.5 constructs Δ1-45aa, Δ 1-92aa, Δ203-318aa and Δ246-318aa) was conducted to localize the regions within NKX2.5 that are important for the synergistic interaction with KLF13 on the ANF promoter. Schematic representations of the NKX2.5 constructs utilized are shown on top of the corresponding synergy analysis. The study was conducted by co-transfecting NIH 3T3 with 2ug of ANF promoter, a constant dose of KLF13 (50ng), and different doses of NKX2.5 (25ng, 50ng and 100ng). Note that the total amount of DNA was kept constant using an empty pCGN vector. Fold promoter activity is expressed as the fold change relative to the control. This experiment was carried out in triplicate.

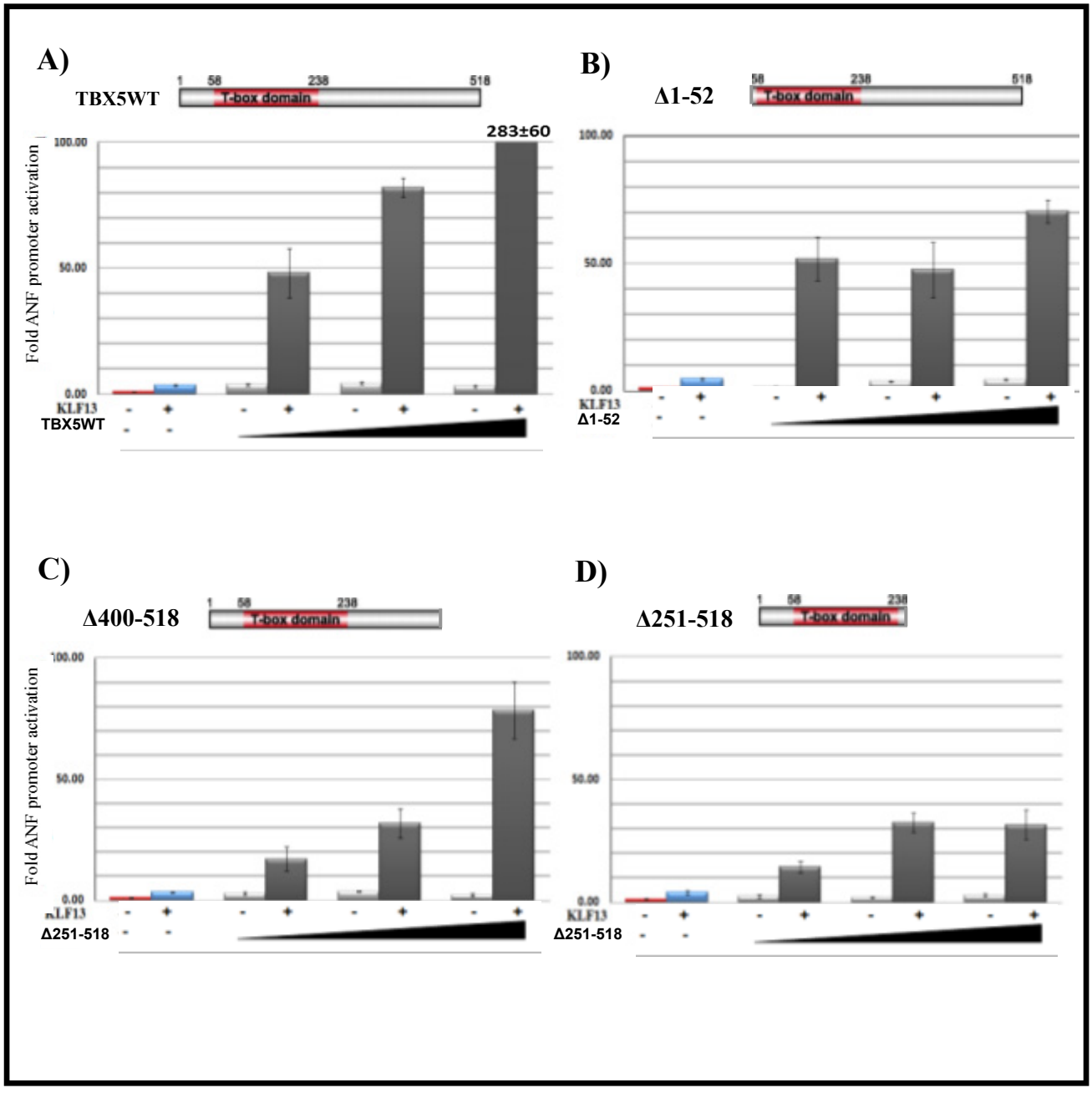
A)
TBX5WT
1
58
238
518
T-box domain
283±60
Fold ANF promoter activation
100.00
50.00
0.00
KLF13
TBX5WT
B)
Δ1-52
T-box domain
KLF13
Δ1-52
C)
Δ400-518
T-box domain
Fold ANF promoter activation
KLF13
Δ251-518
D)
Δ251-518
T-box domain
KLF13
Δ251-518

Figure 3.7: TBX5 domains required for KLF13 and TBX5 synergy.

Deletion/mutation analysis of theTBX5 protein (utilizing the TBX5 constructs Δ1-51aa, Δ400-514aa and Δ251-514aa) was conducted to localize the regions within TBX5 important for the synergistic interaction with KLF13 on the ANF promoter. Schematic representations of the TBX5 constructs utilized are shown on top of the corresponding synergy analysis. The study was conducted by co-transfecting NIH 3T3 with 2ug of ANF promoter, a constant dose of KLF13 (50ng), and different doses of TBX5 (25ng, 50ng and 100ng). Note that the total amount of DNA was kept constant using an empty pCGN vector. Fold promoter activity is expressed as the fold change relative to the control. The experiment was carried out in triplicate.

3.2.5 Physical interaction of KLF13 with TBX5, NKX2.5, and PEX1.

Following the synergy evidence of functional cooperation between KLF13 and the ANF regulators TBX5, NKX2.5, PEX1 and CATF1, we tested whether these synergies are reflective of physical interactions. Thus, pull-down assays were carried out on the binding of KLF13 with our novel functional partners. Indeed the physical binding was evidenced by the ability of the maltose binding protein fusion proteins (MBP)-TBX5 and (MBP)-NKX2.5, and the glutathione S-transferase fusion protein (GST)-PEX1 to retain *in vitro*- translated ^{35}S-labeled-KLF13. MBP and GST were used as negative controls to detect binding specificity. A physical interaction between KLF13 and CATF1 was not detected (data not shown), at least in our binding conditions.

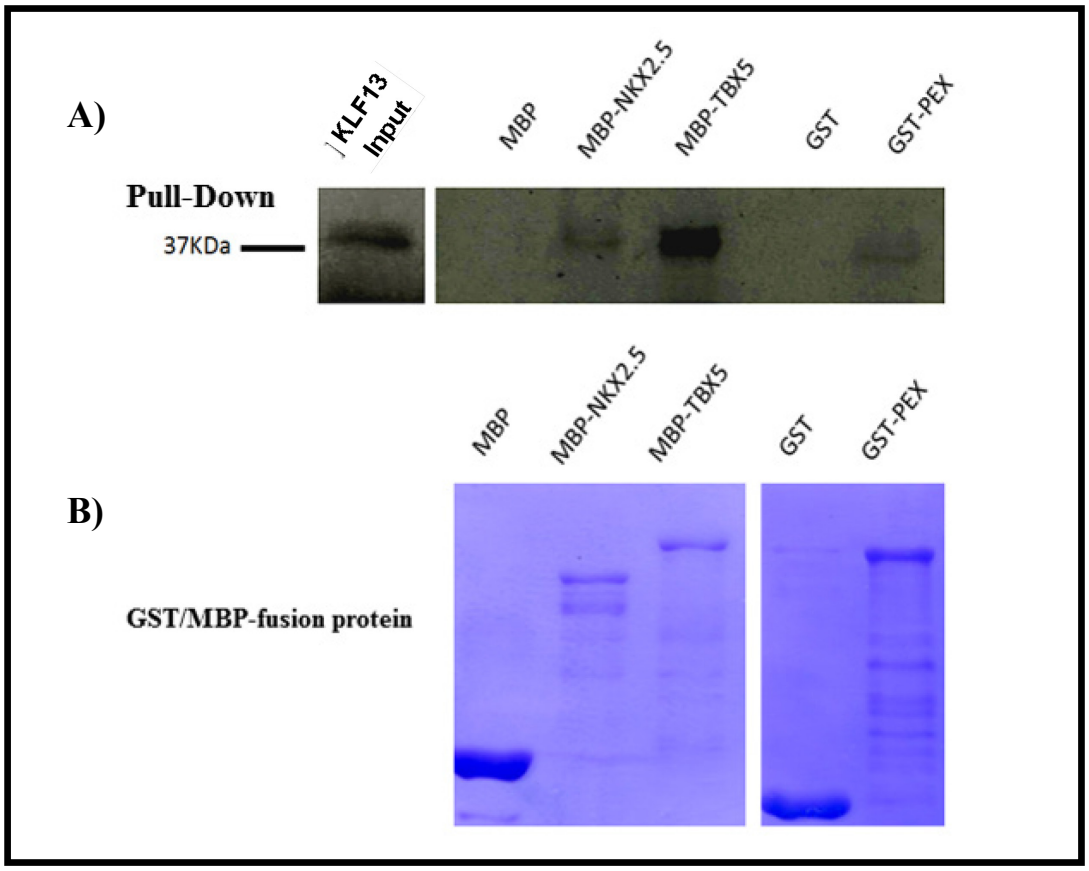
A)
KLF13 Input
MBP
MBP-NKX2.5
MBP-TBX5
GST
GST-PEX
Pull-Down
37KDa
B)
MBP
MBP-NKX2.5
MBP-TBX5
GST
GST-PEX
GST/MBP-fusion protein

Figure3.8: KLF13 physically interacts with TBX5, NKX2.5, and PEX1.

A) Pull-down assays using *in vitro*-translated ^{35}S-labeled-KLF13 and the fusion proteins MBP-TBX5, MBP-NKX2.5 and GST-PEX1. Note how KLF13 is retained on the MBP-NKX2.5, MBP-TBX5, and GST-PEX1 beads. B) Coommassie blue staining of SDS-PAGE gel showing the bacterially produced fusion proteins MBP-TBX5, MBP-NKX2.5 and GST-PEX1.

3.3 Structure-Function Analysis of KLF13

Sequence analysis of KLF13 revealed a DNA-binding domain (AA 169–249) with three typical contiguous C2H2 zinc-fingers, a serine-rich carboxyl-terminal tail (AA 250–288), a basic region adjacent to the amino terminus of zinc-fingers (AA 147–168), and an amino terminal domain (AA 1–146) rich in proline (24/146), serine (10/146), and alanine (30/146) residues, which are known to constitute transcriptional activation domains for a number of transcription factors[112]. In order to assess the functional domains important for DNA binding and the synergistic interaction of KLF13 with the new identified partners we have pursued a structure-function analysis of KLF13. For easy localization and monitoring, HA-tagged KLF13 constructs, which contain deletions on their N- and C-termini, were generated (the deletion-mutants are illustrated in **figure 3.9**).

The expressivities of the generated constructs were validated by transfecting AD 293 cells with each of the constructs and preparing protein extracts for Western blot analysis using anti-HA antibodies. As shown in Fig. 2C, the appropriate size HA-fusion proteins were produced. Note that the two constructs Δ147-288 / 250-288aa and Δ 221-228aa had an up-shift in their molecular weight, possibly due to disturbances of the molecular structure and the associated post-translational modification of the protein. Also note that several constructs gave extra bands possibly due to some posttranslational modifications. Also note that our KLF13 construct is termed KLF13a; a novel isoform of KLF13 was analyzed during this study and it is referred to here as KLF13b. **Section 3.4** will separately discuss this isoform. Note that our protein constructs had different expressivity that might be due to the stability of the expressed protein and its folding or the interference in cellular processes including proliferation and apoptosis (similar observations were found in both the nuclear and cytoplasmic extracts).

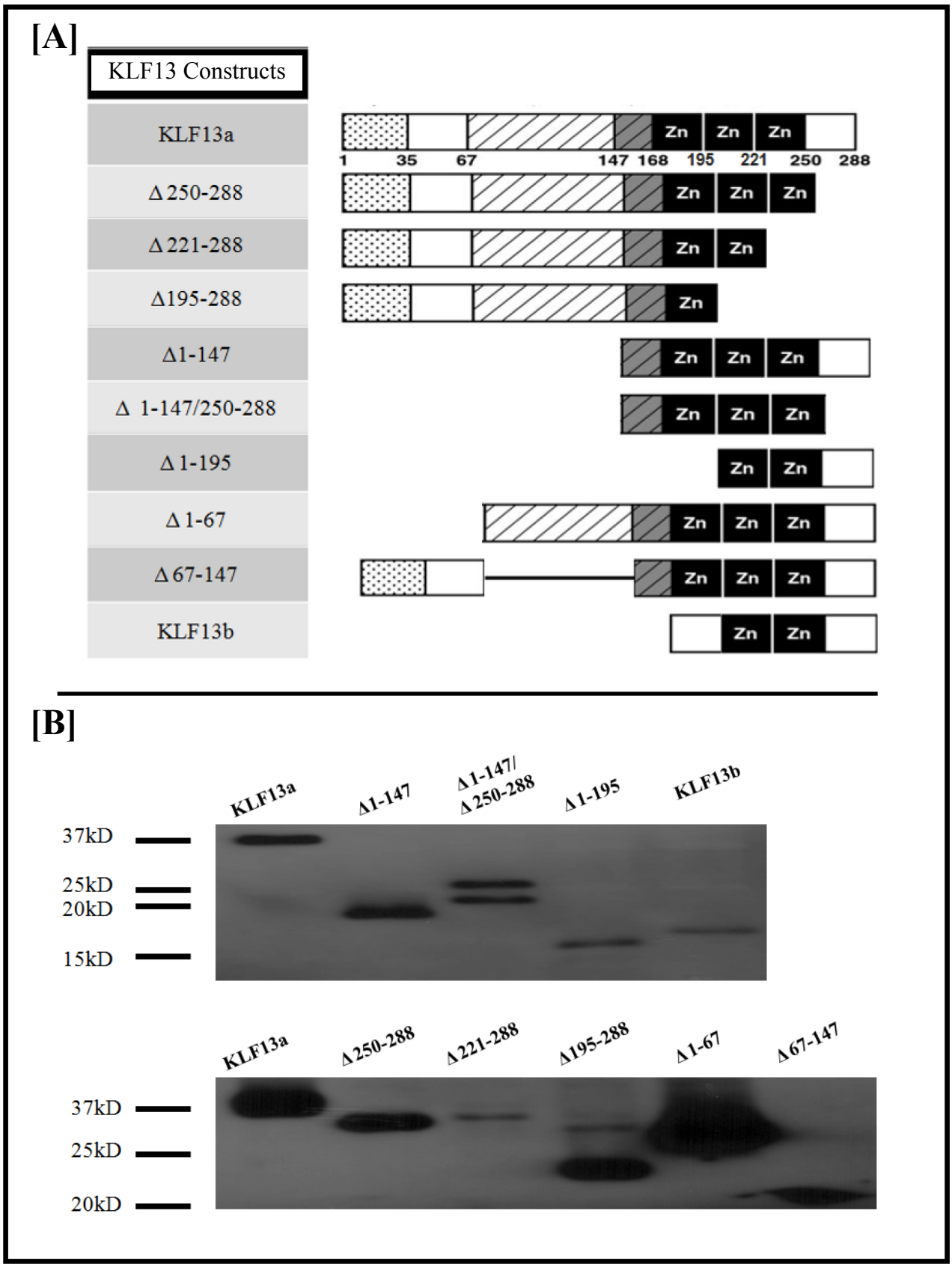
[A]
KLF13 Constructs
KLF13a
Δ250-288
Δ221-288
Δ195-288
Δ1-147
Δ 1-147/250-288
Δ1-195
Δ1-67
Δ67-147
KLF13b
Zn
1
35
67
147
168
195
221
250
288
[B]
KLF13a
Δ1-147
Δ1-147/ Δ250-288
Δ1-195
KLF13b
37kD
25kD
20kD
15kD
KLF13a
Δ250-288
Δ221-288
Δ195-288
Δ1-67
Δ67-147
37kD
25kD
20kD

Figure 3.9: Production of KLF13 constructs. (A) Schematic representation of the HA-tagged KLF13 mutants produced as described under Section 2.1 ‘‘Material and Methods’’. (B) 10μg of each of the construct expressing truncated KLF13 proteins was transfected into AD293 cells, and whole cell extracts were made 48 h post-transfection. 10μg of each extract was separated by SDS-PAGE and Western blotted with an anti-HA antibody.

To identify the domains/regions responsible for KLF13's nuclear localization, the full-sized and truncated HA-KLF13 were expressed in AD 293 cells and cellular localization of the fusion products was monitored by immunofluorescence using an HA-antibody (**figure 3.10**). Fluorescence of HA alone was shown to be present throughout the cell. In contrast, the majority of full-sized HA-KLF13 accumulated in the nucleus, indicating the presence of a strong NLS. Neither the deletion of the N-terminal region of the protein (Δ1-147aa) nor the distal C-terminal tail (Δ 250-288aa) had an effect on the nuclear localization of the protein. It is the serial deletion of a zinc-finger at a time that progressively reduced the nuclear localization of KLF13 constructs. Although at a very low level, even a single zinc-finger was capable of translocating the protein to the nucleus. Similar to the nuclear localization studies of Sp1 [146], our results suggest that the overall tertiary structure formed by the three zinc-fingers is essential for the nuclear localization of KLF13.

To evaluate the requirement of each zinc-finger for DNA-binding, an EMSA using radioactive probe corresponding to the proximal CACCC element of the BNP promoter was conducted on nuclear extracts of several KLF13 deletion constructs that contained various deletions of the zinc-finger motifs. As shown in **figure 3.11**, the full KLF13 and the Δ250-288aa construct, although with a lower intensity band, were capable of binding to the DNA probe. On the other hand, the deletion of the third-zinc finger totally abolished the binding of KLF13 to the consensus CACCC element, suggesting its absolute requirement for DNA binding. Furthermore, both the Δ 1-147aa, which contained the three zinc-fingers, and the Δ 1-195aa construct, which lacked the first zinc-finger, were capable of binding to the DNA probe. Thus, it appears that the first zinc-finger is dispensable for DNA binding and its function might be related to sequence specificity instead.

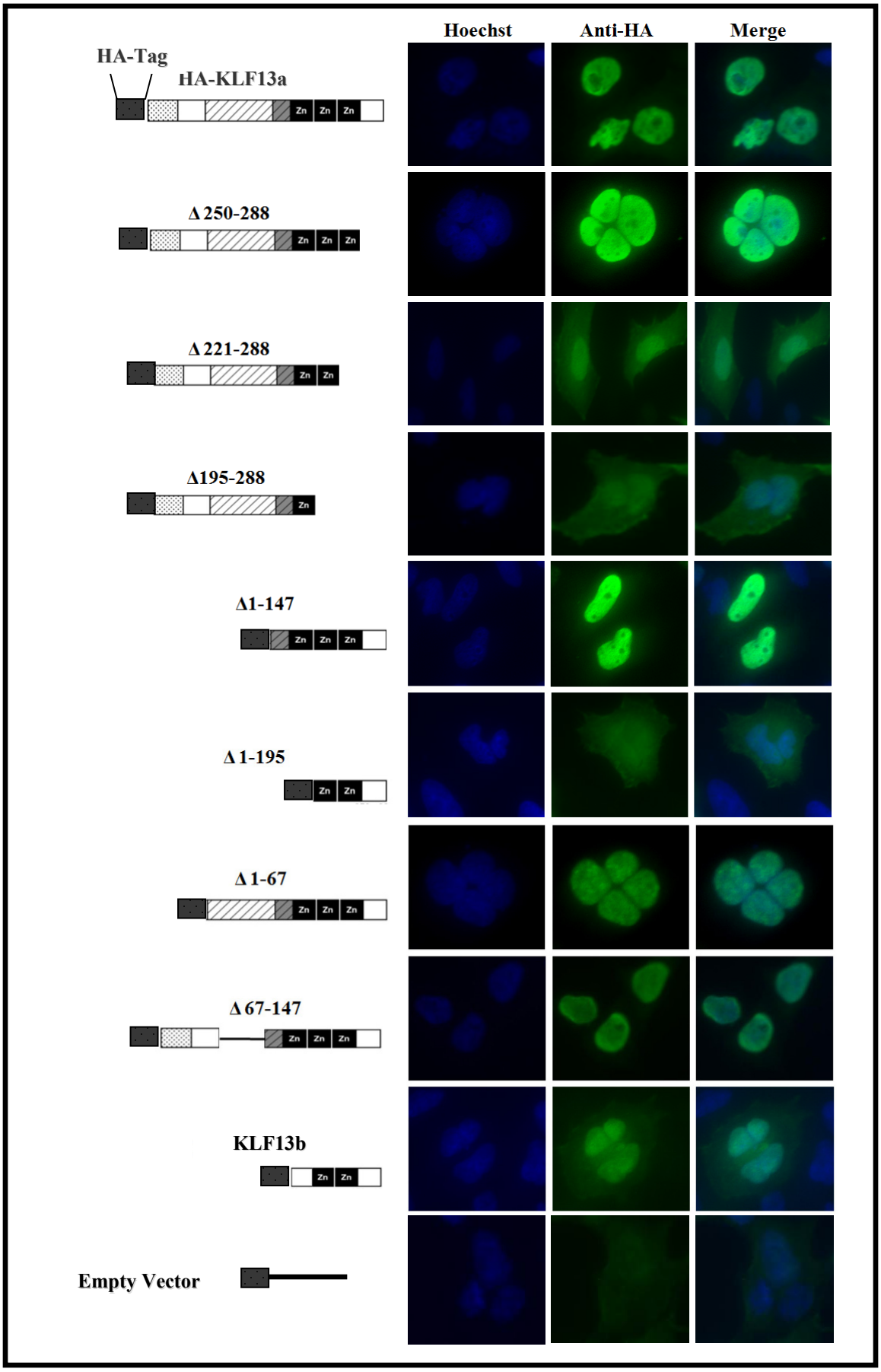
Hoechst
Anti-HA
Merge
HA-Tag
HA-KLF13a
Zn Zn Zn
Δ 250-288
Zn Zn Zn
Δ 221-288
Zn Zn
Δ195-288
Zn
Δ1-147
Zn Zn Zn
Δ 1-195
Zn Zn
Δ 1-67
Zn Zn Zn
Δ 67-147
Zn Zn Zn
KLF13b
Zn Zn
Empty Vector

Figure 3.10: Cellular localization of HA-tagged KLF13 protein constructs.

Fluorescence microscopy for AD293 cells transfected by 10μg of each of the construct represented in the right side. The green color shows the Alexa 488 conjugated secondary antibodies against the anti-HA antibody. The nuclei are visualized by Hoechst 33424 autofluorescence. Staining of cells transfected with the backbone pCGN (empty vector) is used as background controls.

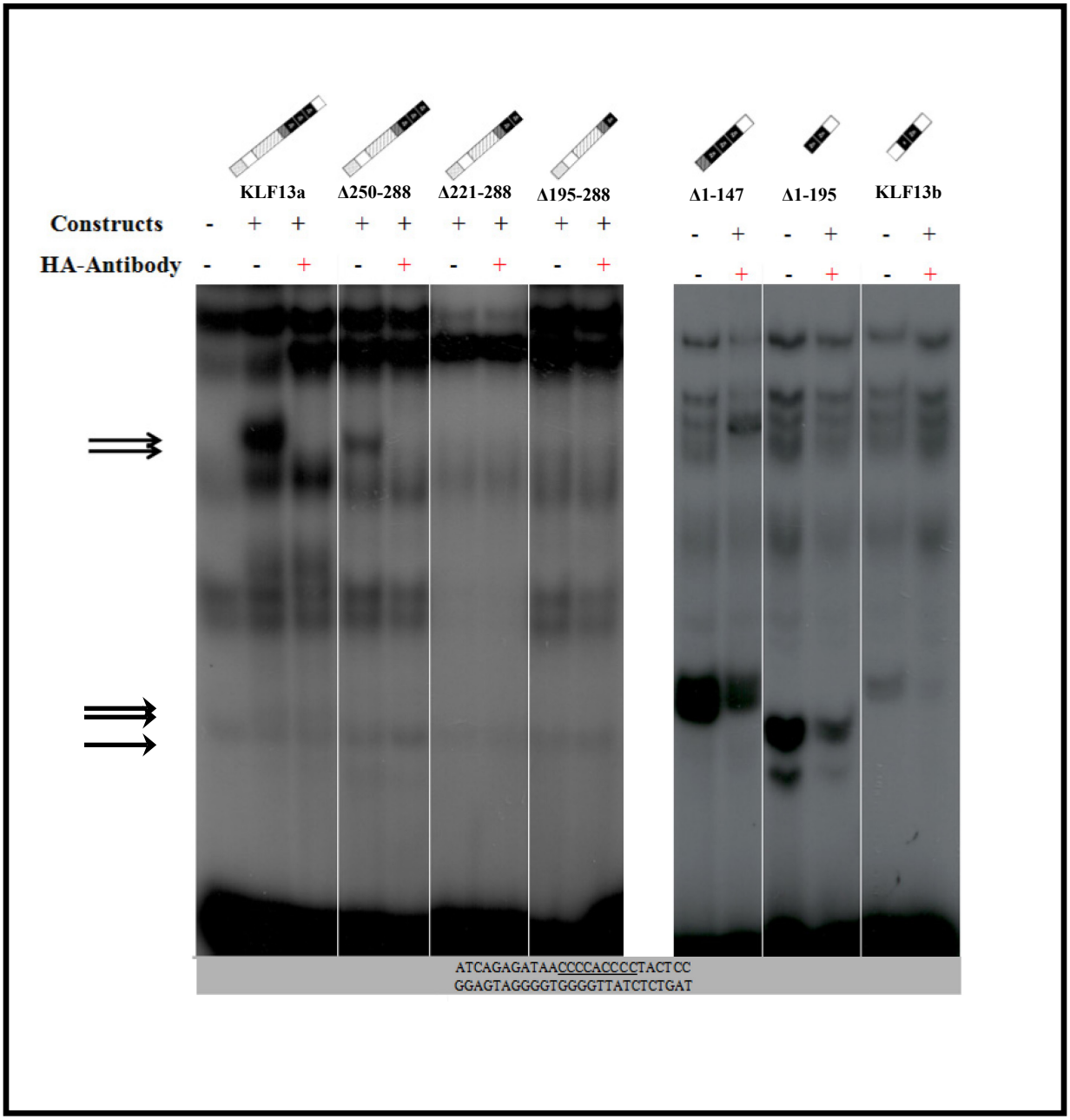
KLF13a
Δ250-288
Δ221-288
Δ195-288
Δ1-147
Δ1-195
KLF13b
Constructs
HA-Antibody
ATCAGAGATAACCCCACCCCTACTCC
GGAGTAGGGGTGGGGTTATCTCTGAT

Figure 3.11: Determining the zinc-finger motifs required for KLF13-DNA binding.

Electrophoretic mobility shift assays (EMSA) of several HA-tagged KLF13 constructs that contained various deletions of the zinc-finger motifs; a schematic representation of the HA-tagged KLF13 mutants utilized is located above the corresponding lanes. The DNA probes utilized here are derived from the proximal CACCC element of the BNP promoter shown previously to be a KLF13 response element. The probe sequence is provided beneath the EMSA film. The radioactive probes were incubated with either the nuclear extract of control or KLF13 transfected AD293 cells. The arrowheads show KLF13 construct binding.

Next, the transcriptional activities of the generated KLF13 constructs were assessed on the proximal -80bp BNP promoter. In comparison to the -699 ANF promoter, the -80bp BNP promoter is shorter and contains fewer known TFs binding elements. In addition, the BNP promoter contains a single CACCC element. **Figure 3.11** shows that deleting the serine- rich C-terminal tail (250-288aa) of the protein did not result in a significant drop in the activation of the BNP promoter, but rather caused a right shift in the dose-response curve, likely reflecting a lower level of protein accumulation. However, and in correlation to our EMSA studies, **figure 3.11** shows that deletion of the last zinc-finger had led to a severe drop in promoter activation, indicating that KLF13 transcriptional activation is dependent on its DNA-binding. The C-terminal region of the protein, Δ 1-147aa, which showed preferential localization to the nucleus and was capable of maintaining DNA-binding, was unable to recapitulate the transcriptional activity of the full-KLF13 construct, indicating the loss of a transactivation domain (TAD) located in the N-terminal region of the protein. While deletion of the 1-67aa did not result in a significant drop in the activation of the BNP promoter but caused a right shift in the dose-response curve, the deletion of 67-147aa decreased significantly the promoter activation, indicating the presence of a TAD within that region.

Together, these results indicate the importance of the structural integrity of the three zinc-fingers for DNA binding, nuclear localization, and transactivational activities of KLF13. In addition, it seems that KLF13's TAD is located within 67-147aa of the protein.

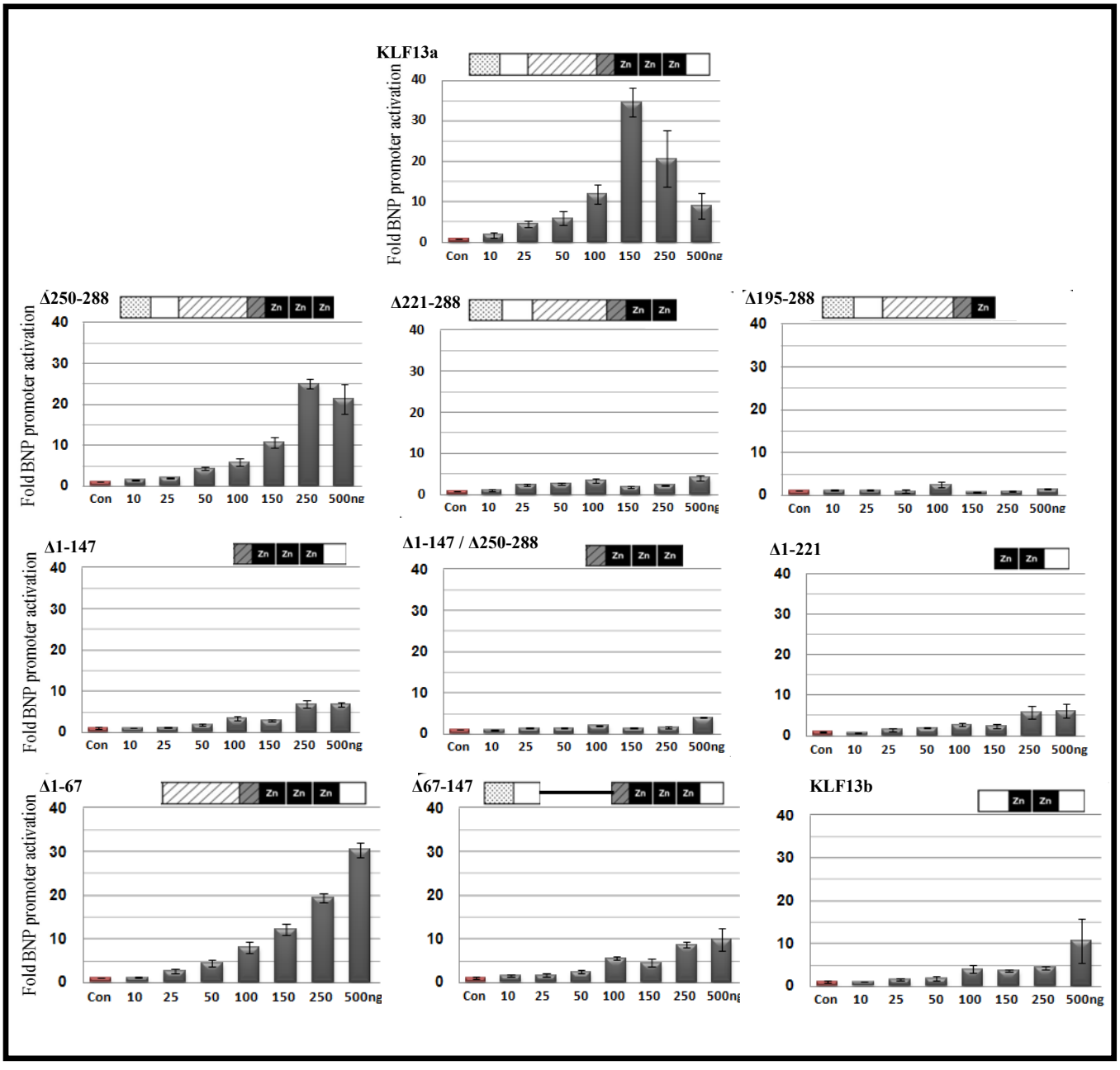
KLF13a
Fold BNP promoter activation
Zn Zn Zn
0 10 20 30 40
Con 10 25 50 100 150 250 500ng
Δ250-288
Δ221-288
Δ195-288
Δ1-147
Δ1-147 / Δ250-288
Δ1-221
Δ1-67
Δ67-147
KLF13b

Figure 3.12: Structure-function analysis of KLF13 using minimal BNP promoter.

Transient co-transfections were carried out in NIH 3T3 cells using an increasing dosage of the indicated/schematized KLF13 constructs and a constant level of the -120bp BNP-Luc reporter. Promoter activity is expressed as a ratio of the luciferase activity recorded with the co-transfection of KLF13 constructs to the activity without KLF13 co-transfection (fold change). The results shown are representations of three different experiments carried out in duplicates.

3.4 Determination of KLF13's synergy domains

In order to determine the important domains of KLF13 for synergy with GATA4, NKX2.5, TBX5, CATF1, and PEX, a synergistic structure-function analysis was pursued. The study was conducted utilizing the KLF13 constructs Δ250-288aa, Δ1-67aa, Δ67-147aa, Δ1-147aa, and Δ1-195aa in a luciferase assay on the ANF promoter. Consistent with our previous results on -137 BNP, **figure 3.12.A** shows that the N-terminal domain (67-147aa) of KLF13 contains a potent transactivational domain, and deletion of that region drastically reduced KLF13-induced transcriptional activity on the -699bp ANF promoter.

The structure-function analysis of KLF13 synergistic activity with GATA4 showed the implication of the N-terminal (1-147aa) in the synergy with GATA-4; a secondary role for the C-terminal tail of KLF13 (250-288aa) is suggested (**figure 3.13.B)**. Consistent with our previous results, GATA-4 was capable of potentiating KLF13 transcriptional activity by approximately 3 folds. Although the Δ1-67aa and Δ67-147aa constructs still maintained a synergistic interaction with GATA-4, the Δ 1-147aa construct with a full deletion of the N-terminal had an abrogated GATA-4 synergistic interaction. It appears that an N-terminal extension to the zinc-finger domain is required for synergy with GATA-4. In addition, although deletion of the serine-rich C-terminal tail (250-288aa) of KLF13 had a reduced fold synergy with GATA-4 by at least one-fold, the C-terminal tail containing constructs Δ1-147aa and Δ1-195aa were unable to induce synergy with GATA-4. Thus, it appears that the serine-rich region has a secondary role for synergy with GATA-4. Intriguingly, these two constructs, Δ1-147aa and Δ1-195aa, inhibited the transcriptional activity of GATA-4 on the ANF promoter. The transcriptional inhibition might be due to the DNA-binding capability of the two constructs, which might disrupt the GATA-4 containing protein-DNA complex on the ANF promoter.

The structure-function analysis of KLF13's synergistic activity with NKX2.5 also implicated the N-terminal (1-147aa) in the synergy with NKX2.5; a secondary role for the C-terminal tail of KLF13 (250-288aa) is also suggested **(figure 3.13.C)**. Consistent with our previous results, NKX2.5 was capable of potentiating KLF13 transcriptional activity by approximately 3.5 fold. Although the Δ1-67aa and Δ67-147aa constructs still maintained a synergistic interaction with NKX2.5, the Δ 1-147aa construct, with a full deletion of the N-terminal, had an abrogated NKX2.5 synergistic interaction. It appears that an N-terminal extension to the zinc-finger domain is required for synergy with NKX2.5. Intriguingly, deletion of the serine-rich C-terminal tail (250-288aa) of KLF13 potentiated the fold synergy with NKX2.5 to approximately seven folds. Thus, it appears that the serine-rich region has a secondary role for synergy with NKX2.5.

The structure-function analysis of KLF13's cooperativity with TBX5 showed that the synergy is mediated via KLF13's zinc-finger domain **(figure 3.13.D)**. A secondary enhancing involvement of the C-terminal tail was also suggested. Consistent with our previous results, TBX5 was capable of potentiating KLF13 transcriptional activity by approximately 6.5 fold. This synergy was still maintained after the deletion of the N-terminal region, 1-147aa, of KLF13. Although Δ67-147aa constructs still maintained a synergistic interaction with TBX5, the Δ1-67aa construct had an abrogated synergy with TBX5. From the full synergistic activity of Δ 1-147aa, it seems that deleting 1-67aa region exposes a domain, located between 67-147aa, inhibitory for synergy with TBX5. Similar to the synergy with GATA-4, deletion of the serine-rich C-terminal tail (250-288aa) of KLF13 reduced the fold synergy with TBX5 by approximately 2.5 fold. Thus, it appears that the serine-rich region has a secondary role in synergy with TBX5.

Similar studies on the synergy of KLF13 with PEX1, represented by **figure 3.13.E**, showed that the synergy is probably mediated via KLF13's zinc-finger domain. A secondary enhancing involvement of the C-terminal tail and an inhibitory role for the N-terminal 67-147aa region are suggested. Consistent with our previous results PEX1 was capable of potentiating KLF13 transcriptional activity by approximately 6 folds. This synergy was still maintained after the deletion of N-terminal region, 1-147aa, of KLF13. Although Δ67-147aa constructs still maintained a synergistic interaction with PEX1, the Δ1-67aa construct had a lower synergy with PEX1. From the synergistic activity of Δ 1-147aa, it seems that deleting the 1-67aa region exposes a domain, located between 67-147aa, inhibitory for the synergy with PEX1. Similar to the synergy with GATA-4 and PEX1, deletion of the serine-rich C-terminal tail (250-288aa) of KLF13 reduced the fold synergy with PEX1 by approximately 1.5 fold.

Studies similar to the aforementioned luciferases assays were also conducted on the synergy of KLF13 with CATF1 **(figure 3.13.F)**. Our data implicated the C-terminal domain 195-288aa in synergy with CATF1; a secondary enhancing role for the C-terminal tail of KLF13 (250-288aa) was also suggested. Consistent with our previous results CATF1 was capable of potentiating KLF13 transcriptional activity by approximately 4.5 folds. None of the N-terminal deletion constructs were able to maintain synergy with CATF1. Intriguingly, Δ1-195aa, which lacks both the N-terminal and the first zinc-finger of KLF13, was able to strongly synergize with CATF1. It appears that deleting the N-terminal domains of KLF13 had a negative effect on the protein structure required for synergy with CATF1. Similar to the case with NKX2.5, deletion of the serine-rich C-terminal tail (250-288aa) of KLF13 potentiated the fold synergy with CATF1 by approximately one fold. Thus, it appears that the serine-rich region has a secondary role in synergy with CATF1.

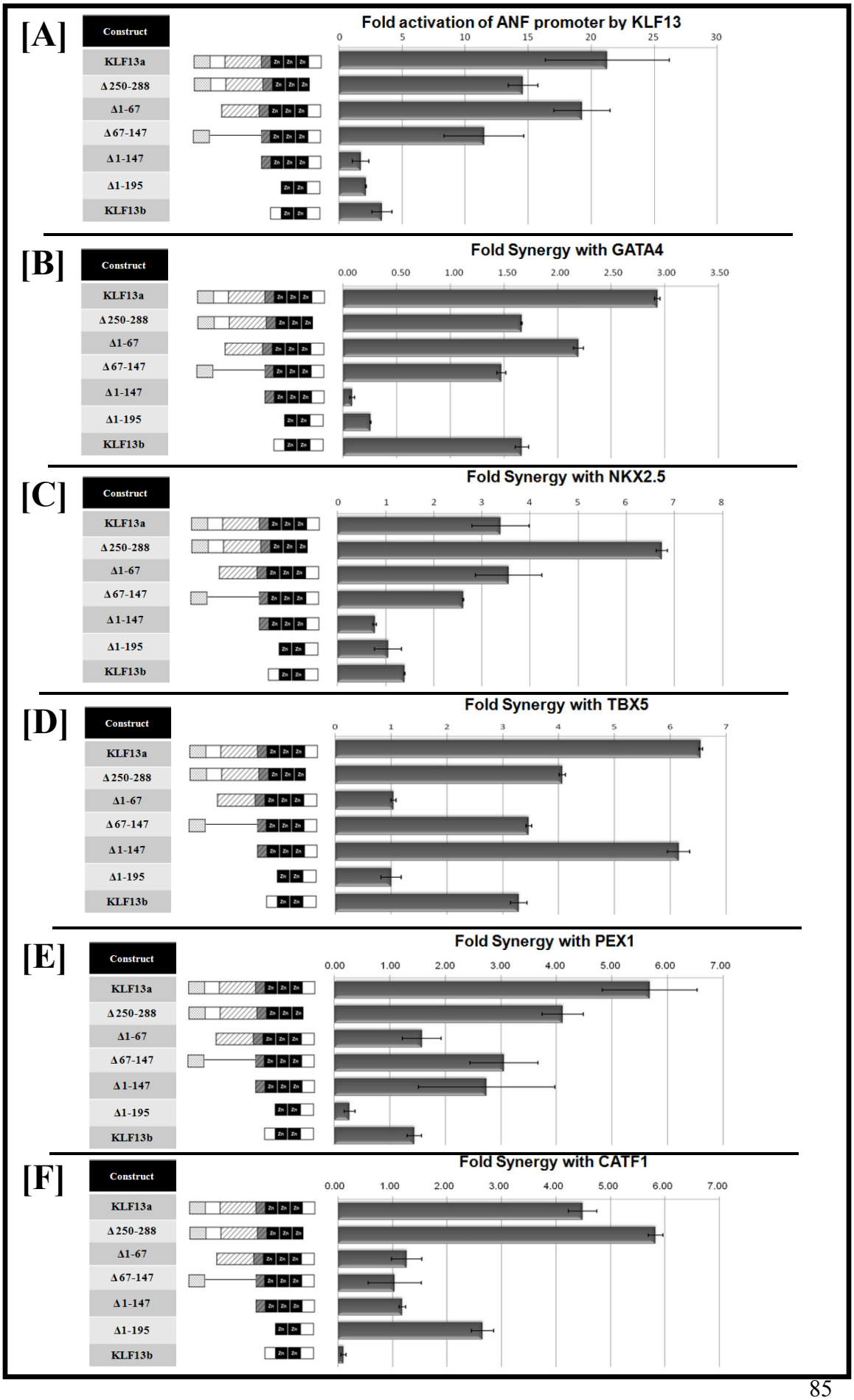
[A]
Construct
KLF13a
Δ250-288
Δ1-67
Δ67-147
Δ1-147
Δ1-195
KLF13b
Fold activation of ANF promoter by KLF13
0
5
10
15
20
25
30
[B]
Construct
KLF13a
Δ250-288
Δ1-67
Δ67-147
Δ1-147
Δ1-195
KLF13b
Fold Synergy with GATA4
0.00
0.50
1.00
1.50
2.00
2.50
3.00
3.50
[C]
Construct
KLF13a
Δ250-288
Δ1-67
Δ67-147
Δ1-147
Δ1-195
KLF13b
Fold Synergy with NKX2.5
0
1
2
3
4
5
6
7
8
[D]
Construct
KLF13a
Δ250-288
Δ1-67
Δ67-147
Δ1-147
Δ1-195
KLF13b
Fold Synergy with TBX5
0
1
2
3
4
5
6
7
[E]
Construct
KLF13a
Δ250-288
Δ1-67
Δ67-147
Δ1-147
Δ1-195
KLF13b
Fold Synergy with PEX1
0.00
1.00
2.00
3.00
4.00
5.00
6.00
7.00
[F]
Construct
KLF13a
Δ250-288
Δ1-67
Δ67-147
Δ1-147
Δ1-195
KLF13b
Fold Synergy with CATF1
0.00
1.00
2.00
3.00
4.00
5.00
6.00
7.00

Figure 3.13: Structure-function analysis of KLF13 domains involved in synergy with GATA-4, NKX2.5, TBX5, CATF1, and PEX1 on the -699bp ANF promoter.

Transfections were carried out using the -699bp ANF promoter. In (A) KLF13 expression vectors were co-transfected with the ANF reporter, whereas in (B, C, D, E and F) GATA-4, NKX2.5, TBX5, PEX1, and CATF1 expression vectors was also included, respectively. The synergy results represent the ratio of promoter activation by KLF13 in the presence of its functional partner over the sum of promoter activation by KLF13 and its partner alone.

3.3. Analysis of KLF13's alternative splicing isoform.

During the course of this study a splice variant isoform of KLF13 was successfully cloned. In this uncharacterized variant the cryptic exon 1b is alternatively used to generate an isoform with only two C2H2-type zinc-fingers, instead of exon 1a of the first isoform which encodes the first N-terminal zinc-finger and the N-terminal tail of KLF13a (figure **3.14.A**). Here we will refer to the first and longer identified isoform as KLF13a and the novel and shorter one as KLF13b. To assess the distribution of the two KLF13 transcripts in different tissues during development (ED 11.5, 13.5, 16.5 and 30 day- old male mice) we used two pairs of oligonucleotides designed to span the splice junctions. As shown in **figure 3.14.B**, KLF13a was detected in all the tissue (heart, lung, brain, limb and liver) analyzed at ED 11.5 with a very weak band in the heart, lung and liver. In the same embryonic stage KLF13b was detected robustly in brain and lung tissues, but it was not detected in heart, limb or liver tissues. At ED 13.5 and 16.5 the two isoforms were detected in all tissues analyzed except for the second isoform in the liver; a low expression of the first isoform in ED 16.5 was also observed. In male adult mice, expression of the two isoforms was differentially regulated. KLF13a was robustly expressed in the brain, thyroid, thymus, and brown fat in comparison to the other tissues analyzed. On the other hand, KLF13b showed a robust expression in the kidney and liver and a relatively lower expression in the ventricles, atria, skeletal muscles, spleen, brain, and thymus. In some adult tissues (including liver, kidney, thyroid, and brown fat), the abundance of the two isoforms was inversely correlated. In other adult tissues (bone, lung, small intestine) the expression of the two isoforms was barely detectable. The different spatiotemporal expressivity of the two isoforms, especially in E11.5 and in adult mice, raises the possibility of differential regulation and function of the two isoforms during development.

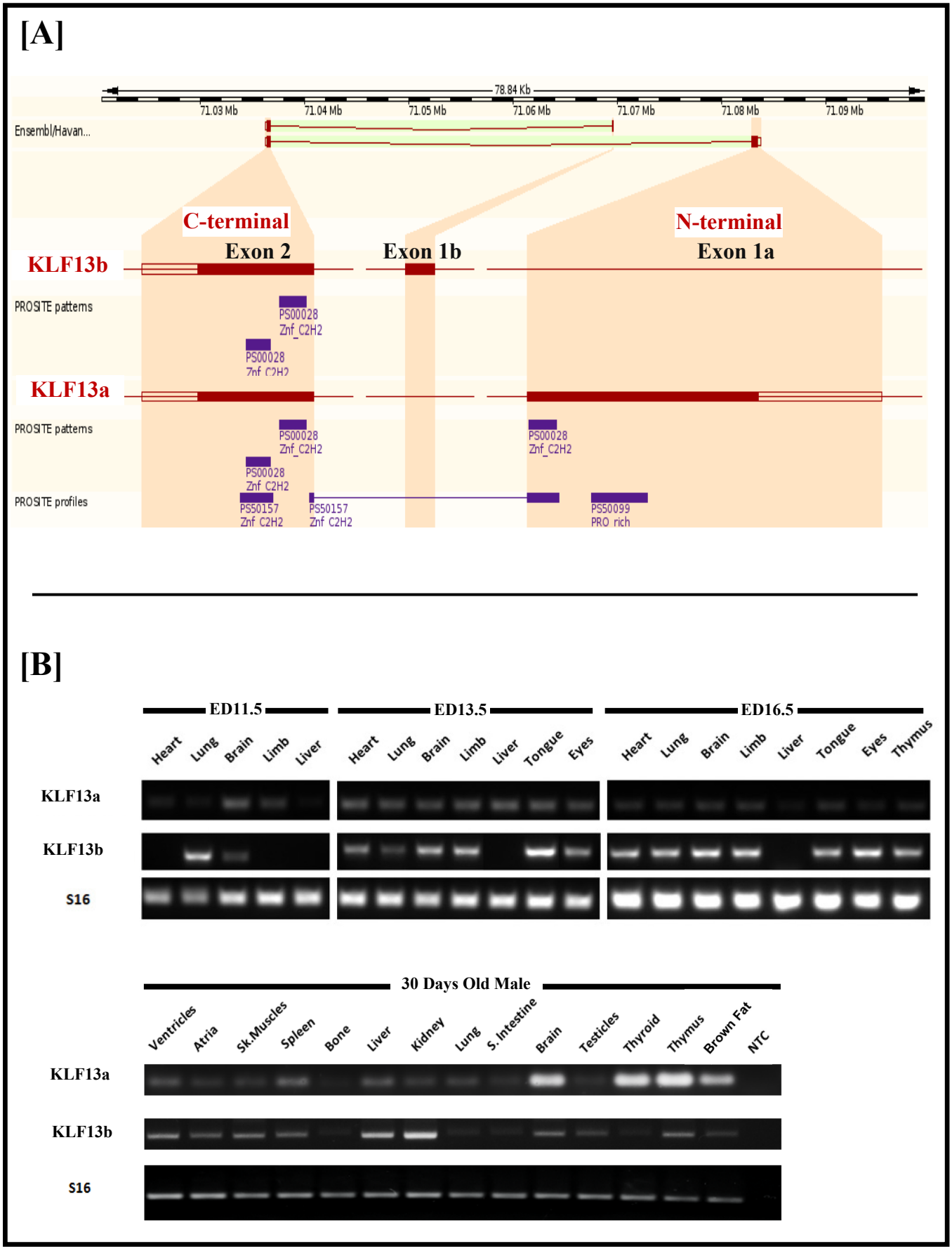
[A]
78.84 Kb
71.03 Mb
71.04 Mb
71.05 Mb
71.06 Mb
71.07 Mb
71.08 Mb
71.09 Mb
Ensembl/Havan...
C-terminal
N-terminal
Exon 2
Exon 1b
Exon 1a
KLF13b
PROSITE patterns
PS00028
Znf_C2H2
KLF13a
PROSITE patterns
PS00028
Znf_C2H2
PROSITE profiles
PS50157
Znf_C2H2
PS50099
PRO_rich
[B]
ED11.5
ED13.5
ED16.5
Heart
Lung
Brain
Limb
Liver
Tongue
Eyes
Thymus
KLF13a
KLF13b
S16
30 Days Old Male
Ventricles
Atria
Sk.Muscles
Spleen
Bone
Liver
Kidney
Lung
S.Intestine
Brain
Testicles
Thyroid
Thymus
Brown Fat
NTC
KLF13a
KLF13b
S16

Figure 3.14: Schematic representation of the KLF13 isoforms and their distributions during embryonic development. A) Schematic representation of the KLF13 locus. The N-terminal encoding exon 1, encoding the transactivation domain and the N-terminal zinc-finger, is spliced out and an alternative cryptic exon is used to generate an isoform with only two C2H2-type zinc-fingers. The illustration was generated by www.ensembl.org. B) RT-PCR carried out using primers specific to each of the isoforms in different tissues during development (ED 10.5, 13.5 and 16.5).

To assess the biochemical properties of the novel splice variant, KLF13b, we carried out its analysis in conjunction with the generated KLF13 clones. We first sub-cloned the isoform into a pCGN expression vector to generate the HA-tagged protein. As shown in Fig. 2C, the appropriate size HA-fusion KLF13-Isoform was produced (**figure 3.9.B**). In AD 293 cells transfected with the HA-KLF13b expression vector, immunofluorescence microscopy toward the HA-tag showed a lower nuclear localization preference of the isoform in comparison to the KLF13a (**figure 3.10**). The discrepancy between the isoforms' nuclear localization might be contributed to the lack of the first zinc finger in the second isoform or/and different posttranslational modifications in KLF13b. Note that the Δ1-195aa construct had a lower nuclear localization preference thus indicating a positive contribution of the alternative exon 1 on the nuclear localization of the splice variant isoform KLF13b. Using EMSA, KLF13b was capable of maintaining DNA binding to the proximal CACCC element of the BNP promoter (**figure 3.11**). This DNA-binding of the isoform is consistent with our previous hypothesis that the N-terminal zinc-finger is dispensable for DNA binding and its function might be related to sequence specificity rather than binding.

The transcriptional activity of the novel isoform was assessed using the ANF and BNP promoters. **Figure 3.12** shows that although the isoform is capable of activating the single CACCC element containing the BNP promoter, this activation could not recapitulate the full activity of KLF13a, indicating the absence of a potent trans-activation domain in the alternative exon 1b. We then directly tested whether KLF13b antagonizes KLF13a transcriptional activity. As seen in **figure 3.15**, when increasing doses of KLF13b cotransfected with KLF13a, an inhibition of promoter activation was observed. Thus, it appears that the presence of two KLF13 isoforms constitutes an additional level of control to the CACCC element mediated transcriptional regulation.

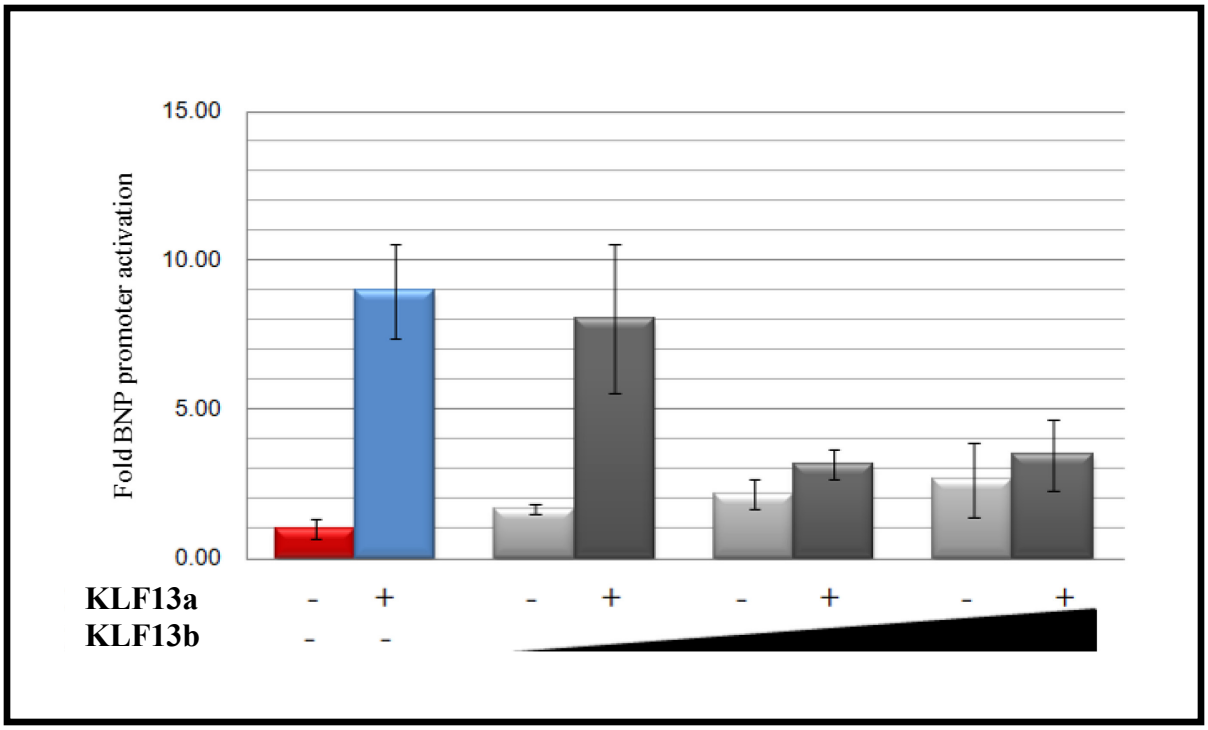
15.00
10.00
5.00
0.00
Fold BNP promoter activation
KLF13a - + - + - + - +
KLF13b - -

Figure 3.15: KLF13b antagonizes KLF13a transcriptional activity on the -699bp ANF promoter.

The study was conducted with a constant dose of Full-KLF13 (50ng) and different doses of the KLF13-Isoform (25ng, 50ng and 75ng). Promoter activity is expressed as a ratio of the luciferase activity recorded with the co-transfection of Full-KLF13, KLF13-Isoform constructs, or both to the activity without KLF13 co-transfection (fold change). The experiment was carried out in triplicate.

The synergy of KLF13b with GATA-4, TBX5, NKX2.5, PEX1, and CATF1 was also analyzed in conjunction with those of the generated KLF13 clones (**figure 3.13**). Of the synergistic partners KLF13b was capable of maintaining a strong synergy with GATA-4 (1.6 fold synergy) and TBX5 (3.5 fold synergy). Interestingly, the protein product of exon 2, the Δ1-195aa construct, failed in recapitulating the synergistic interaction with GATA-4 or TBX5. Thus it appears that exon 1b of KLF13b is involved in the interactions with GATA-4 and TBX5. In the case of NKX2.5 and PEX1, a lower synergistic interaction (lower than 1.5fold synergy) was observed with KLF13b. Interestingly, the low synergy with NKX2.5 was not significantly different than synergy with the protein product of exon 2, the Δ1-195aa construct. Thus, it seems that the alternative exon 1b does not contribute to the functional partnership with NKX2.5 and rather via the two zinc-fingers. On the other hand, the protein product of exon 2, the Δ1-195aa construct interacted antagonistically with PEX1. However, KLF13b was capable of maintaining low synergy with PEX1. Thus, it appears that the synergy is mediated via the alternative exon 1b. Intriguingly, although a strong synergistic interaction (2.5 fold synergy) was observed when exon 2 and CATF1 were co-transfected, an antagonistic functional interaction was observed with CATF1 and KLF13b. Thus, it appears that the alternative exon 1b mediates the antagonistic interaction between KLF13b and CATF1 on the ANF promoter.

4. Discussion:

In this thesis we show that KLF13, a member of the kruppel-like factors (KLFs) family, genetic network cardiac growth and differentiation. identified at least three KLF13 binding sites on the ANF promoterTBX5, NKX2.5, PEX1, and CATF1 on the ANF promoter. In addition our structure-function analysisof KLF13 and the dissected partnership profile with the other transcription factors suggested a possible mechanism of action that involves the histone acetyltransferases CBP/p300. Also, we KLF13 isoforms distinct biochemical properties and spatiotemporal expression. The existence of alternatively spliced KLF13 isoform may provide a new paradigm that may help to decipher the genotype-phenotype relation in patients with congenital heart diseases.

4.1. CACCC boxes, KLFs and cardiac transcription.

Analysis of several cardiac promoters revealed the presence of several CACCC boxes (putative binding sites of the KLF family) within their regulatory domains, which their importance in regulating cardiac transcription. Among them, the ANF promoter was found to harbour at least three of these CACCC elements; other promoters also include BNP, cardiac actin, β-myosin heavy chain and cardiac troponin C (cTnC) [48]. Interestingly, multiple KLF proteins have preferential binding to similar GC/GT-rich elements attributed to the highly homolog C-terminal DNA-binding zinc-finger motifs. It is the heterogeneity of the N-terminal domains that may explain in part the diverse biochemical mechanisms by which KLFs regulate transcription under various physiological conditions and their diverse influence on cellular processes [112, 120]. The disparate interaction with a diverse repertoire of cofactors not only allows the distinct KLF members

to differentially regulate a distinct subset of genes, but also divergently regulates the same gene using the same DNA-element [120].

ve the function of KLFs in the heart: KLF5 in cardiac fibroblasts [116], two KLF15 [117] [118] and a brief describing a cardiac phenotype in systemic KLF10-null mice [119]. r, describes the role of KLF13 in cardiomyocytes during embryonic development [48]. In our attempt to understand the of KLF13 during development, we identified the cardiac master regulator GATA4 as functional partner of KLF13 in regulating BNP promoter activity via an evolutionary conserved CACCC box. highly enriched in the heart during embryonic development in the atrial myocardium and the endocardial layer, at D10.5, in a pattern that overlaps that of GATA-4. Thus, our results suggest a role of KLF13 in the regulatory network of early stages of cardi [121]. The importance of in the heart was by the observed cardiac defects in KLF13 knockdown Xenopus embryos exhibit ventricular hypotrabeculation, atrial septal defects, hypoplastic myocardium delayed atrioventricular cushion formation and maturation of valves [121]. Some of these defects (e.g. myocardial hypoplasia and atrial septal defects) were also observed in mice with reduced GATA-4 levels or activity [147]. Interestingly, KLF13 and GATA-4 the cyclin D1 promoter a role for these proteins in embryonic cardiomyocyte proliferation, may explain the hypoplastic hypotrabeculat observed in mice hypomorphic with KLF13 or GATA-4.

Most of studies KLF13 were towards analysis of its contribution to the hematopoietic system; is a key regulator of erythropoiesis and is involved in the development of B and T cells at multiple stages [133, 148]. KLF13 expression was documented in several hematopoietic tissues including the spleen, liver, and thymus. Interestingly, viable KLF13 -/- mice ha reduced numbers of circulating erythrocytes, larger

spleens, and increased thymuses. It was found that KLF13 the cell cycle progression marker cyclin B. the anti-apoptotic factor BCL-XL [149].

In a step towards analyzing KLF13's mechanism of action and in deciphering its role in the genetic networks regulating cardiac development, we pursued the identification of factor(s) that might cooperate with KLF13 on the ANF promoter. Our use of ANF as the primary model with which to study KLF13's cardiac-specific transcription was prompted by its early expression during development and its atrial co-prevalence with KLF13. Using the ANF and through the identification of three KLF13 regulatory elements (centered at -365, -515 and -535) that were juxtaposed to several cardiac response elements including GATA, PERE, NKE, TBE and CARE, we stumbled upon a novel functional interaction of KLF13 with the cardiac transcription factors TBX5, NKX2.5, PEX1 and CATF1 that potentiates KLF13 transcriptional activity on the ANF promoter. A direct physical interaction was shown to accompany KLF13's synergy with TBX5, NKX2.5 and PEX1. Interestingly loss of function of either NKX2.5 or TBX5 was associated with similar septal defects and reduced heart mass as those seen in KLF13 loss-of-function, thus indicating the integration of these transcription factors in to a common pathway [134].

4.2. KLF13 and NKX2.5.

The homeobox gene NKX2.5 is one of the earliest known markers of vertebrate heart development. It is expressed quite early during development, at EDD 7.5 in mice, and continues to be expressed at a high level in the heart through adulthood [52]. Targeted disruption of the murine homolog resulted in embryonic lethality at EDD 9–10 due to the failure of the heart tube to progress to the looping stage [52]. Detailed analysis of the null mice indicated that NKX2.5 is required for proper chamber specification [11]. Humans carrying mutations in the NKX2.5 homolog (**Figure 1.2.B**), most of which occur within the

homeodomain, suffer from septal defects, conduction abnormalities, thinning of the ventricular myocardium, and hypotrabeculation [11, 71]. Moreover, mice with conditional knockout (CKO) of NKX2.5, in the specific lineage originating from Islet-1 (Isl1) expressing progenitors, demonstrated persistent truncus arteriosus, trunkwhich is an interruption of the aortic arch, and membranous-type ventricular septal defects [150]. Interestingly, these defects overlap with the defects seen in KLF13 loss-of-function in xenopous embryos [134] and KLF13-/- mice [not published]. The earlier expression of NKX2.5, the atrial co-localization with KLF13, the overlapping defects upon loss-of-function, and the synergistic transcriptional activation all point to an integrated interaction between KLF13 and NKX2.5 during cardiac development, specifically in the atria. Our reported functional and physical interactions between NKX2.5 and KLF13 suggest ways in which mutations in NKX2.5 may alter protein-protein interactions with KLF13 and disrupt the tightly regulated spatial and temporal gene expression that is essential during cardiac development. In addition, NKX2.5, TBX5, and GATA-4 expression were reduced in KLF13-depleted xenopous embryos starting from stage 20 before the appearance any histological abnormalities. However, it is possible that KLF13 participates in a positive feedback loop that enhances expression of the cardiac transcription factors GATA-4, TBX5 and NKX2.5 to regulate cardiac gene expression in a spatiotemporal dose-dependent manner.

Our reported transcriptional interaction between NKX2.5-KLF13 is the first between members of the KLF and the NKX families. However, NKX2.5 was shown to interact with other members of zinc-finger-containing transcription factors including GATA-4 (contains two C4-type zinc-fingers) and ZAC1 (contains seven C2H2-type zinc-fingers). Interestingly, ZAC1 did not only show a strong functional synergy with NKX2.5 on the

ANF promoter utilizing theGC boxes, but ZAC1's zinc-fingers 5 and 6 physically associated with the homeodomain of NKX2.5 [151]. Although our synergy studies indicated the importance of the N-terminal domain of KLF13 to its functional partnership with NKX2.5, the physical interaction could be mediated in a homeodomain, zinc-finger-mediated fashion. Physical structure-function analysis of the interaction between KLF13 and NKX2.5 is ongoing in our lab.

ZAC1 is strongly expressed in the heart from cardiac crescent stages with a chamber-restricted pattern at the looping stage [151]. Homozygous and paternally derived heterozygous mice carrying an interruption in the ZAC1 locus showed decreased levels of chamber and myofilament genes, increased apoptotic cells, partially penetrant lethality, morphological defects including atrial and ventricular septal defects, and thinning of the ventricular walls [151]. It is interesting to test the binding of KLF13 to the identified ZAC1 binding elements, GC boxes, on the ANF promoter. It is possible that KLF13 and ZAC1 compete with each other for physical interaction with the homeodomain of NKX2.5. If NKX2.5 alternatively uses KLF13 and NKX2.5, it could be a unique mechanism to regulate cardiac spatiotemporal gene expression during development.

4.3. KLF13 and TBX5.

TBX5 is the gene mutated in human Holt-Oram Syndrome (HOS), a dominant disorder characterized primarily by upper fore-limb defects and heart abnormalities [91]. Intriguingly, the atrial septal defects and ventricular hypoplasia seen in HOS patients overlap with the defects seen in KLF13, NKX2.5 and GATA-4 loss-of-function [134]. An overlapping spatiotemporal expression is remarkable for TBX5, NKX2.5, GATA-4 and KLF13, especially in the atria and the outflow tract [92]. Mechanistically, TBX5 was shown to associate directlyphysically, and synergistically, with numbers of cardiac

transcription factors including NKX2.5 and GATA-4 to activate the expression of chamber-specific genes such as ANF in vitro [86]. Our reported KLF13-TBX5 physical and synergistic interaction emphasizes on the instructive role of TBX5 and the combinatorial interaction with KLF13, NKX2.5, and GATA-4 in lineage specification and morphogenesis of future chambers [86, 92].

To date, over 37 mutations in the TBX5 gene have been associated with Holt-Oram syndrome, and the majority introduce a premature stop codon within the T-box domain [152]. The deleterious effect of TBX5 mutations that effect the interactions with GATA4 and NKX2.5 support the existence of a tri-complex composed of the three transcription factors to regulate the expression of a subset of genes required for cardiac septal formation. The demonstration of a synergistic and physical interaction between TBX5 and KLF13 suggests similar conclusions in which mutations in TBX5 may alter protein-protein interaction with KLF13 which leads to a disruption in the tightly regulated spatial and temporal gene expression during cardiac development. Analysis of TBX5 point mutations can function as a Rosetta stone in understanding how a disruption of the combinatorial interactions of transcription factors can lead to specific birth defects [15].

Our reported transcriptional interaction between KLF13 and TBX5 is a first between the two transcriptional families. However, TBX5 was shows to interact with other members of zinc-finger containing transcription factors including the GATA-4 (a two C4-type zinc-finger containing protein) and SALL4 (an eight C2H2-type zinc-finger containing protein) [99, 100, 153]. Remarkably, coimmunoprecipitation showed the importance of the first zinc-finger motif of SALL4 and the C-terminal domain of TBX5 for the interaction between the proteins [153]. Our synergy analysis indicated the importance of the C-

terminal zinc finger domain of KLF13 and the C-terminal domain of TBX5 for maintenance of the synergy between the two proteins. Currently, a structure-function analysis of the physical interaction is ongoing in our lab.

Interestingly, human mutations in SALL4 were also implicated in upper limb and heart defects similar to those seen in TBX5 mutants. Although SALL4 showed a strong functional synergy with TBX5 on the Fgf10 promoter (Fibroblast growth factor 10), critical for limb outgrowth, the ANF promoter SALL4 counteracted the activation by TBX5. Interestingly, SALL4 did not influence the activation of the ANF promoter by NKX2.5 and GATA4, indicating that its repressive effects are specific to activation by TBX5[153]. Although the exact binding element of SALL4 is not yet determined [153], it is possible that its C2H2 type zinc-fingers could bind to KLF13 binding elements on the ANF promoter. It is possible that SALL4 and KLF13 compete for DNA-binding on specific CACCC elements and for the C-terminal protein-protein binding motif of TBX5 to regulate the spatiotemporal gene expression during cardiac development for chamber specification.

4.4. KLF13 and PEX1.

PEX1, Phenylephrine-induced Complex-1, is a novel transcription factor that is implicated in α1-adrenergic signalling in the heart. The protein contains 13 zinc-fingers of the C2H2 kruppel-like family zinc-fingers and binds to a GC-rich evolutionarily-conserved phenylephrine response element (PERE) on the proximal ANF promoter. Showing an expression overlap with KLF13, PEX1 expression is maintained throughout embryonic development in the atria and in the ventricular walls and trabeculae [94]. Physiologically, PEX1 upregulation was associated with hypertension and cardiac hypertrophy. Interestingly, PEX1 was shown to physically and functionally interact with GATA4 to cooperatively activate transcription of ANF and other hypertrophy induced genes [94, 95].

KLF13's role in cardiomyocyte embryonic proliferation; the physical and functional interaction of KLF13 with PEX1 and GATA4 proteins that mediate the nuclear response to α1-adrenergic receptors; and the overlapping spatiotemporal expression between KLF13, PEX1 and ANF during development are all indicative of the possible role of KLF13-PEX1 interactions in cardiac remodelling during hypertrophy. Remarkably, other KLF members were shown to have a role in cardiac hypertrophy ; these include KLF5 (null mice have reduced hypertrophic remodelling in response to angiotensin II infusion [116]), KLF15 (downregulated with hypertrophic stimulation and null mice developed severe eccentric hypertrophy and LV dysfunction with pressure overload [117]), and KLF10 (null male mice developed spontaneous pathological hypertrophy by 16 months of age [119]). Structure-function analysis of PEX1 is currently underway in our lab along with the domain(s) responsible for the interaction of KLF13 and GATA-4. However, similar to TBX5, our synergy study of KLF13 showed that the C-terminal, zinc-finger containing domain is capable of maintaining synergy with PEX1.

4.5. KLF13 and CATF1.

The CATF1 protein is a helicase protein renowned for its Swiss Army Knife-like multi-functionality. It was implicated in broad molecular processes including DNA replication, recombination, pre-mRNA splicing, and transcription [102, 103]. Several putative helicases were shown to be or proposed to be involved in the regulation of transcription [154]. However, very few were shown to also harbor features of classical transcriptional regulators such as sequence-specific DNA-binding and/or autonomous transcriptional activation. CATF1 was found to possess a sequence-specific, ATP-dependent DNA-binding activity. This allows it to bind to a hypersensitive, cis-acting myocyte-specific cardiac response element (CARE) located in the proximal region of the

ANF promoter; in addition, CATF1 was also found to have transactivational capabilities. The helicase-truncated CATF1 is also capable of dose-dependently activating the ANP promoter, supporting the hypothesis that CATF1 functions as a transcription factor (data not published). Here we not only report that KLF13 is capable of binding to the same CARE element on the ANF promoter, but also that it functionally interacts with CATF1 to potentiate the ANF promoter in a CARE element-dependent manner. KLF13 is the first identified functional partner of CATF1; however physical binding is still pending. To confirm independency of KLF13-CATF1 synergy from the DNA helicase activity of CATF1, it would be interesting to test if a helicase-truncated CATF1 is also capable of maintaining the same synergistic interaction with KLF13. In addition it is possible that ATP binding could modulate CATF1 activity with KLF13.

The fact that CATF1 transcripts are enriched in the embryonic and perinatal myocardium raises the possibility that these helicases might add another level of spatiotemporal transcriptional control. Also, it is possible that CATF1 is essential for proper temporal expression of muscle isoforms important for adequate remodelling and compensatory responses of the heart to changing load and demand. Intriguingly, several mutations in CATF1 outside the helicase domain were linked to dilated cardiomyopathy (DCM) defined by ventricular chamber enlargement and systolic dysfunction that ultimately manifests itself in progressive heart failure, arrhythmias, thromboembolism, and premature death [108, 110]. Our demonstrated KLF13-CATF1 synergistic transcriptional activation might suggest a mechanism by which mutations in CATF1 might alter protein-protein interaction with KLF13 and disrupt the tightly regulated spatial and temporal gene expression that is essential during cardiac development. Further structure-function analysis

of CATF1 is needed for a better understanding of its involvement in transcriptional activities during development.

4.6. A novel isoform of KLF13.

Few members of the KLF family were shown to exhibit splice variants (i.e. KLF6, KLF10, and KLF8). Of these, KLF6b, KLF6c, and KLF8b are truncated isoforms that contain deletions in the zinc-finger motifs [114]. Interestingly, the isoform of the KLF6 protein antagonizes the ability of full length KLF6 to suppress cell proliferation and induce cellular differentiation. KLF6 inactivation and KLF6b overexpression have been associated not only with the progression of a number of human cancers, but more importantly with patient survival [155]. Thus, alternative splicing adds another regulatory mechanism by which members of the KLF family influence growth and development.

During the course of the thesis, a second isoform of KLF13 was identified. Our study reveals a new mechanism for regulating KLF13 expression and activity that involves the alternative splicing of the KLF13 gene to produce two isoforms with distinct spatiotemporal distributions and activities. In this uncharacterized variant, an alternative N-terminal cryptic exon 1b is used to generate an isoform with only two C2H2-type zinc-fingers, thus splicing out exon 1a of the first isoform which encodes the first N-terminal zinc finger and the N-terminal tail of KLF13a. Although KLF13b retained the abilities of DNA binding and nuclear localization, it lacked a potent TAD. Interestingly, we found that KLF13b competes for the same DNA CACCC element as KLF13a and hinders its transcriptional activity. Moreover, KLF13b was capable of maintaining strong functional synergy with GATA-4 and TBX5. These data point to a possible mechanism of gene regulation in which an isoform-lacking TADs not only act as competitors for DNA binding

sites but also as modulators of gene expression by having different transcriptional activities and distinct repertoires of interacting partners.

In addition to their distinct biochemical properties, the expression patterns of KLF13 isoforms suggest a differential role during development. For example, the first isoform (ED 11.5) is expressed in the heart, limb, and liver earlier than the second isoform (ED 13.5). In addition, while KLF13b was not detected during embryonic development, KLF13a was shown to have a robust expression by ED 13.5. The earlier expression of KLF13a (as early as ED 9.5) might be attributed to its role in cardiomyocyte proliferation; the later expression of KLF13b (ED 13.5) might be due to a role associated with septation and/or maturation of the heart. Note that by ED13.5, heart morphogenesis is near completion and, importantly, myocyte proliferation is tempered downat this stage . More functional studies are needed to decipher the physiological role of the two isoforms during embryonic development and postnatally. Currently our lab is testing the effect of the isoforms on proliferation and apoptosis by over-expressing the isoforms in proliferating C2C12 cells and testing their proliferation and differentiation profiles.

It is possible that KLF13 isoforms (a and b) work in a manner similar to those of TBX5 isoforms (a and b). The distinct biochemical properties and patterns of expression of TBX5 isoforms suggest a differential role in cellular proliferation. *In vivo* and *in vitro* studies concluded that while the expression of TBX5a correlated with proliferative growth, the expression of TBX5b was predominant in more differentiated, less proliferative cells. Thus, isoform ratio and switching might add another level of control during cardiac development.

4.7. Structure-function analysis.

In a step towards analyzing KLF13's mechanism of action and to decipher its role in the genetic networks regulating cardiac development we pursued a structure-function characterization of KLF13. Here we report, using cloning and transfection techniques, the coarse identification of the domains central for KLF13 DNA-binding and nuclear localization. In addition we identified a new transactivational domain of KLF13.

The distinctive feature of the KLF family is the presence of three contiguous and highly conserved C2H2 zinc-fingers that compose a DNA-binding domain at the carboxyl terminus of the protein. The zinc-finger domains enable the KLF family members to bind to related GC/GT rich sites on the major groove of DNA [112, 113]. We demonstrated that the last two zinc-fingers contained on the C-terminal region were capable of binding to the KLF13 response element (CACCC element). Interestingly, deleting the third zinc-finger left the protein incompetent in DNA binding. Thus, as a premature statement, we are assumingsuggests that the last two zinc-fingers (ZF2 and ZF3) are the zinc-fingers mediating DNA binding. On the other hand it is strongly suggested that the first zinc-finger exists to mediate a secondary role, possibly specificity of DNA binding, nuclear localization, or/and even protein-protein binding interface. The DNA recognition mode of the KLF zinc-fingers is currently predicted based on the *in silico* structural analysis of the Zif268–DNA complex. Based on the *in silico* Wolfe model, each zinc-finger recognizes a nucleotide triplet, and thus the three zinc-finger repeats of the KLFs recognize nine base pairs in total. The amino acid residues determinant of sequence specificity and critical for the direct interaction with the DNA bases are four highly conserved amino acids positioned at −1, 2, 3, and 6 from the N-terminal end of the α-helix in each zinc-finger. Interestingly, using *in silico* analysis, the first ZF1 has the least preference for DNA bases, at which it is predicted

to prefer the sequence 5′-NGN-3′, where N is any base. As for ZF2, the four amino acid positions important for DNA binding are completely conserved among the KLFs and the ZF2 was found to prefer the sequence 5′-GCG-3′. In the case of ZF3, the amino acid at the 6th position is not completely conserved among the KLF family members. However, it was predicted to prefer 5′-(G/T)GG-3′ in the case of KLF13. Not only is the aforementioned *in silico* analysis/prediction highly consistent with numerous reports on the sequence preferences of KLFs for the CACCC-box (GC-box) in promoter or enhancer regions, but it also partially explains our reported dispensability of ZF1 to KLF13's DNA-binding to the CACCC element [136]. Intriguingly, Laity *et al* 2006 suggested that a number of novel strategies have evolved for C2H2 zinc-finger containing transcription factors to achieve high DNA-binding affinity and specificity with only two or even one ZF motif [156]. A notable example is that of the two Krüppel-like, C2H2, zinc-fingers containing the transcription factor ZFF29. Although the protein contains only two zinc-fingers, the remnants of "an archaic third zinc-finger" can be detected by the presence of conserved inter-finger sequences, i.e. TGEKP, and cysteine and histidine residues [157].

In comparison to the conserved zinc-finger motifs of the KLF family, the locations and structures of the NLS are variable [120]. Normally, the NLS is important for protein translocation across the nuclear membrane via nuclear transport proteins in an ATP-dependent fashion [112]. Song *et al* 2002, conducted a sequence analysis of KLF13 and predicted the presence of an enriched stretch of basic amino acids (Arg/Lys) typical of a nuclear localization signal (NLS) region adjacent to the start of the zinc-finger DNA-binding domain (147–168aa) [112]. In their study utilizing GFP-fusion KLF13 constructs, the 147-168aa region of KLF13 was identified as a potent NLS sequence [112]. Here we report that the structural integrity of the zinc-finger domain, not the 147-168aa region that contains the

NLS, is required to target the protein to the nucleus. Progressive C-terminal deletion of the zinc-fingers, maintaining the 147-168aa region, dramatically reduced nuclear localization of the protein. As no putative NLS (core or bipartite) rich in basic amino acids was found within the finger region we concluded that the three zinc fingers serve as the NLS for KLF13. The idea that the zinc-fingers can participate and sufficiently localize a protein to the nucleus is not novel or unique to KLF13 alone. Several basic regions were identified in many KLF family members, but they proved useless for nuclear localization in some KLFs including KLF1 [115, 136]. Similar to KLF13, Pandya *et all* demonstrated that the NLS of KLF1 is contained specifically within the three Kruppel zinc-fingers [158]. All three zinc-fingers were found to be necessary for efficient nuclear localization; deletion of any one finger resulted in partial loss of nuclear targeting, whereas deletion of any two zinc-fingers resulted in predominant cytoplasmic accumulation [158]. Thus, we conclude that KLF13 contains a multifunctional zinc-finger domain. It is worth mentioning that in addition to DNA-binding and nuclear localization, this domain was also in protein-protein interactions with the coactivators CBP/p300 and PCAF [140, 159].

Our deletion analysis of KLF13 has also revealed that the region 67–147aa contains a transactivation domain. This region is rich in the amino acids alanine (19%) and proline (20%) with five arginine residues embedded within 84-98aa. This region has no obvious resemblance to any other proteins including the closest family members KLF9 and KLF16 [112]. Hydrophobic amino acid residues are well known to be enriched in regions mediating protein-protein interactions. It is not radical to think that protein-protein contact between KLF13's transactivation domain and the basal transcriptional machinery may involve both charged residues and hydrophobic interaction. It is that the protein-protein interaction is initiated by contact between charged amino acids however this interaction is reinforced and

stabilized by the stronger hydrophobic forces [112, 160]. Intriguingly, *Song et al* have also identified a transactivationalal domain within the N-terminal region 1-67aa and a repression domain was localized to the 67–147aa region of the protein. These data combined suggest that, in addition to the well-known bifunctional EKLF subfamily (KLF1, KLF2, and KLF4), KLF13 can also function as an activator and repressor depending upon the targeting promoters, the interacting proteins, and the cellular context [112]. Figure 4.1 demonstrates our current model of KLF13's structural / functional domains.

4.8. KLF13's combinatorial interaction.

Previously, Song *et al* demonstrated that the coactivator p300/CBP acts synergistically in stimulating KLF13 transcriptional activity, which points to the involvement of acetyltransferases in the transcriptional activity of KLF13 [112]. Utilizing the RANTES promoter, a chemokine vital for T lymphocyte maturation, a thorough examination of the interaction between transcriptional machinery and chromatin was undertaken to decode the molecular events that accompany changes in gene expression.

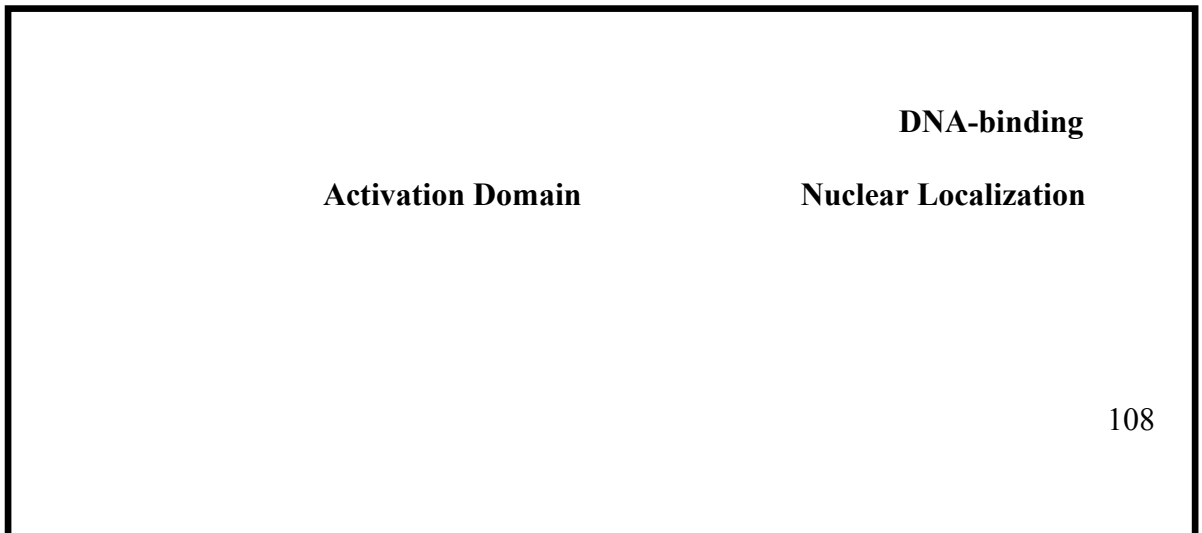

Figure 4.1: Schematic representation of KLF13 protein structure. The coxes on the top half of the figure represent the functional domains recognized by our current study. The solid lines on the bottom half of the figure represent regions required for the interaction with the proteins identified under the line (supported by physical interactions studies). The dotted lines on the bottom half of the figure represent regions required for the interaction with the proteins identified under the line (not yet supported by physical interactions studies).

In the study, KLF13 was found to act as a 'linchpin' for the recruitment of numerous co-factors important for chromatin remodelling to orchestrate the activation of RANTES expression in T lymphocytes. These co-factors were found to include the MAPK Nemo-like kinase (NLK), p300/CBP, PCAF, and Brahma-related gene 1, which are vital to commence timed changes in phosphorylation, acetylation of histones and ATP-dependent chromatin remodeling near the TATA box of the RANTES promoter. Accordingly, relaxing the RANTES promoter for RNA polymerase II recruitment and transcriptional initiation [161] [162].

Compellingly, numerous studies have reported that the transcription factors GATA-4 [89] and NKX2.5 [85] also functionally and physically interact with p300/CBP. In cardiac myocytes, the p300 protein serves as an adaptor for the cardiac-specific zinc-finger transcription factors GATA-4 and GATA-5, and these interactions are required for the full transcriptional activities of these factors [163]. Also, the novel transcriptional co-activator TAZ (transcriptional co-activator with PDZ-binding motif), recognized as a key TBX5 co-activator, was also found to mediate its transcriptional regulation via interactions with histone acetyltransferases p300/CBP and PCAF [101]. Our data regarding the domains mediating protein-protein interaction between KLF13-NKX2.5 and KLF13-GATA-4 support a hypothesis of a p300/CBP-mediated synergy model similar to that of KLF13 on the RANTES promoter (**figure 4.2**). While the C-terminal zinc-finger domain of KLF13 functionally and physically mediates the interaction with p300/CBP, our study has indicated that the N-terminal domain of KLF13 is functionally important for synergy with GATA-4 and NKX2.5. Reciprocally, while the synergy of KLF13 was shown to be physically mediated via the N-terminal zinc finger of GATA-4, the synergy with p300 was physically localized to the C-terminal zinc-finger of GATA-4. Also, while NKX2.5-p300 interaction is physically mediated via the 9-19aa region of NKX2.5, our study indicated that the synergy of KLF13 with NKX2.5 is functionally mediated via the (48-92aa) region of the protein. However, triple synergy studies between KLF13- p300/CBP-NKX2.5, KLF13-p300/CBP-GATA-4, and the KLF13 domains mediating the physical interaction with NKX2.5 and GATA-4 are needed to confirm our model. Importantly, our model might also encompass multifaceted protein-protein interactions that include KLF13 with TBX5, PEX1 and CATF1.

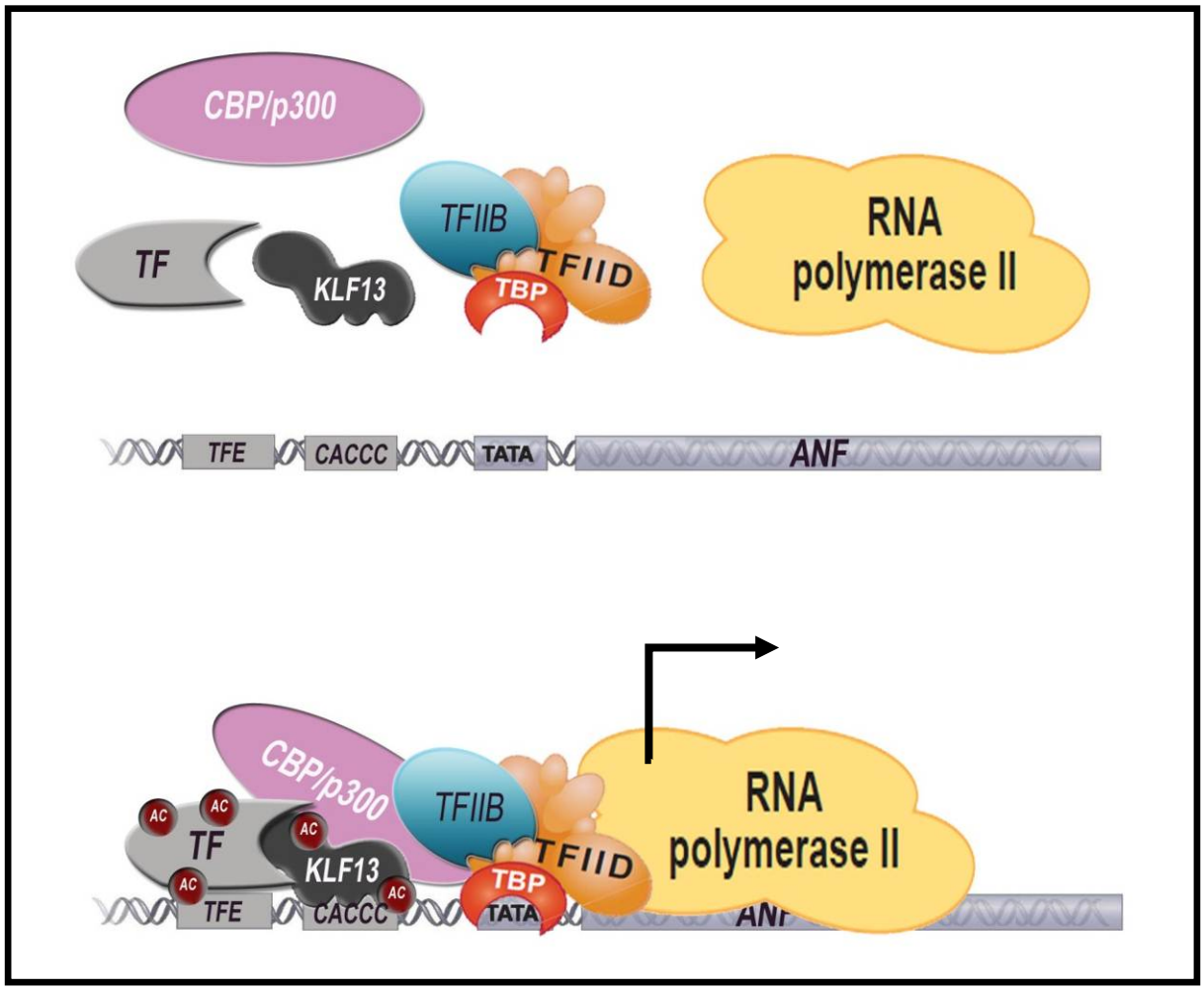

Figure 4.2: A hypothetical model for the molecular mechanism of KLF13 synergy with the transfection factors NKX2.5 and GATA-4. The model illustrates the bridging functionality of p300/CBP. In addition, the figure shows the acetylation of several residues in NKX2.5, GATA-4 and KLF13.

Conclusions:

In conclusion, we showed that KLF13, a cardiac-enriched member of kruppel-like factors (KLFs) family, is an integrated member of the genetic networks controlling cardiac growth and differentiation. We report a novel synergistic partnership between KLF13 and the individual cardiac transcription factors TBX5, NKX2.5, PEX1 and CATF1 that potentiates their transcriptional activity on the ANF promoter. Also, the functions of selected structural regions of KLF13 were analyzed; a novel transcriptional activation

domain, the nuclear localization region/zinc-fingers, and the DNA binding zinc-fingers were identified. Analyses of these structural features were the first step in defining the KLF13 mechanism of action. Assisted by our structure-function studies, dissecting the partnership profile of KLF13 with the other transcription factors directed us to a possible mechanism of action that involves the recruitment and protein-acetylation by histone acetyltransferases CBP/p300. More tedious dissections of the partnership profile (physical and functional) of KLF13 with the newly identified collaborators are needed to fully understand the recruitment and the combinatorial interactions between these transcription factors on the ANF promoter. These studies may partially explain how specific mutations in cardiac transcription factors (e.g. TBX5, GATA4 and NKX2.5) might contribute to similar phenotypes.

Our preliminary data regarding $KLF13^{-/-}$ mice implicates the protein in the proper development of the atria, the right ventricles, and the out-flow tract. The spatial localizations of these cardiac defects suggest the importance of $KLF13^{-/-}$ for the proper development of the secondary heart field and/or its derivatives. It is possible that KLF13 acts on the same genetic pathways that TBX5 and GATA4 are epart of to direct proper cardiac development. Due to the low penetrance of $KLF13^{-/-}$ and possible compensatory mechanisms, it would be interesting to assess the contribution of the interactions of KLF13 and TBX5 (important for atrial development) or GATA5 (important for out-flow tract and valve development) during cardiac development by crossing mice mutant in KLF13 and others that are mutant in TBX5 or GATA5. We are expecting severe and new undetected cardiac defects to develop specially in the outflow tract upon mutating these genes. These studies will provide a new paradigm that may help to decipher the genotype-phenotype relation in patients with congenital heart diseases.

Moreover, we present that the two KLF13 isoforms have distinct biochemical properties and spatiotemporal expression. The existence of alternatively spliced KLF13 isoforms may provide a new paradigm that might help to decipher the genotype-phenotype relation in patients with congenital heart diseases.

6. References

1. Martin-Puig, S., Z. Wang, and K.R. Chien, *Lives of a Heart Cell: Tracing the Origins of Cardiac Progenitors.* Cell stem cell, 2008. **2**(4): p. 320-331.
2. Buckingham M, M.S., Zaffran S., *Building the mammalian heart from two sources of myocardial cells.* Nat Rev Genet., 2005. **6**(11): p. 826-35.
3. Srivastava, D., *Making or Breaking the Heart: From Lineage Determination to Morphogenesis.* Cell, 2006. **126**(6): p. 1037-1048.
4. Wu, S.M., K.R. Chien, and C. Mummery, *Origins and Fates of Cardiovascular Progenitor Cells.* Cell, 2008. **132**(4): p. 537-543.
5. Bruneau, B.G., *The developmental genetics of congenital heart disease.* Nature, 2008. **451**(7181): p. 943-948.
6. Koshiba-Takeuchi, K., et al., *Cooperative and antagonistic interactions between Sall4 and Tbx5 pattern the mouse limb and heart.* Nat Genet, 2006. **38**: p. 175 - 183.
7. Abraham, D., et al., *The Role of the Homeodomain Transcription Factor Nkx2-5 in the Cardiovascular System*, in *Advances in Vascular Medicine*, Springer London. p. 113-130.
8. Linask, K.K.a.L., J. W. , *Early heart development: Dynamics of endocardial cell sorting suggests a common origin with cardiomyocytes.* American Journal of Anatomy, 1993. **196**: p. 62-69.
9. Packham, E.A. and J. David Brook, *Interaction makes the heart grow stronger.* Trends in Molecular Medicine, 2003. **9**(10): p. 407-409.
10. Olson, E.N. and D. Srivastava, *Molecular Pathways Controlling Heart Development.* Science, 1996. **272**(5262): p. 671-676.
11. Nemer, M., *Genetic insights into normal and abnormal heart development.* Cardiovascular Pathology. **17**(1): p. 48-54.
12. Alsan, B.H. and T.M. Schultheiss, *Regulation of avian cardiogenesis by Fgf8 signaling.* Development, 2002. **129**(8): p. 1935-1943.
13. Frank, D.U., et al., *An Fgf8 mouse mutant phenocopies human 22q11 deletion syndrome.* Development, 2002. **129**(19): p. 4591-4603.
14. Lee, Y., et al., *The Cardiac Tissue-Restricted Homeobox Protein Csx/Nkx2.5 Physically Associates with the Zinc Finger Protein GATA4 and Cooperatively Activates Atrial Natriuretic Factor Gene Expression.* Mol. Cell. Biol., 1998. **18**(6): p. 3120-3129.
15. Garg, V., et al., *GATA4 mutations cause human congenital heart defects and reveal an interaction with TBX5.* Nature, 2003. **424**(6947): p. 443-447.
16. Morin, S., et al., *GATA-dependent recruitment of MEF2 proteins to target promoters.* EMBO J, 2000. **19**(9): p. 2046-2055.
17. Belaguli, N.S., et al., *Cardiac Tissue Enriched Factors Serum Response Factor and GATA-4 Are Mutual Coregulators.* Mol. Cell. Biol., 2000. **20**(20): p. 7550-7558.
18. Dai, Y.-S., et al., *The Transcription Factors GATA4 and dHAND Physically Interact to Synergistically Activate Cardiac Gene Expression through a p300-dependent Mechanism.* Journal of Biological Chemistry, 2002. **277**(27): p. 24390-24398.
19. MOORMAN, A.F.M. and V.M. CHRISTOFFELS, *Cardiac Chamber Formation: Development, Genes, and Evolution.* Physiol. Rev., 2003. **83**(4): p. 1223-1267.
20. Bruneau, B.G., *Transcriptional Regulation of Vertebrate Cardiac Morphogenesis.* Circ Res, 2002. **90**(5): p. 509-519.

21. Takeuchi, J.K., et al., *Tbx20 dose-dependently regulates transcription factor networks required for mouse heart and motoneuron development.* Development, 2005. **132**(10): p. 2463-2474.
22. Bruneau, B.G., *Chromatin remodeling in heart development.* Current Opinion in Genetics & Development. **20**(5): p. 505-511.
23. Bernstein, B.E., A. Meissner, and E.S. Lander, *The Mammalian Epigenome.* Cell, 2007. **128**(4): p. 669-681.
24. Simone, C., *SWI/SNF: The crossroads where extracellular signaling pathways meet chromatin.* Journal of Cellular Physiology, 2006. **207**(2): p. 309-314.
25. Kouzarides, T., *Chromatin Modifications and Their Function.* Cell, 2007. **128**(4): p. 693-705.
26. Yao, T.-P., et al., *Gene Dosage-Dependent Embryonic Development and Proliferation Defects in Mice Lacking the Transcriptional Integrator p300.* Cell, 1998. **93**(3): p. 361-372.
27. Kawamura, T., et al., *Acetylation of GATA-4 Is Involved in the Differentiation of Embryonic Stem Cells into Cardiac Myocytes.* Journal of Biological Chemistry, 2005. **280**(20): p. 19682-19688.
28. Haberland, M., R.L. Montgomery, and E.N. Olson, *The many roles of histone deacetylases in development and physiology: implications for disease and therapy.* Nat Rev Genet, 2009. **10**(1): p. 32-42.
29. de Bold, A.J., et al., *A rapid and potent natriuretic response to intravenous injection of atrial myocardial extract in rats.* Life Sciences, 1981. **28**(1): p. 89-94.
30. Sudoh, T., et al., *A new natriuretic peptide in porcine brain.* Nature, 1988. **332**(6159): p. 78-81.
31. Hayek, S. and M. Nemer, *Cardiac Natriuretic Peptides: From Basic Discovery to Clinical Practice.* Cardiovascular Therapeutics, 2010: p. no-no.
32. de Bold, A.J., B.G. Bruneau, and M.L. Kuroski de Bold, *Mechanical and neuroendocrine regulation of the endocrine heart.* Cardiovascular Research, 1996. **31**(1): p. 7-18.
33. Suo, M., *The role and mechanisms of angiotensin II in regulating the natriuretic peptide gene expression in response to cardiac overload*, in *Department of Pharmacology and Toxicology, University of Oulu*. 2002, University of Oulu: Oulu.
34. McBride, K. and M. Nemer, *Regulation of the ANF and BNP promoters by GATA factors: Lessons learned for cardiac transcription.* Canadian Journal of Physiology and Pharmacology, 2001. **79**(8): p. 673-681.
35. Argentin, S., et al., *Developmental stage-specific regulation of atrial natriuretic factor gene transcription in cardiac cells.* Mol. Cell. Biol., 1994. **14**(1): p. 777-790.
36. R T Lee, K.D.B., J M Pfeffer, M A Pfeffer, E J Neer, and C E Seidman, *Atrial natriuretic factor gene expression in ventricles of rats with spontaneous biventricular hypertrophy.* J Clin Invest. , 1988. **81**(2): p. 431–434.
37. John, S., et al., *Genetic decreases in atrial natriuretic peptide and salt-sensitive hypertension.* Science, 1995. **267**(5198): p. 679-681.
38. Y Ogawa, H.I., N Tamura, S Suga, T Yoshimasa, M Uehira, S Matsuda, S Shiono, H Nishimoto, and K Nakao, *Molecular cloning of the complementary DNA and gene that encode mouse brain natriuretic peptide and generation of transgenic mice that overexpress the brain natriuretic peptide gene.* J Clin Invest. , 1994. **93**(5): p. 1911–1921.

39. Ruskoaho, H., *Atrial natriuretic peptide: synthesis, release, and metabolism.* Pharmacological Reviews, 1992. **44**(4): p. 479-602.
40. Hunyady, B., et al., *Immunohistochemical Localization of Somatostatin Receptor SST2A in the Rat Pancreas.* Endocrinology, 1997. **138**(6): p. 2636-2639.
41. Posch, M., et al., *Molecular genetics of congenital atrial septal defects.* Clinical Research in Cardiology. **99**(3): p. 137-147.
42. Olson, E.N., *A decade of discoveries in cardiac biology.* Nat Med, 2004. **10**(5): p. 467-474.
43. Joziasse, I., et al., *Genes in congenital heart disease: atrioventricular valve formation.* Basic Research in Cardiology, 2008. **103**(3): p. 216-227.
44. Hartman, J.L., IV, B. Garvik, and L. Hartwell, *Principles for the Buffering of Genetic Variation.* Science, 2001. **291**(5506): p. 1001-1004.
45. Rutherford, S.L., *Between genotype and phenotype: protein chaperones and evolvability.* Nat Rev Genet, 2003. **4**(4): p. 263-274.
46. Bentham, J. and S. Bhattacharya, *Genetic Mechanisms Controlling Cardiovascular Development.* Annals of the New York Academy of Sciences, 2008. **1123**(1): p. 10-19.
47. Xin, M., et al., *A threshold of GATA4 and GATA6 expression is required for cardiovascular development.* Proceedings of the National Academy of Sciences, 2006. **103**(30): p. 11189-11194.
48. Lavallee, G., et al., *The Kruppel-like transcription factor KLF13 is a novel regulator of heart development.* EMBO J, 2006. **25**(21): p. 5201-5213.
49. Biben, C. and R.P. Harvey, *Homeodomain factor Nkx2-5 controls left/right asymmetric expression of bHLH gene eHand during murine heart development.* Genes & Development, 1997. **11**(11): p. 1357-1369.
50. Habets, P.E.M.H., et al., *Cooperative action of Tbx2 and Nkx2.5 inhibits ANF expression in the atrioventricular canal: implications for cardiac chamber formation.* Genes & Development, 2002. **16**(10): p. 1234-1246.
51. Jay, P.Y., et al., *Nkx2-5 mutation causes anatomic hypoplasia of the cardiac conduction system.* The Journal of Clinical Investigation, 2004. **113**(8): p. 1130-1137.
52. Lyons, I., et al., *Myogenic and morphogenetic defects in the heart tubes of murine embryos lacking the homeo box gene Nkx2-5.* Genes & Development, 1995. **9**(13): p. 1654-1666.
53. Pashmforoush, M., et al., *Nkx2-5 Pathways and Congenital Heart Disease: Loss of Ventricular Myocyte Lineage Specification Leads to Progressive Cardiomyopathy and Complete Heart Block.* Cell, 2004. **117**(3): p. 373-386.
54. Tanaka, M., et al., *The cardiac homeobox gene Csx/Nkx2.5 lies genetically upstream of multiple genes essential for heart development.* Development, 1999. **126**(6): p. 1269-1280.
55. Watt, A.J., et al., *GATA4 is essential for formation of the proepicardium and regulates cardiogenesis.* Proceedings of the National Academy of Sciences of the United States of America, 2004. **101**(34): p. 12573-12578.
56. Reiter, J.F., et al., *Gata5 is required for the development of the heart and endoderm in zebrafish.* Genes & Development, 1999. **13**(22): p. 2983-2995.
57. Crispino, J.D., et al., *Proper coronary vascular development and heart morphogenesis depend on interaction of GATA-4 with FOG cofactors.* Genes & Development, 2001. **15**(7): p. 839-844.

58. Vong, L., et al., *MEF2C is required for the normal allocation of cells between the ventricular and sinoatrial precursors of the primary heart field.* Developmental Dynamics, 2006. **235**(7): p. 1809-1821.
59. Marguerie, A., et al., *Congenital heart defects in Fgfr2-IIIb and Fgf10 mutant mice.* Cardiovascular Research, 2006. **71**(1): p. 50-60.
60. Cai, C.-L., et al., *Isl1 Identifies a Cardiac Progenitor Population that Proliferates Prior to Differentiation and Contributes a Majority of Cells to the Heart.* Developmental cell, 2003. **5**(6): p. 877-889.
61. Firulli, A.B., et al., *Heart and extra-embryonic mesodermal defects in mouse embryos lacking the bHLH transcription factor Hand1.* Nat Genet, 1998. **18**(3): p. 266-270.
62. Srivastava, D. and E.N. Olson, *A genetic blueprint for cardiac development.* Nature, 2000. **407**: p. 221-226.
63. Yamagishi, H., *Tbx1 is regulated by tissue-specific forkhead proteins through a common Sonic hedgehog-responsive enhancer.* Genes Dev., 2003. **17**: p. 269-281.
64. Christoffels, V.M., et al., *Chamber Formation and Morphogenesis in the Developing Mammalian Heart.* Developmental Biology, 2000. **223**(2): p. 266-278.
65. Mommersteeg, M.T.M., et al., *Molecular Pathway for the Localized Formation of the Sinoatrial Node.* Circ Res, 2007. **100**(3): p. 354-362.
66. Mori, A.D., et al., *Tbx5-dependent rheostatic control of cardiac gene expression and morphogenesis.* Developmental Biology, 2006. **297**(2): p. 566-586.
67. Ko, L.J. and J.D. Engel, *DNA-binding specificities of the GATA transcription factor family.* Mol. Cell. Biol., 1993. **13**(7): p. 4011-4022.
68. Grepin, C., et al., *A hormone-encoding gene identifies a pathway for cardiac but not skeletal muscle gene transcription.* Mol. Cell. Biol., 1994. **14**(5): p. 3115-3129.
69. Arceci, R.J., et al., *Mouse GATA-4: a retinoic acid-inducible GATA-binding transcription factor expressed in endodermally derived tissues and heart.* Mol. Cell. Biol., 1993. **13**(4): p. 2235-2246.
70. Grepin, C., et al., *Inhibition of transcription factor GATA-4 expression blocks in vitro cardiac muscle differentiation.* Mol. Cell. Biol., 1995. **15**(8): p. 4095-4102.
71. Bartlett, H., G. Veenstra, and D. Weeks, *Examining the Cardiac NK-2 Genes in Early Heart Development.* Pediatric cardiology. **31**(3): p. 335-341.
72. Molkentin, J.D., et al., *Requirement of the transcription factor GATA4 for heart tube formation and ventral morphogenesis.* Genes & Development, 1997. **11**(8): p. 1061-1072.
73. Clark KL, Y.K., and Benson DW., *Transcription factors and congenital heart defects.* Annu Rev Physiol, 2006: p. 97-121.
74. David J.Whyatt, E.d.a.F.G., *The two zinc finger-like domains of GATA-1 have different DNA binding specificities.* The EMBO Journal, 1993. **12**(13): p. 4993-5005.
75. Pikkarainen, S., et al., *GATA transcription factors in the developing and adult heart.* Cardiovascular Research, 2004. **63**(2): p. 196-207.
76. Morrisey, E.E., et al., *GATA-4 activates transcription via two novel domains that are conserved within the GATA-4/5/6 subfamily.* J. Biol. Chem., 1997. **272**: p. 8515-8524.
77. Durocher, D., et al., *The cardiac transcription factors Nkx2-5 and GATA-4 are mutual cofactors.* EMBO J, 1997. **16**(18): p. 5687-5696.

78. Svensson, E.C., et al., *A Functionally Conserved N-terminal Domain of the Friend of GATA-2 (FOG-2) Protein Represses GATA4-Dependent Transcription.* Journal of Biological Chemistry, 2000. **275**(27): p. 20762-20769.
79. Hiroi, Y., et al., *Tbx5 associates with Nkx2-5 and synergistically promotes cardiomyocyte differentiation.* Nat Genet, 2001. **28**(3): p. 276-280.
80. Harvey, R.P., *NK-2Homeobox Genes and Heart Development.* Developmental Biology, 1996. **178**(2): p. 203-216.
81. Akazawa, H. and I. Komuro, *Cardiac transcription factor Csx/Nkx2-5: Its role in cardiac development and diseases.* Pharmacology & Therapeutics, 2005. **107**(2): p. 252-268.
82. Chen, C. and R. Schwartz, *Recruitment of the tinman homolog Nkx-2.5 by serum response factor activates cardiac alpha-actin gene transcription.* Mol. Cell. Biol., 1996. **16**(11): p. 6372-6384.
83. Liu, Z. and V. Karmarkar, *Groucho/Tup1 family co-repressors in plant development.* Trends in Plant Science, 2008. **13**(3): p. 137-144.
84. Muhr, J., et al., *Groucho-Mediated Transcriptional Repression Establishes Progenitor Cell Pattern and Neuronal Fate in the Ventral Neural Tube.* Cell, 2001. **104**(6): p. 861-873.
85. Li, T., et al., *Carboxyl Terminus of NKX2.5 Impairs its Interaction with p300.* Journal of Molecular Biology, 2007. **370**(5): p. 976-992.
86. Stennard, F.A. and R.P. Harvey, *T-box transcription factors and their roles in regulatory hierarchies in the developing heart.* Development, 2005. **132**(22): p. 4897-4910.
87. Ryan, K. and A.J. Chin, *T-box genes and cardiac development.* Birth Defects Research Part C: Embryo Today: Reviews, 2003. **69**(1): p. 25-37.
88. Clabby, M.L., et al., *Retinoid X Receptor Î± Represses GATA-4-mediated Transcription via a Retinoid-dependent Interaction with the Cardiac-enriched Repressor FOG-2.* Journal of Biological Chemistry, 2003. **278**(8): p. 5760-5767.
89. Dai, Y.-S. and B.E. Markham, *p300 Functions as a Coactivator of Transcription Factor GATA-4.* Journal of Biological Chemistry, 2001. **276**(40): p. 37178-37185.
90. Charron, F., et al., *Cooperative Interaction between GATA-4 and GATA-6 Regulates Myocardial Gene Expression.* Mol. Cell. Biol., 1999. **19**(6): p. 4355-4365.
91. Rallis, C., et al., *Tbx5 is required for forelimb bud formation and continued outgrowth.* Development, 2003. **130**(12): p. 2741-2751.
92. Liberatore, C.M., R.D. Searcy-Schrick, and K.E. Yutzey, *Ventricular Expression of tbx5 Inhibits Normal Heart Chamber Development.* Developmental Biology, 2000. **223**(1): p. 169-180.
93. A. Ardati, a.M.N., *A nuclear pathway for alpha 1-adrenergic receptor signaling in cardiac cells.* EMBO J, 1993. **12**(13): p. 5131-5139.
94. Debrus, S., et al., *The Zinc Finger-Only Protein Zfp260 Is a Novel Cardiac Regulator and a Nuclear Effector of {alpha}1-Adrenergic Signaling.* Mol. Cell. Biol., 2005. **25**(19): p. 8669-8682.
95. Komati, H., et al., *ZFP260 an inducer of cardiac hypertrophy and a nuclear mediator of endothelin-1 signaling.* Journal of Biological Chemistry.
96. Kulisz, A. and H.-G. Simon, *An Evolutionarily Conserved Nuclear Export Signal Facilitates Cytoplasmic Localization of the Tbx5 Transcription Factor.* Mol. Cell. Biol., 2008. **28**(5): p. 1553-1564.

97. Ghosh, T.K., et al., *Physical Interaction between TBX5 and MEF2C Is Required for Early Heart Development.* Mol. Cell. Biol., 2009. **29**(8): p. 2205-2218.
98. Krause, A., et al., *Tbx5 and Tbx4 transcription factors interact with a new chicken PDZ-LIM protein in limb and heart development.* Developmental Biology, 2004. **273**(1): p. 106-120.
99. Basson, C.T., *Mutations in human TBX5 cause limb and cardiac malformation in Holt-Oram syndrome.* Nature Genet., 1997. **15**: p. 30-35.
100. Basson, C.T., *Different TBX5 interactions in heart and limb defined by Holt-Oram syndrome mutations.* Proc. Natl Acad. Sci. USA, 1999. **96**: p. 2919-2924.
101. Murakami, M., et al., *A WW domain protein TAZ is a critical coactivator for TBX5, a transcription factor implicated in Holt-Oram syndrome.* Proc Natl Acad Sci USA, 2005. **102**: p. 18034 - 18039.
102. Guenther, U.-P., et al., *IGHMBP2 is a ribosome-associated helicase inactive in the neuromuscular disorder distal SMA type 1 (DSMA1).* Human Molecular Genetics, 2009. **18**(7): p. 1288-1300.
103. Maddatu, T.P., et al., *Transgenic rescue of neurogenic atrophy in the nmd mouse reveals a role for Ighmbp2 in dilated cardiomyopathy.* Human Molecular Genetics, 2004. **13**(11): p. 1105-1115.
104. Grohmann, K., et al., *Characterization of Ighmbp2 in motor neurons and implications for the pathomechanism in a mouse model of human spinal muscular atrophy with respiratory distress type 1 (SMARD1).* Human Molecular Genetics, 2004. **13**(18): p. 2031-2042.
105. Sebastiani, G., et al., *Localization of the <i>Catf1</i> transcription factor gene to mouse Chromosome 19.* Mammalian Genome, 1995. **6**(2): p. 147-148.
106. Mizuta, T.-R., et al., *Isolation of cDNA encoding a binding protein specific to 5'-phosphorylated single-stranded DNA with G-rich sequences.* Nucleic Acids Research, 1993. **21**(8): p. 1761-1766.
107. McBride, K., et al., *fos/jun repression of cardiac-specific transcription in quiescent and growth-stimulated myocytes is targeted at a tissue-specific cis element.* Mol. Cell. Biol., 1993. **13**(1): p. 600-612.
108. Maddatu, T.P., et al., *Dilated cardiomyopathy in the nmd mouse: transgenic rescue and QTLs that improve cardiac function and survival.* Human Molecular Genetics, 2005. **14**(21): p. 3179-3189.
109. de Planell-Saguer, MariÃ n., et al., *Biochemical and genetic evidence for a role of IGHMBP2 in the translational machinery.* Human Molecular Genetics, 2009. **18**(12): p. 2115-2126.
110. Fatkin, D., R. Otway, and Z. Richmond, *Genetics of Dilated Cardiomyopathy.* Heart Failure Clinics. **6**(2): p. 129-140.
111. Grohmann, K., et al., *Infantile spinal muscular atrophy with respiratory distress type 1 (SMARD1).* Annals of Neurology, 2003. **54**(6): p. 719-724.
112. Song, A., et al., *Functional Domains and DNA-binding Sequences of RFLAT-1/KLF13, a KrÃ¼ppel-like Transcription Factor of Activated T Lymphocytes.* Journal of Biological Chemistry, 2002. **277**(33): p. 30055-30065.
113. Pearson, R., et al., *Krüppel-like transcription factors: A functional family.* The International Journal of Biochemistry & Cell Biology, 2008. **40**(10): p. 1996-2001.
114. Simmen, R.C.M., et al., *The emerging role of Kruppel-like factors in endocrine-responsive cancers of female reproductive tissues.* J Endocrinol. **204**(3): p. 223-231.

115. Kaczynski, J., T. Cook, and R. Urrutia, *Sp1- and Kruppel-like transcription factors.* Genome Biology, 2003. **4**(2): p. 206.
116. Shindo, T., et al., *Kruppel-like zinc-finger transcription factor KLF5/BTEB2 is a target for angiotensin II signaling and an essential regulator of cardiovascular remodeling.* Nat Med, 2002. **8**(8): p. 856-863.
117. Fisch, S., et al., *Kruppel-like factor 15 is a regulator of cardiomyocyte hypertrophy.* Proceedings of the National Academy of Sciences, 2007. **104**(17): p. 7074-7079.
118. Yoshida, T., et al., *Smooth and Cardiac Muscle-selective Knock-out of KrÃ¼ppel-like Factor 4 Causes Postnatal Death and Growth Retardation.* Journal of Biological Chemistry. **285**(27): p. 21175-21184.
119. Rajamannan, N.M., et al., *TGFβ inducible early gene-1 (TIEG1) and cardiac hypertrophy: Discovery and characterization of a novel signaling pathway.* Journal of Cellular Biochemistry, 2007. **100**(2): p. 315-325.
120. Lomberk, G. and R. Urrutia, *The family feud: turning off Sp1 by Sp1-like KLF proteins.* Biochem. J., 2005. **392**(1): p. 1-11.
121. Saptarsi, M.H., A.I. Osama, and K.J. Mukesh, *Kruppel-like Factors (KLFs) in muscle biology.* Journal of molecular and cellular cardiology, 2007. **43**(1): p. 1-10.
122. Narla, G., et al., *Targeted Inhibition of the KLF6 Splice Variant, KLF6 SV1, Suppresses Prostate Cancer Cell Growth and Spread.* Cancer Research, 2005. **65**(13): p. 5761-5768.
123. Martin, K.M., et al., *Selective modulation of the SM22alpha promoter by the binding of BTEB3 (basal transcription element-binding protein 3) to TGGG repeats.* Biochem. J., 2003. **375**(2): p. 457-463.
124. Richard, B., et al., *Angiotensin II and tumor necrosis factor-alpha upregulate survivin and Kruppel-like factor 5 in smooth muscle cells: Potential relevance to vein graft hyperplasia.* Surgery, 2006. **140**(2): p. 289-296.
125. Gray, S., et al., *Abstract 1393: Targeting of KLF15 Reveals a Critical Role in the Vascular Smooth Muscle Cell Response to Injury.* Circulation, 2006. **114**(18_MeetingAbstracts): p. II_266-a-.
126. Liu, Y., et al., *Kruppel-like Factor 4 Abrogates Myocardin-induced Activation of Smooth Muscle Gene Expression.* Journal of Biological Chemistry, 2005. **280**(10): p. 9719-9727.
127. Asano, H., X.S. Li, and G. Stamatoyannopoulos, *FKLF-2: a novel Kruppel-like transcriptional factor that activates globin and other erythroid lineage genes.* Blood, 2000. **95**(11): p. 3578-3584.
128. Yamamoto, J., et al., *A KrÃ¼ppel-like factor KLF15 Contributes Fasting-induced Transcriptional Activation of Mitochondrial Acetyl-CoA Synthetase Gene AceCS2.* Journal of Biological Chemistry, 2004. **279**(17): p. 16954-16962.
129. Matsumoto, N., et al., *Cloning the cDNA for a New Human Zinc Finger Protein Defines a Group of Closely Related KrÃ¼ppel-like Transcription Factors.* Journal of Biological Chemistry, 1998. **273**(43): p. 28229-28237.
130. Song, A., et al., *RFLAT-1: A New Zinc Finger Transcription Factor that Activates RANTES Gene Expression in T Lymphocytes.* Immunity, 1999. **10**(1): p. 93-103.
131. Martin, K.M., et al., *Mouse BTEB3, a new member of the basic transcription element binding protein (BTEB) family, activates expression from GC-rich minimal promoter regions.* Biochem. J., 2000. **345**(3): p. 529-533.
132. Martin, K.M., J.C. Metcalfe, and P.R. Kemp, *Expression of Klf9 and Klf13 in mouse development.* Mechanisms of Development, 2001. **103**(1-2): p. 149-151.

133. Gordon, A.R., et al., *Splenomegaly and Modified Erythropoiesis in KLF13â€"/â€" Mice.* Journal of Biological Chemistry, 2008. **283**(18): p. 11897-11904.
134. Nemer M, H.M., *The KLF family of transcriptional regulators in cardiomyocyte proliferation and differentiation.* Cell Cycle, 2007. **6**(2): p. 117-21.
135. LePichon, J.-B., et al., *A 15q13.3 homozygous microdeletion associated with a severe neurodevelopmental disorder suggests putative functions of the TRPM1, CHRNA7, and other homozygously deleted genes.* American Journal of Medical Genetics Part A. **152A**(5): p. 1300-1304.
136. Toshio Nagashima, F.H., Takashi Umehara, and a.S. Yokoyama, *Molecular Structures of Krüppel-like Factors*, in *The Biology of Krüppel-like Factors*, R.F. Nagai, Scott L.; Kasuga, Masato, Editor. 2009, Springer: Tokyo, Japan. p. 268.
137. Wolfe SA, N.L., Pabo CO, *DNA recognition by Cys2His2 zinc finger proteins.* Annu Rev Biophys Biomol Struct, 1999. **29**: p. 183–212.
138. Nedved, M.L. and G.R. Moe, *Cooperative, non-specific binding of a Zinc finger peptide to DNA.* Nucleic Acids Research, 1994. **22**(22): p. 4705-4711.
139. Zhou, M., et al., *KrÃ¼ppel-Like Transcription Factor 13 Regulates T Lymphocyte Survival In Vivo.* The Journal of Immunology, 2007. **178**(9): p. 5496-5504.
140. Song, C.-Z., et al., *Functional Interaction between Coactivators CBP/p300, PCAF, and Transcription Factor FKLF2.* Journal of Biological Chemistry, 2002. **277**(9): p. 7029-7036.
141. Kaczynski, J., et al., *The Sp1-like Protein BTEB3 Inhibits Transcription via the Basic Transcription Element Box by Interacting with mSin3A and HDAC-1 Co-repressors and Competing with Sp1.* Journal of Biological Chemistry, 2001. **276**(39): p. 36749-36756.
142. Grzenda, A., et al., *Sin3: Master scaffold and transcriptional corepressor.* Biochimica et Biophysica Acta (BBA) - Gene Regulatory Mechanisms. **1789**(6-8): p. 443-450.
143. Huang, B., et al., *Interaction of PRP4 with KrÃ¼ppel-Like Factor 13 Regulates CCL5 Transcription.* The Journal of Immunology, 2007. **178**(11): p. 7081-7087.
144. Brown, C.O., et al., *The Cardiac Determination Factor, Nkx2-5, Is Activated by Mutual Cofactors GATA-4 and Smad1/4 via a Novel Upstream Enhancer.* Journal of Biological Chemistry, 2004. **279**(11): p. 10659-10669.
145. Georges, R., et al., *Distinct Expression and Function of Alternatively Spliced Tbx5 Isoforms in Cell Growth and Differentiation.* Mol. Cell. Biol., 2008. **28**(12): p. 4052-4067.
146. Ito, T., et al., *Role of zinc finger structure in nuclear localization of transcription factor Sp1.* Biochemical and Biophysical Research Communications, 2009. **380**(1): p. 28-32.
147. Zeisberg, E.M., et al., *Morphogenesis of the right ventricle requires myocardial expression of Gata4.* The Journal of Clinical Investigation, 2005. **115**(6): p. 1522-1531.
148. Susan V. Outram, A.R.G., Ariadne L. Hager-Theodorides, James Metcalfe, Tessa Crompton and Paul Kemp *KLF13 influences multiple stages of both B and T cell development.* Cell Cycle, 2008. **7**(13): p. 2047-2055.
149. McConnell, B.B. and V.W. Yang, *Mammalian KrÃ¼ppel-Like Factors in Health and Diseases.* Physiological Reviews. **90**(4): p. 1337-1381.

150. Hajrasouliha, A.R., et al., *Abstract 2173: Nkx2.5 is Required for Development of the Outflow Tract Through Regulation of Semaphoring 3C Expression and Neural Crest Cells Migration.* Circulation, 2009. **120**(18_MeetingAbstracts): p. S605-b-.
151. Yuasa, S., et al., *Zac1 Is an Essential Transcription Factor for Cardiac Morphogenesis.* Circ Res. **106**(6): p. 1083-1091.
152. Zaragoza, M.V., et al., *Identification of the TBX5 transactivating domain and the nuclear localization signal.* Gene, 2004. **330**: p. 9-18.
153. Koshiba-Takeuchi, K., et al., *Cooperative and antagonistic interactions between Sall4 and Tbx5 pattern the mouse limb and heart.* Nat Genet, 2006. **38**(2): p. 175-183.
154. Ali, F.V.F.-P.a.S., *The DEAD box RNA helicases p68 (Ddx5) and p72 (Ddx17): novel transcriptional co-regulators.* Biochemical Society Transactions, 2008. **36**: p. 609–612.
155. DiFeo, A., G. Narla, and J.A. Martignetti, *Emerging Roles of Kruppel-Like Factor 6 and Kruppel-Like Factor 6 Splice Variant 1 in Ovarian Cancer Progression and Treatment.* Mount Sinai Journal of Medicine: A Journal of Translational and Personalized Medicine, 2009. **76**(6): p. 557-566.
156. Laity, J.H., *Cys2His2 Zinc Finger Proteins*. Handbook of Metalloproteins. 2006: John Wiley & Sons, Ltd.
157. Asano, H.M., Takashi. Naoe, Tomoki. Saito, Hidehiko. and Stamatoyannopoulos, George., *Molecular cloning and characterization of ZFF29: a protein containing a unique Cys2His2 zinc-finger motif.* Biochem. J., 2004. **384**(3): p. 647-653.
158. Pandya, K. and T.M. Townes, *Basic Residues within the Kruppel Zinc Finger DNA Binding Domains Are the Critical Nuclear Localization Determinants of EKLF/KLF-1.* Journal of Biological Chemistry, 2002. **277**(18): p. 16304-16312.
159. Song, C.-Z., et al., *Functional Interplay between CBP and PCAF in Acetylation and Regulation of Transcription Factor KLF13 Activity.* Journal of Molecular Biology, 2003. **329**(2): p. 207-215.
160. Strub, C., et al., *Mutation of exposed hydrophobic amino acids to arginine to increase protein stability.* BMC Biochemistry, 2004. **5**(1): p. 9.
161. Ahn, Y.-T., et al., *Dynamic Interplay of Transcriptional Machinery and Chromatin Regulates "Late" Expression of the Chemokine RANTES in T Lymphocytes.* Mol. Cell. Biol., 2007. **27**(1): p. 253-266.
162. Krensky, A.M. and Y.-T. Ahn, *Mechanisms of Disease: regulation of RANTES (CCL5) in renal disease.* Nat Clin Pract Neph, 2007. **3**(3): p. 164-170.
163. Yanazume, T., et al., *Biological role of p300 in cardiac myocytes.* Molecular and Cellular Biochemistry, 2003. **248**(1): p. 115-119.